Hang Gao

Nitrogen loss from intertidal permeable Wadden Sea sediments

Bremen, April 2011

Nitrogen loss from intertidal permeable Wadden Sea sediments

Dissertation
zur Erlangung des
Doktorgrades der Naturwissenschaften
im Fachbereich Geowissenschften
der Universitaet Bremen
vorgelegt von

Hang Gao

Bremen, April 2011

Die vorliegende Arbeit wurde in der Zeit von October 2006 bis April 2011 am Max-Planck-Institute fuer marine Mikrobiologie in Bremen angefertigt.

Gutachter:
Prof. Dr. Kai-Uwe Hinrichs
Dr. Marcel MM Kuypers

Pruefer:
Prof. Dr. Gerhard Bohrmann
Dr. Marlene M Jensen

Weitere Mitglieder des Pruefungsausschusses:
Dr. Yu-Shih Lin
Friedrich Schroeder

Datum des Promotionskolloquiums: 01. Juni 2011

Abstract

In the oceanic nitrogen (N) cycle, the sedimentary N_2 production accounts for 50-70 % of global marine N-loss. Coastal regions or continental shelves, where terrestrial riverine systems and the oceans intersect, play a role as a significant N-sink in the marine N-cycle by regulating the fixed-N flow at the land-sea boundary. Although continental shelf sediments cover only 7.5 % of the global marine seafloor, they contribute > 60 % of benthic N-loss. The majority of the seafloor on continental shelves worldwide is covered by permeable sediments. Advection, instead of diffusion, is the predominant mass transport in these permeable sediments. The particle and solute exchanges between water column and sediments under advective conditions exceed those under diffusive conditions by several orders of magnitude. Advective pore water flows allow oxygen penetration to greater depths, expanding the biogeochemical oxic zone in permeable sediments. However, so far little is known about N-loss in these sediments, and the impacts of advection on N- loss and N-cycling processes in general. The aim of this thesis is to investigate the extent and mechanisms of N-loss in the Wadden Sea permeable sediments under simulated *in situ* advective conditions. Spatial and temporal N-loss rates were determined in order to assess the significance of the Wadden Sea permeable sediments, and furthermore these sediments from this worldwide tidal flat system were used as a case study to elucidate the role of permeable sediments in the global marine N-loss. Potential links between N-loss and other N-cycling processes such as nitrification are further explored, especially under the influence of fluctuating oxic-anoxic conditions.

Using a modified core ^{15}N-incubation method with one-pulse perfusion to simulate advections, and with simultaneous multiple-sensor measurements, active N-loss via denitrification was found to occur under oxic conditions. Such occurrence was further corroborated by slurry incubations with ^{15}N-labelled substrates by O_2 microsensor measurement and on-line measurement using membrane inlet mass spectrometry (MIMS). In the overlapped zone of O_2 and NO_x^- (nitrate and/or nitrite), instantaneous N_2 production was observed under aerobic conditions, while NO_x^- was co-respired with O_2. These combined results show that permeable Wadden Sea sediments are characterized by some of the highest denitrification rates (≥190 µmol N m^{-2} h^{-1}) under aerobic conditions

(with oxygen concentrations of up to 90 µM) in the marine environment. This is the first time that the substantial N-loss in permeable sediments has been attributed to aerobic denitrification under oxic-anoxic oscillations driven by advection.

To examine the significance of N-loss in permeable Wadden Sea sediments over an annual cycle, N-loss rates were determined across three seasons. The impacts of advection were also evaluated by comparing three incubation methods: (i) intact core incubations simulating diffusive transport, (ii) intact core incubations simulating advective transport conditions, or (iii) slurry incubations. Nitrogen loss rates under simulated advective conditions exceeded those under diffusive conditions by 1-2 orders of magnitude, and were comparable to rates determined in slurries. Intensive N loss rates (mean 207 ± 30 µmol m^{-2} h^{-1}) were measured in permeable Wadden Sea sediments with little temporal and spatial variation. Furthermore, NO_x^- fluxes over a full annual cycle were empirically simulated by 2-dimensional model with *in situ* monitoring data as input parameters, including temperatures, bottom current velocities and NO_x^- concentrations in water column. Combined with actual rate measurements across seasons and sites, the annual N-loss in permeable Wadden Sea sediments was estimated to be 745 mmol N m^{-2} y^{-1}, which agrees well with previous N budget calculations for the Wadden Sea. These results in the case study of the Wadden Sea verify that permeable sediments, accounting for up to 68 % of the continental shelves, are an important N-sink in the global marine N-cycle.

The expansion of the oxic biogeochemical zone in permeable sediments due to advection may favor aerobic processes such as nitrification. Hence, the occurrence of nitrification and its interaction with N-loss processes in permeable Wadden Sea sediments were evaluated using ^{15}N-isotope paring experiments. Net NO_x^- production was determined under aerobic conditions in these sediments, verifying the active occurrence of nitrification. In addition, the NO_x^- produced by nitrification could be immediately channeled to N-loss to produce N_2. Instead of anammox (at very low rates of <2 µmol N m^{-2} h^{-1}, and <1 % of total N-loss), aerobic denitrification predominated in these permeable sediments. Moreover, the coupled nitrification-denitrification was found to represent up to 17 % to total N-loss, particularly apparent in surficial (permeable) sediments where the influence from advection was the strongest. The rest of total N-loss (83 %) might be attributed to NO_x^- from the overlying water due to advection. In this

study, the contribution of coupled nitrification-denitrification to N-loss may be underestimated as O_2 limitation could have occurred due to the one-pulse percolation method used in incubations. Furthermore, potential gross nitrification rates were estimated by calculating the amount of NO_3^- produced via ammonium oxidation by the consumed O_2 during incubations (according to the O_2/NO_3^- stoichiometry ratio of 138/16), while conservative gross nitrification rates were obtained by summing the directly measured net NO_x^- production rate and the portion coupled to denitrification. Potential gross nitrification rates indicate that nitrification is a significant *in situ* NO_x^- source in these sediments and might play a more important role in coupling with denitrification in the summer with depleted NO_x^- in overlying water compared to in the winter/spring with enriched NO_x^- in water column. The potential gross nitrification is substantially greater than the conservative gross nitrification, implying that other NO_x^--consuming processes such as dissimilatory nitrate reduction to ammonium (DNRA) or assimilation are occurring. This study provides direct and quantitative evidence that nitrification plays a key role in linking N-sources and N-sinks in permeable Wadden Sea sediments.

Kurzfassung

Im marinen Stickstoffkreislauf ist die benthische Produktion von molekularem Stickstoff (N_2) für 50-70% des Verlust an biologisch verfügbarem Stickstoff (N-Verlust) verantwortlich. Der Kontinentalschelf und insbesondere die Küstenregionen, in denen Flusssysteme und Ozeane aufeinandertreffen, spielen wegen ihrer regulatorischen Effekte auf die Stickstoffflüsse an der Land-Meer Grenze als Stickstoffsenken eine wichtige Rolle. Obwohl Schelf-Sedimente nur 7,5% des gesamten marinen Meeresboden bedecken, tragen sie mehr als 60% zum globalen benthischen N-Verlust bei. Weltweit ist der überwiegende Teil des Kontinentalschelfs von permeablen Sedimenten bedeckt. In diesen Sedimenten ist Advektion statt molekulare Diffusion der dominierende Massentransportprozess. So übersteigt der durch Advektion hervorgerufene Austausch von partikulären und gelösten Substanzen zwischen Wassersäule und Sedimenten jenen durch Diffusion hervorgerufenen um mehrere Größenordungen. Advektive Porenwasserflüsse ermöglichen ein Eindringen von Sauerstoff in größere Tiefen des Sediments und erweitern somit vertikal die oxische Zone in den Sedimenten. Es ist wenig über den N-Verlust in diesen Sedimenten und den Einfluss der Advektion auf den Stickstoffverlust und den Stickstoffkreislauf bekannt. Das Ziel dieser Studie ist die Untersuchung des Ausmaßes und der Mechanismen des N-Verlusts in permeablen Sedimenten des Wattermeeres unter simulierter *in situ* Advektion. Die zeitliche und räumliche Variabilität der N-Verlustraten wurden bestimmt, um deren Rolle in den permeablen Wattenmeersedimente abschätzen zu können. Darüberhinaus wurden die Sedimente dieses einzigartigen Wattenmeersystems auf die Bedeutung der permeablen Sedimente für den globalen Stickstoffverlust hin untersucht. Potentielle Verknüpfungen zwischen Stickstoffverlust und anderen Prozessen des Stickstoffkreislaufs, wie z. B. Nitrifikation, wurden insbesondere unter dem Aspekt fluktuierender Sauerstoffkonzentrationen erforscht.

Mittels einer modifizierten ^{15}N-Inkuationsmethode von Sedimentkernen, bei der die Advektion durch eine „one-pulse“ Durchströmung simuliert wurde, sowie mittels gleichzeitiger Mikrosensormessungen verschiedener Parameter, wurde gezeigt das Stickstoffverlust durch Denitrifikation auch unter oxischen Bedingungen stattfindet. Durch Inkubationen von Sedimentsuspensionen mit ^{15}N-markiertem Substraten, in Verbindung mit Sauerstoff-Mikrosensormessungen und Massenspektrometermessungen

wurden diese Erkentnisse bestätigt. In einer Zone, in welcher sowohl Sauerstoff als auch Nitrat bzw. Nitrit (NO_x^-) vorhanden waren, wurde N_2-Produktion unter oxischen Bedingunen gefunden während NO_x^- zusammen mit O_2 veratmet wurde. Kombiniert zeigen diese Ergebnisse, dass in den permeablen Wattenmeersedimente eine der höchsten marinen Denitrifikationsraten (≥190 µmol N m^{-2} h^{-1}) unter aeroben Bedingungen (mit Sauerstoffkonzentrationen bis zu 90 µM) gefunden wurden. Zum ersten Mal wurde gezeigt, dass aerobe Denitrifikation unter advektionsgetriebenen wechselnden Sauerstoffbedingungen verantworlich für den hohen N_2-Verlust in permeablen Sedimenten ist.

Um die saisonale Variabilität des N-Verlusts in permeablen Wattenmeersedimenten zu untersuchen, wurden N-Verlustraten während drei Jahreszeiten bestimmt. Desweiteren wurde der Einfluß der Advektion durch den Vergleich von drei ^{15}N-Inkubationsmethoden untersucht: (i) Inkubation mit ganzen Kernen unter simuliertem diffusiven Transportbedingungen (ii) Inkubationen mit ganzen Kernen unter simulierten advektiven Transportbedingungen und (iii) Inkubationen von Sedimentsuspensionen („slurries“). Die unter advektiven Bedingungen gemessenen N-Verlustraten waren um 1-2 Größenordnungen höher als diejenigen, welche unter diffusiven Transportbedingungen gemessen wurden und waren vergleichbar zu den N-Verlustraten der „slurry“ Inkubationen. Diese hohen N-Verlustraten (durchschnittlich 207 ± 30 µmol m^{-2} h^{-1}) in Wattenmeersedimenten zeigten eine sehr geringe zeitliche und räumlich Variabilität. Die experimentellen Ergebnisse wurden mit einem mathematischen Model verglichen, das den NO_x^- Fluss aus der Wassersäule in das Sediment berechnet. Eingangsgrößen waren Temperatur, Strömungsgeschwindigkeiten und NO_x^--Konzentrationen des Bodenwassers, die im zeitlichen Verlauf von einer *in situ* Messstation aufgezeichnet wurden. In Kombination mit den gemessenen Raten wurde der jährliche N-Verlust in den permeablen Wattenmeersedimenten auf 745 mmol N m^{-2} y^{-1} geschätzt, was in Übereinstimmung mit vorherigen Berechnungen des Stockstoffbudgets für das Wattenmeer ist. Diese Ergebnisse zeigen, dass permeable Sedimente eine bedeutende Stickstoffsenke im globalen marinen Stickstoffkreislauf sein können.

Die, aufgrund von Advektion, vergrößerte oxischen Zone in permeablen Sedimenten fördert auch aerobe Pozesse wie Nitrifikation. Daher wurden in einer

weiteren Studie Nitrifikationraten gemessen und die Verknüpfung von Nitrifikation zu den N-Verlustprozessen mit Hilfe von ^{15}N-Inkubationen untersucht. Die netto-NO_x^--Produktion, die in diesen Sedimenten unter aeroben Bedingungen gefunden wurde deutet auf signifikante Nitrifikationsraten hin. Die produzierten NO_x^--Verbindungen können direkt durch N-Verlustprozesse verbraucht und zu Stickstoffgas umgewandelt werden. Während Anammox als N-Verlustprozess eine geringe Bedeutung hat (<2 µmol N m^{-2} h^{-1}, und <1 % des gesamten N-Verlusts), ist in den permeablen Sedimenten die aerobe Denitrifikation der dominierende Prozess. Weiterhin wurde festgestellt, dass gekoppelte Nitrifikation-Denitifikation für bis zu 17% des gesamten N-Verlusts verantworlich ist, besonders in den Oberflächensedimenten, wo die Advektion am ausgeprägtesten ist. Der übrige Teil des N-Verlusts (83%) wird gespeist von NO_x^- aus der Wassersäule, eingetragen durch Advektion. Es besteht die Möglichkeit, dass der Beitrag von gekoppelter Nitrifikation-Denitifikation zum N-Verlust sogar unterschätzt wurde, da die auf den O_2 Verbrauch gestützte Berechnung der NO_x^- Produktion (basierend auf dem O_2/NO_3^- Stöchometrieverhältnis von 138/16) wesentlich höher waren. Die hohen Nitifikationsraten zeigen, dass Nitrifikation eine wichtige NO_x^--Quelle in diesen Sedimenten darstellt und gekoppelt mit Denitrifikation besonders dann eine herausragende Bedeutung hat, wenn niedrige NO_x^--Konzentrationen in der Wassersäule zu finden sind (z.B. im Sommer). Die über den O_2 Verbrauch brechnete Nitrifikation ist wesentlich höher als die experimentell gemessene Kopplung von Nitrifikation-Denitifikation. Es ist deshalb gut möglich, dass weitere NO_x^--Verbrauchende Prozesse, wie z. B. dissimilatorische Nitratreduktion zu Ammonium (DNRA) oder Assimilation stattfinden. Diese Studie liefert direkten und quantitativen Beweis, dass Nitrifikation eine Schlüsselrolle in der Kopplung von Stickstoffquellen und –senken in permablen Wattenmeersedimenten spielt.

Introduction

1 Nitrogen in the marine environment

In the Ocean, primary production is sustained by the supply of essential nutrients, including inorganic carbon (C), nitrogen (N) and phosphorous (P). Of these elements, a relatively consistent atomic ratio of 106:16:1 has been found in the phytoplanktonic biomass as well as in the release from the phytoplankton-driven organic matter remineralization and resultant sea water composition (Redfield et al., 1963). This distribution of C:N:P, also known as the 'Redfield ratio', is often used as a criterion to differentiate between N-limitation and P-limitation in aquatic systems (Falkowski 1997; Tyrrell 1999). However, instead of the value 16:1, a lower N:P ratio ($[NO_3^-] : [PO_4^{3-}] \leq$ 15:1) has been often found in surface seawater (Tyrrell 1999). Therefore, nitrogen is considered as the most limiting nutrient in surface waters of large parts of the Ocean (Ryther and Dunstan 1971). Hence, the dynamics of the N-cycle controls phytoplankton productivity (Falkowski 1997; Tyrrell 1999; Canfield et al. 2005; Elser et al. 2007), and links N-cycling to biological CO_2-sequestration in the Ocean (Falkowski 1997; Altabet et al. 2002; Gruber 2004).

1.1 Nitrogen cycling processes

Nitrogen in the environment is present in multiple forms, which can be divided into two categories: reactive (fixed) N and non-reactive (non-fixed) (Galloway et al. 2003). The reactive forms of nitrogen include inorganic nitrogen, such as ammonium, nitrite and nitrate. Their combined concentrations in the surface ocean are usually scarce due to biological production, with regard to much higher concentrations in the deep sea. Dinitrogen ($N \equiv N$) is the most common non-reactive form—a stable molecule with triple bonds that require high-energy conversion to ammonia to become bioavailable. This so-called "N_2-fixation" is the major input of fixed N into the oceans. Once ammonia is incorporated by microbes into organic N, it is transformed into other different reactive N forms, such as nitrite and nitrate, or remineralized back to ammonium (Remineralization). These reactive N forms are assimilated by microbes to form their biomass (Assimilation) or are involved in other transformations. Under aerobic or suboxic conditions, ammonium is oxidized to nitrate via nitrite (Nitrification), while

nitrate and nitrite are reduced through a series of intermediate gaseous nitrogen oxide products and ultimately turned into dinitrogen (Denitrification). These major redox transformations in the marine N-cycle are strictly mediated by microbes, and have been well studied for decades (Figure 1). However, recent studies of the marine nitrogen balance indicate that N_2-fixation could be largely underestimated. In the meantime, novel N-loss pathways and additional coupling processes have been discovered (Brandes et al. 2007). All these have led to a revision of our understanding of the nitrogen cycle, and of nitrogen balance in the present day Ocean (Figure 1).

1.1.1 N_2 fixation

N_2-fixation is a process in which the non-reactive N_2 gas is converted into bioavailable ammonia by either high-temperature abiotic reactions (lighting or Haber-Bosch) or biologically via specialized N_2-fixing microbes. In the oceans, only the latter has been observed. N_2 fixation produces ammonia, which is assimilated by organisms and incorporated into their biomass. Organic forms of N may include particulate organic N (PON) and dissolved organic N (DON), which together constitute complex mixture of compounds with a wide range of compositions and thus lability (Figure 1).

For years, it was believed that the non-heterocystous cyanobacterium *Trichodesmium* was the main N_2-fixer in the open ocean. However, recent studies have revealed diverse bacterial N_2-fixing communities in the Atlantic and Pacific Oceans, and suggested that the capability for nitrogen fixation is mere widespread throughout the water column (Capone 2001; Zehr et al. 1998; 2000). The prevalence of unicellular N_2-fixers, in particular, suggest that biological N_2 fixation may contribute twice as much to oceanic N_2-fixation compared to previous estimates (Montoya et al. 2004), and that the abundance of filamentous and bloom forming N_2-fixing *Trichodesmium* spp. may have been underestimated (Davis and McGillicuddy 2006). In addition, it has been suggested that significant N_2 fixation may occur in close proximity to zones of active N-loss in the water column (Deutsch et al. 2007) and recent results also indicate the occurrence of N_2 fixation in deep-sea hydrothermal vents (Mehta et al. 2003; Mehta and Baross 2006). Therefore, the current estimates for N_2 fixation as an oceanic N-input remain conservative, and are expected to be greater in reality.

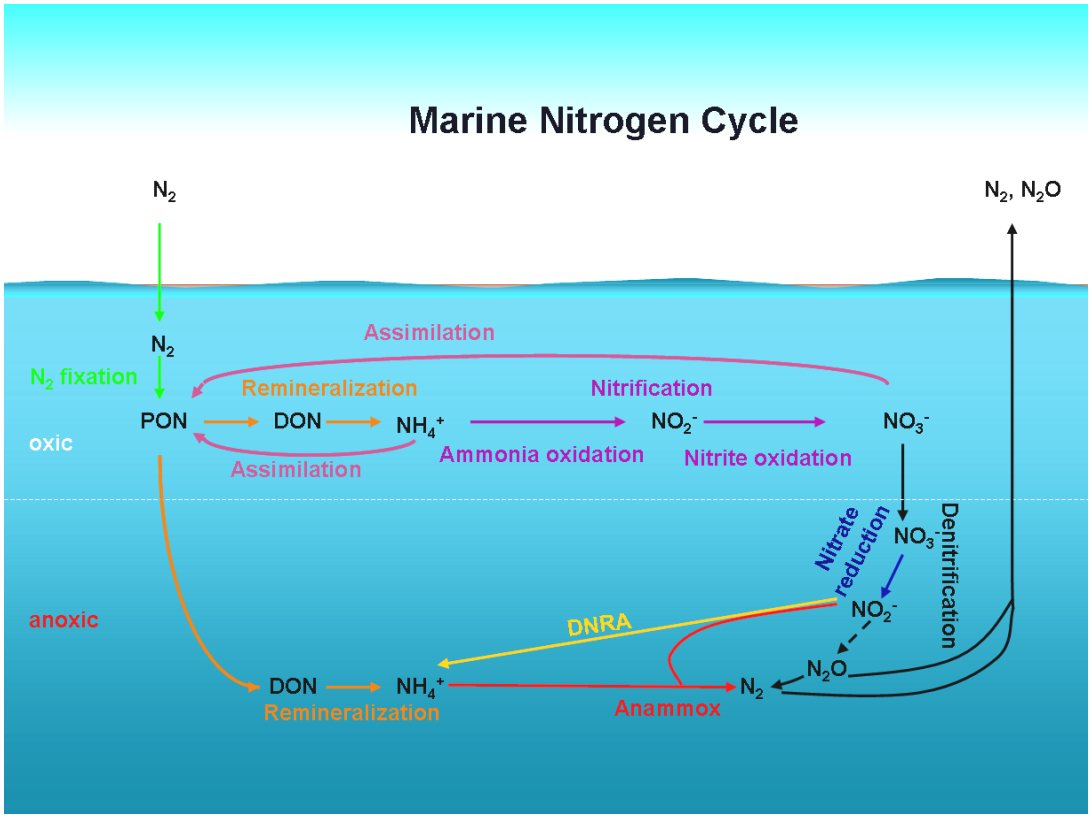

Figure 1: Currently understood nitrogen cycle in the marine environment. The arrows mark the transformation processes among all N forms. Marine N_2-fixation is the biological conversion of N_2 into ammonia, which is incorporated into organic N forms. Organic N, such as particulate organic N (PON) and dissolved organic N (DON), is transformed biologically to release ammonium via remineralization. Ammonium, the most reduced natural form of N, is either biologically assimilated or oxidized to nitrate via nitrite under oxic/suboxic conditions through nitrification. Nitrate, the most oxidized form of N and the most abundant biologically utilizable form, is biologically assimilated or is reduced through a series of intermediate gaseous nitrogen oxide products (e.g. NO, N_2O) and is ultimately turned into N_2 gas via denitrification. N loss is also achieved by the N_2 production via anaerobic ammonium oxidation with nitrate (anammox). In addition, nitrate/nitrite can also be directly reduced to ammonium via dissimilatory nitrate reduction to ammonium (DNRA).

1.1.2 Nitrification

Ammonium (NH_4^+) is generally formed from the decomposition of organic matter or via dissimilatory nitrate reduction to ammnonium (DNRA). Nitrification is a two/step process, in which NH_4^+ is oxidized via NO_2^- to NO_3^- by two distinct groups of primarily lithoautotrophic microorganisms. That is, the energy in the oxidative processes is harvested for the formation of organic carbon from CO_2. The final product, NO_3^-, may then serve as a source for assimilation by organisms, or as a terminal electron acceptor in the denitrification or anammox pathway to produce N_2, or be reduced via DNRA (Joye

and Anderson 2008; Thamdrup and Dalsgaard 2008). Nitrification thereby links the mineralization of organic N to the potential N-loss through denitrification and anammox (Seitzinger, 1990; Sloth et al., 1992; Kuypers et al. 2005; Lam et al. 2007), and connects oxidative and reducing pathways in the N cycle (Joye et al., 1995; Zehr and Ward 2002).

1.1.3 Denitrification

Before the 1990's, marine N-loss was mainly attributed to heterotrophic denitrification, in which nitrate is ultimately turned into N_2 gas through a series of intermediate gaseous nitrogen oxide products (e.g. NO, N_2O) and lost to the atmosphere. 'Heterothrophic' denitrification has been considered the major remineralization process in suboxic settings, i.e. organic matter is respired via NO_3^- after O_2 is depleted. Although denitrification is usually considered as an anaerobic process, an aerobic denitrifier, *Thiosphaera pantotropha*, has been firstly isolated from wastewater (Robertson and Kuenen, 1983). The potential significance of aerobic denitrification in the natural environments, however, is not yet clear. Apart from its use in the respiration of organic matter, denitrification can also occur autotrophically, when NO_2^- is used as electron acceptor for the oxidation of e.g. sulphide, while producing N_2. It has recently been reported to be important in certain marine anoxic water columns (Hannig et al. 2007; Lavik et al. 2009; Jensen et al. 2009).

Coupled nitrification-denitrification is a term that describes the process via which ammonium in the oxic/suboxic zone is oxidized to nitrate, and almost immediately denitrified to N_2. This coupling relationship is very important in the marine environments, especially sediments. This coupling may explain how the N_2 flux from the sediments can be much greater than that supported by diffusive NO_3^- supply alone (e.g., in muddy sediments; Devol 1991).

1.1.4 Anammox

'Anammox' stands for the "anaerobic ammonium oxidation with nitrite". It was first discovered in a fluidized bed reactor (Mudler et al. 1995), although its occurrence had been hypothesized for suboxic water column back in the 1960's (Richard, 1965). Anammox activities in the marine environment was first reported four decades later in the sediments of the Skagerrak using a modified isotope paring technique (IPT) that can

distinguish N_2 produce from anammox and denitrification (Thamdrup and Dalsgaard 2002). Anammox activities were later reported also in the marine suboxic water columns of Golfo Dulce (Dalsgaard et al. 2003) and the Black Sea (Kuypers et al. 2003). It was, however, in the latter study that marine anammox bacteria were first identified in a marine natural setting. From subsequent studies, it is clear that anammox is a quantitatively important N-sink in the marine systems (Dalsgaard et al. 2003; Engstroem et al. 2005; Kuypers et al. 2006). Anammox predominates as the N-loss pathway in oxygen minimum zones (OMZ) of Namibia, Eastern Tropical South Pacific (ETSP) and the Arabian Sea (Dalsgaard et al. 2003). Anammox has also been found in many investigated marine sediments with varied contributions ranging from <1% to 80 % of total N_2 production. It is considered of little importance in shallow estuarine and coastal sediments due to the high carbon remineralization rates therein (Engstroem et al. 2005; Thamdrup and Dalsgaard 2008). It has been proposed that in general, the relative contribution to N_2 production via anammox is negatively correlated with the availability of organic substrates (Dalsgaard et al. 2005; Kuypers et al. 2006). N_2 production via anammox, in the OMZ water columns and benthic environments combined, may account for 25-50 % of overall marine N_2 production (Dalsgaard et al. 2003; Devol 2003; Hulth et al. 2005). Hence, the discovery of anammox has substantially changed our perception of the marine N cycle in the last decade.

1.1.5 Dissimilatory nitrate reduction to ammonium (DNRA)

In recent years, dissimilatory nitrate reduction to ammonium (DNRA) has been recognized as an environmentally relevant reaction in marine systems, especially in anoxic sediments in the presence of substantial free sulfide (Boon et al. 1986; An et al. 2002; Gardner et al. 2006). DNRA bypasses N_2 production as an N-sink by producing ammonium instead, from the reduction of nitrate/nitrite mediated by organisms that can be either autotrophic or heterotrophic (Fossing et al. 1995; Thamdrup et al. 1996; Jorgensen et al. 1999). This process may enhance ammonium fluxes to the oxic/anoxic interface. When coupled with nitrification, it may serve as a ‘short circuit’ in the N cycle to preserve fixed N that can support higher production (An et al. 2002; Gardner et al. 2006). Alternatively, it may lead to N_2 production via anammox (Kartal et al. 2007; Lam et al. 2009).

1.2 The oceanic nitrogen budget

1.2.1 Nitrogen budget in pre-industrial era

In the pre-industrial era, in the absence of significant anthropogenic inputs, the N source in the marine environment was mainly due to pelagic N_2 fixation, and the N cycle was considered to be in a relatively steady state (Eppley and Peterson 1979). The marine nitrogen budget is mainly driven by six terms (Brandes et al. 2007): N_2 fixation (including benthic and pelagic N_2 fixation), riverine inputs and atmospheric deposition as N sources, whereas sediment organic burial, and water column and benthic N_2 production (including denitrification and anammox) are the N sinks (Fig 2). In the preindustrial era, marine N_2 fixation as the major N-source term is conservatively estimated to be 125 Tg N yr^{-1}. Other substantial N-sources were. riverine input (41 Tg N yr^{-1}) and atmospheric deposition (15-20 Tg N yr^{-1}) (Gruber and Sarmiento 1997; Duce et al. 2008). Among these, the total anthropogenic reactive N-input was small, only around one tenth of N_2 fixation in the ocean ecosystem (Galloway et al. 2003). Hence, the marine N-source was essentially influenced by natural N-input rather than anthropogenic N. Water column and benthic N_2 production were more important sinks than sediment burials, although there is a wide variation in estimates for each N-loss term (Gruber and Sarmiento 1997).

1.2.2 Nitrogen budget in Anthropocene

Due to the massive impact of human activities on the environment, the last ~150 years, have been termed the Anthropocene (Falkowski et al. 2000; Crutzen and Rammanathan 2000). Reactive N due to human activities in the early 1990's increased by an order of magnitude relative to 1860 levels with the increased utilization of agricultural fertilizers for food production, other industrial production activities and fossil fuel combustion (Galloway et al. 2004). These human activities affect N-inputs through the input pathways of riverine and ground water and atmospheric deposition, respectively. The marine N budget has been substantially altered during the Anthropocene (Figure 2) (Vitousek et al. 1997; Codispoti et al. 2001; 2003; Galloway et al. 2003). Although N_2 fixation remains the most important N source for the present

ocean with an estimated N input of 125 Tg N yr^{-1} (Gruber et al 2004; Codispoti 2007), the input of atmospheric fixed N to the ocean has increased four-fold to 67-84 Tg N yr^{-1} since 1860, and over two-thirds of which is attributed to human activities (Duce et al. 2008; Schlesinger 2009). Riverine and groundwater input has also doubled to 80 Tg N yr^{-1} due to human activities (Codispoti et al. 2001; Codispoti 2007).

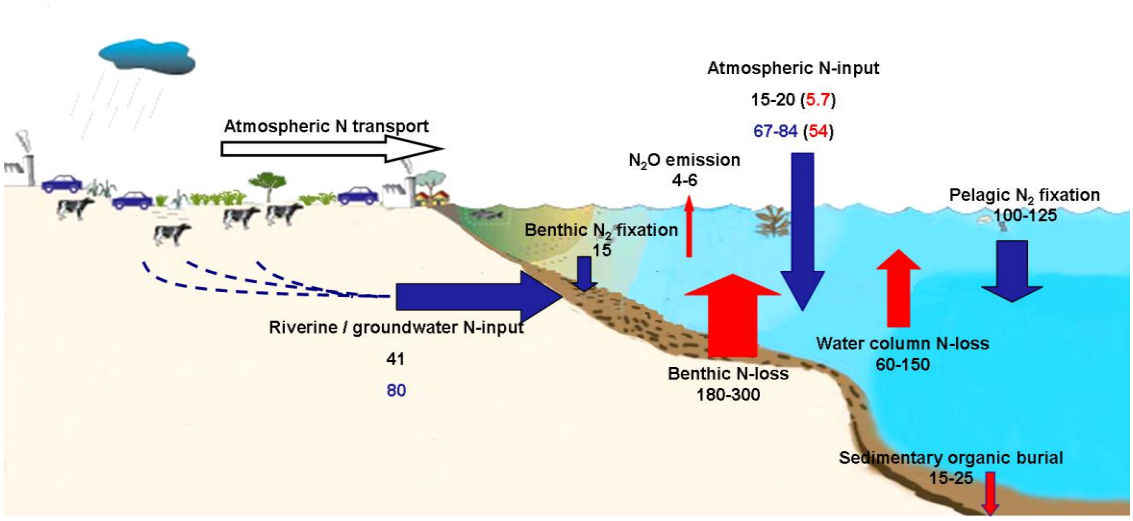

Figure 2: Marine nitrogen budget in the preindustrial era and Anthropocene. The estimated values of N-input and output are in the unit of Tg N yr^{-1}, referred to Gruber and Sarmieto (1997), Gruber (2004), Galloway et al. (2004), Codispoti et al. (2001;2007), Duce (2008) and Schlesinger (2009). Black numbers are estimates in the preindustrial era, blue numbers are estimates in anthropocene, and red numbers are the contribution by human activities. Blue arrows present the nitrogen sources (inputs) and red arrows present the nitrogen sinks (outputs).

These increases in N-inputs result in various environmental problems. The increased riverine and groundwater inputs of reactive N result in higher frequencies and intensity of eutrophication. This further leads to harmful algal blooms, hypoxia and even the episodic accumulation of sulfidic bottom waters in coastal regions (Rabalais 2002; Lavik et al. 2009) as well as the expanded oxygen minimum zone (OMZ) (Breitburg et al. 2009). These changes in the marine environments might influence the N-cycle in the present and future Ocean.

The increasing inputs of anthropogenic fixed-N have influenced the N-removal in the marine environments. The N-removal rates in the rivers and coastal regions were found to have increased with the increasing riverine anthropogenic N inputs. However, the overall efficiency of N removal seemed to have decreased instead (Seitzinger 2008;

Mulholland et al. 2008). Moreover, with the increase of incomplete denitrification, the emission of intermediate gaseous product—N_2O, an ozone-depleting greenhouse gas, increase correspondingly up to 4-6 Tg N yr^{-1} from the ocean (Duce et al. 2008; Schlesinger 2009).

The oceanic N cycle has long been assumed to be in a steady state (Eppley and Peterson 1979). N* has been used to assess the marine nitrogen balance, which is defined as the derivation from the linear relationship between nitrate (N) and phosphate (P) of the form $N^* = N - r_{nitr}^{N:P} P + 2.9 \mu molkg^{-1}$, where $r_{nitr}^{N:P}$ is the constant N:P stoichiometric ratio during the organic matter remineralization and where 2.9 μmol kg^{-1} is a constant to bring the global mean value to zero (Gruber and Sarmieto 1997). Based on the estimate mainly due to N* in the water column, N sources and sinks were considered to be in balance (Gruber and Sarmieto 1997, 2002; Gruber 2004). However, extrapolations from direct rate measurements showed that total N-loss might be as much as 200 Tg N yr^{-1} greater than total N-gain, such that the oceanic fixed N budget might be unbalanced (Codispoti et al. 2001; Codispoti 2007). This discrepancy might be due to an underestimation of N_2-fixation as direct rate determinations of N fixation are constrained to certain groups of autotrophs in the photic zone, while it is now becoming apparent that more diverse organisms are involved in this process. Alternatively, we might be in a transition state from imbalance to balance, or both (Codispoti 2007). Nowadays, the global N-cycle is substantially affected by intensive human activities. The N-balance in the present ocean remains questionable, requiring the further understanding of marine N-losses and gains.

2 N-loss from marine continental shelf sediments

2.1 Sediments as major nitrogen sinks

In the oceanic nitrogen cycle, benthic N_2 production is considered to be the main N-sink. Although the rate estimates from oceanic benthic N_2 production vary in a wide range from 180 to 500 Tg N yr^{-1} (Middelburg et al. 1996; Brandes and Devol 2002; Gruber et al. 2004; Codispoti 2007), all recent studies indicate that it is the major marine N sink, accounting for up to 70% of total marine N-loss (Codispoti et al. 2001; Codispoti 2007; Galloway et al. 2004). Benthic N-loss can be divided into those that occur in the

deep sea and in coastal sediments. Although shelf sediments (0-200 m) make up only 7.5 % of marine sediments globally, N-loss from shelf sediments account for as much as 170-300 Tg N yr^{-1} (Devol and Christensen 1993; Devol 1997; Laursen and Seitzinger 2002), equivalent to > 60 % of the oceanic benthic N loss according to the N budget proposed by Codispoti (2007). As a result, the sediments, especially shelf sediments, play a significant role in global marine N budget.

2.2 The coastal zone

The coastal region, as a transition zone between land and ocean, plays an important role in the marine N cycle by regulating anthropogenic N inputs to the open ocean (Figure 2). The flux of nitrogen from land and atmosphere to the estuaries and the coastal ocean has increased substantially in recent decades due to industrial activities (Galloway et al. 2002; Howarth et al. 2006). For instance, the riverine N input to the coastal region has nearly doubled to 80 Tg N yr^{-1} since industrialization (Gruber and Sarmiento 1997; Gruber 2004; Seitzinger et al. 2005; Boyer et al. 2006). Although the N-removal in streams and rivers increases correspondingly, the efficiency of N removal in streams and rivers has been found to decrease instead (Seitzinger 2008; Mulholland et al. 2008). So far, there is a consensus that the riverine N fluxes will continue to increase in the future (Howarth et al. 2002; Seitzinger et al. 2002; Galloway et al. 2004; Green et al. 2004; Mulholland et al. 2008). As most riverine nitrogen input is removed by N-loss processes in estuarine and continental shelf sediments before ever reaching the coastal ocean (Codispoti 2007), it is crucial to have a clear understanding of the N-loss mechanisms in coastal regions and thus how they might respond to the increased nitrogen load.

2.3 Role of the permeable sediments in nitrogen loss

Continent shelves are dominated by coarse-grained sediments, which account for 50-68 % of continental margin (Emery 1968; Johnson and Baldwin 1986), yet the role of sandy permeable sediments in N-loss has been largely ignored. Because coarse-grain sediments contain little organic matter, most previous N-loss studies have been focused on the more organic-rich muddy or fine-grained shelf sediments under diffusive conditions.

Sandy permeable sediments differ from muddy sediments, in that material transports within are dominated by advection instead of diffusion (Huettel and Gust 1992; Huettel 1996). Advection leads to high fluxes of organic matter and electron acceptors from the water column into the seafloor, and oscillating oxic-anoxic conditions that allow marine sands to efficiently filter nutrients and thus facilitate N-removal (Precht et al. 2004; Werner et al. 2006). Previous studies on N_2 production in permeable sediments employed the methods based on diffusion, and the impact of advection on N loss was largely neglected (Lohes et al. 1996; Eyre and Ferguson 2002; Vance-Harris and Ingall 2005). However, recent laboratory studies using ^{15}N-labeling experiments showed that denitrification rates in sandy sediments under simulated advective conditions were substantially enhanced relative to those measured under diffusive conditions (Cook et al. 2006; Rao et al. 2007; 2008). Although these studies suggest that N loss in permeable sediments with advective pore water flow is much higher than previously perceived, there have been no reported, systematic investigations of N-loss with respect to its pathways (e.g. denitrification and anammox) and spatio-temporal *in situ* rate distribution. The role of permeable sediments in marine N-removal remains poorly characterized.

3 Nitrogen loss from the Wadden Sea

3.1 The Wadden Sea

The Wadden Sea is one of the largest tidal flat systems in the world, covering 500 km of coastline and encompassing a total area of 14,700 km^2. It is located in the southeastern part of the North Sea, stretching from Den Helder in the Netherlands in the southwest, along the northwestern German coast, to its northern boundary at Skallingen north of Esbjerg in Denmark (van Beusekom et al. 2001). A number of major European rivers, including the Rhine/Meuse, Ems, Weser and Elbe, flow into the Wadden Sea. The catchment areas of these rivers are a combined 231,000 km^2 and include areas that are highly impacted by industries and agriculture, and are densely populated (>100 million inhabitants) (van Beusekom et al. 2001).

The Wadden Sea is strongly influenced by hydrological dynamics driven by wind and tides. In particular, tidal flats are intensively impacted by western winds and semi-diurnal tides such that they are covered by approximately 1.5-2.5 m of water for 4-6

hours during high tides and become exposed for 6-8 hours during low tides. The whole ecosystem provides a multitude of transitional zones between land, sea and freshwater. Water runoff from land and water masses from the sea are repeatedly mixed and flushed with the tides before being taken up by the long shore current to eventually be released to the Atlantic Ocean.

Instead of natural rock formations, sediments prevail in the Wadden Sea. The seafloor of the Wadden Sea is dominated by permeable sandy sediments, which is of fluvial and glacial origin, redistributed by strong currents and waves. The fine-grained sediments, thought to be primarily derived from recent riverine sources, were often found fringing the mainland shore and sometimes presenting along the tidal divides. In general, sandy tidal flats comprise of 75 %, mixed flats 18 % and mud flats 7 % of the back-barrier intertidal area. Almost all subtidal and offshore sediments are sandy (Common Wadden Sea Secretariat 2008).

3.2 Permeable sediments as a bio-filter

The characteristics described above allow the Wadden Sea to function as a gigantic coastal filter system, facilitated by the permeable sediments therein. Pore-water advection is driven mainly by pressure gradients from wave actions and bottom currents interacting with surface topography of ripples (Ziebis et al. 1996; Precht and Huettel 2004b; Franke et al. 2006). Advection causes solute exchange at rates orders of magnitude higher than would be the case due to molecular diffusion alone, and this allows direct transfer of suspended particles into permeable sediment strata (Precht and Huettel 2004a). High primary productivity has been measured recently in these sandy sediments (Billerbeck et al. 2007). Primary productivity by microphytobenthos is recognized as the main source of organic carbon for benthic life in light-exposed coastal sediments (MacIntyre et al. 1996; Underwood and Kromkamp, 1999). Moreover, the significant and rapid carbon fluxes from microphytobenthos to other benthic microorganisms have been demonstrated by recent studies (Middelburg et al. 2000; Cook et al. 2007). The microphytobenthos, often dominated by benthic diatoms, and bacteria, are thus typically closely associated in biofilms on the sand grains (Huettel et al. 2003). High extracellular enzyme activities and bacterial carbon production rates have been reported in the subtidal sandy sediments in the Wadden Sea, suggesting that biological

activities are supported by the rapid flux of carbohydrates from microphytobenthic primary production (Böer et al. 2008).

Photosynthetic production drives high mineralization rates, in the forms of settling phytodetritus and via photosynthetic products excreted by the microphytobenthos (Goto et al. 2001; Rusch et al. 2003). Accordingly, high mineralization rates of organic matter and high oxygen consumption rates have recently been found comparable to or even higher than rates in fine-grained, organic rich sediments (de Beer et al. 2005; Werner et al. 2006; Rusch et al. 2006). Recent studies indicate that this accelerated organic matter mineralization is caused by advective transport (Huettel and Rusch 2000; Ehrenhauss et al. 2004a; de Beer et al. 2005; Werner et al. 2006) and a stimulation of biogeochemical cycling is proportional to the extent of pore-water exchange as well (Ehrenhauss et al. 2004b; de Beer et al. 2005).

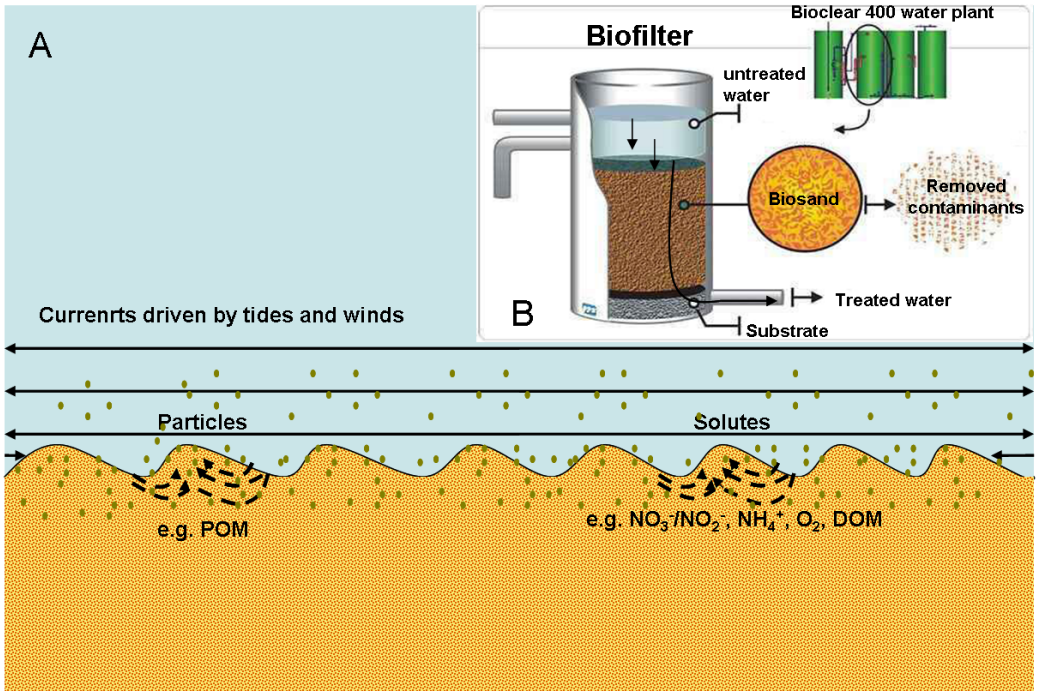

Figure 3: Sand sediments as a bio-filter for maintaining the particles and solutes by filtration. (A) The advective transport of particles and inorganic nitrogen fractions in permeable sandy sediments. (B) Analogous example of a sand Bio-filter at a wastewater treatment plant (Source: http://www.watertiger.net/mainstream/mainstream.htm).

Inward and outward advective flows of pore-water associated with migrating sandy sediment ripples generates vertical oscillations in oxic and anoxic conditions as redox

zones move horizontally through the surface layer of the seabed. The dynamic redox conditions found in permeable marine sediments resemble those found in wastewater treatment plants (Gray 1990) (Figure 3). Recent studies of permeable sediments showed that the oxic-anoxic oscillation driven by the advective pore water flow corresponded with deep O_2 penetration, down to 5 cm sediment depth (Franke et al. 2006; Werner et al. 2006; Jansen et al. 2009). This results in an expansion of the oxic biogeochemical zone (BGZ) compared to the diffusive system (Figure 4). Consequently, permeable marine sediments of the Wadden Sea are also very active sites of nutrient cycling (Werner et al. 2006; Billerbeck et al. 2006a; 2006b). NO_x^-, as an indicator of the redox state of the habitat, has been shown to be present in the zone of 0-5 cm depth due to the flushing with bottom water at *Hausstarnd* in the Wadden Sea sand flat (Böer et al. 2009).

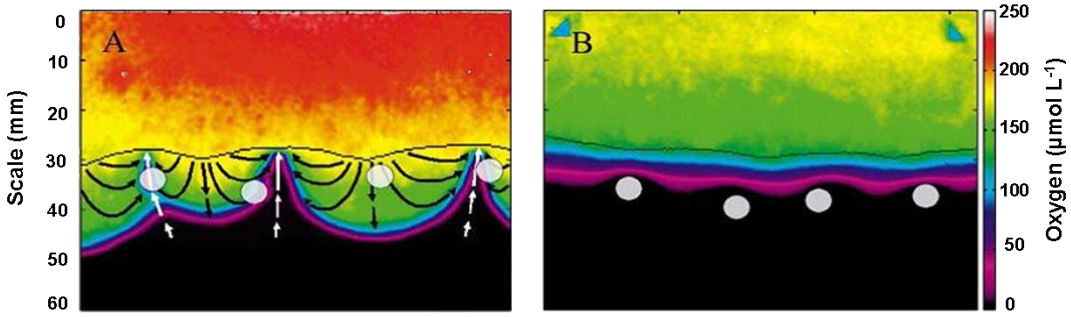

Figure 4: Oxygen penetration under scenarios of advective pore water flow (A) and diffusive pore water flow (B). Circles show the positions of *U. lactuca* discs, black horizontal lines the sediment surface, and the arrows indicate the approximate streamlines of the porewater flow estimated according to Shum and Sundby (1996). Source: Franke et al. 2006.

3.3 The N-budget of the Wadden Sea

The total estimated annual N input to the Wadden Sea approaches 0.74 to 0.82 Tg N y^{-1} as a combination of different source categories, e.g. hinterland drainages, riverine inputs, inputs from the North Sea and atmosphere (van Beusekom et al. 2001). Among the N-sources, the riverine input accounts for 83 %. The nitrogen input to the Wadden Sea is at present dominated by dissolved inorganic fractions (NO_3^-, NO_2^- and NH_4^+), with nitrate and ammonium accounting for the majority of the dissolved inorganic N in sea water (van Beusekom et al. 2001). A clear annual cycle in dissolved inorganic N

concentrations was observed, with low values in summer and autumn, and high values in winter and spring (van Beusekom et al. 2001).

Denitrification is considered a major N sink in the Wadden Sea (van Beusekom and de Jonge 1998; Philippart et al. 2000). However, only a few direct measurements have been conducted, including studies, in the western Dutch Wadden Sea using the acetylene inhibition method (AIM) (Kieskamp et al. 1991) and in the Sylt Rømø Basin with the isotope pairing method (Jensen et al. 1996). Reported denitrification rates were up to 55 mmol m^{-2} h^{-1}. However, these rates were measured using a method that assumed diffusive conditions as occurred in muddy sediments, despite the fact that the Wadden Sea is dominated by permeable sediments where mass transfer is predominantly driven by advection. As such, the role of permeable sediments in the N-loss from the Wadden Sea has largely been ignored. Moreover, the exact dissimilatory pathways responsible for N-loss, e.g. denitrification, anammox and nitrification coupled to denitrification, have not been investigated in these permeable sediments under near *in situ* advective conditions.

Objectives of this thesis

The aim of this thesis is therefore to evaluate the impact of advection on N loss rates from the Wadden Sea permeable sediments, and their response to the deeply-penetrating oxygen. To simulate advection, a modified method based on intact core incubation amended with ^{15}N-labelled substrates was used to determine N-loss rates and the responsible pathways. This method involved one-pulse percolation of sediment porewater with aerated seawater containing ^{15}N-amendments down to 5 cm-depth (the zone generally influenced by advection). In parallel, the response of N-loss processes to the concurrence of O_2 and NO_x^- at advective depths was investigated using multiple methods, such as multiple microsensor measurements in intact sediment cores, simultaneous determinations of O_2 concentrations and N_2 productions in sediment slurries, and in a simulated aerated flow-through slurry system with online measurement by membrane inlet mass spectrometry (MIMS).

Furthermore, another aim of this study was to estimate the annual *in situ* N-loss from permeable Wadden Sea sediments with spatial and temporal consideration. An experimental approach (modified intact core incubation with one-pulse percolation) was used to measure the spatial variation of N-loss rates under simulated in situ advective

conditions at different Wadden Sea sand flats. The experimental approaches of intact core and slurry incubations were applied to investigate the difference of N loss under diffusive and near *in situ* advective conditions, and to study their seasonal variations. To further confirm the reliability of the experimental results on N loss, a model simulation of NO_x^- availability was developed based on a two-dimensional model considering the annual *in situ* monitoring parameters of *in situ* sediment topography, temperature, bottom current velocities and NO_x^- concentrations in the overlying sea water. The empirical model results were expected to provide the insight on the potential NO_x^- source due to *in situ* advection for the annual substantial N loss measured in the experiments. Therefore, the role of permeable sediments in global marine N-loss could be evaluated with the experimental investigation combined with the model simulation.

Apart from the NO_x^- influx driven by advection into permeable sediments, nitrification is an *in situ* NO_x^- source for the dissimilatory N processes in the sediments. However, few studies to date have been performed in permeable sediments to investigate coupled nitrification-denitrification by direct rate determinations, and the role of nitrification in N-cycling in these sediments. Oxic-anoxic fluctuations due to advective porewater flows may favor aerobic nitrification and further coupling to denitrification in these sediments. Therefore, another goal of this work is to quantify nitrification and coupled nitrification-denitrification based on direct rate determinations under aerobic conditions. The role of nitrification in permeable sediments and its influence on N-loss and overall nitrogen cycling in these sediments are further evaluated.

References

Altabet, M. A., M. J. Higginson, and D. W. Murray. 2002. The effect of millennial-scale changes in Arabian Sea denitrification on atmospheric CO_2. Nature **415:** 159-162

An, S., and W. S. Gardner. 2002. Dissimilatory nitrate reduction to ammonium (DNRA) as a nitrogen link, versus denitrification as a sink in a shallow estuary (Laguna Madre/ Baffin Bay, Texas). Mar. Ecol. Prog. Ser. **237:**41–50

Billerbeck, M., U. Werner, K. Bosselmann, E. Walpersdorf, and M. Huettel. 2006a. Nutrient release from an exposed intertidal sand flat. Mar. Ecol-Prog. Ser. **316:** 35-51

Billerbeck, M., U. Werner, L. Polerecky, E. Walpersdorf, D. de Beer, and M. Huettel. 2006b. Surficial and deep pore water circulation governs spatial and temporal scales of nutrient recycling in intertidal sand flat sediment. Mar. Ecol-Prog. Ser. **326:** 61-76

Boon, P. I., D. J. W. Moriarty, and G. Saffigna. 1986. Nitrate metabolism in sediments from seagrass (Zostera capncorni) beds of Moreton bay, Australia. Mar Biol. **91:**269-275

Boyer, E. W., R. W. Howarth, J. N. Galloway, F. J. Dentener, P. A. Green, and C. J. Vörösmarty. 2006. Riverine nitrogen export from the continents to the coasts. Global Biogeochem. Cycles **20:** GB1S91

Böer, S. I., S. I. C. Hedtkamp, J. E. E. van Beusekom, J. A. Fuhrman, A. Boetius, and A. Ramette. 2009a. Time- and sediment depth-related variations in bacterial diversity and community structure in subtidal sands. The ISME Journal **3:**780-791

Böer, S. I., C. Arnosti, J. E. E. van Beusekom, and A. Boetius. 2009. Temporal variations in microbial activities and carbon turnover in subtidal sandy sediments. Biogeosciences **6:** 1149–1165

Brandes, J. A., and A. H. Devol. 2002. A global marine-fixed nitrogen isotopic budget: Implications for Holocene nitrogen cycling. Global Biogeochem. Cycles **16:** 1120

Brandes, J. A., A. H. Devol, and C. Deutsch. 2007. New developments in the marine nitrogen cycle. Chem. Rev. **107:** 577-589

Breitburg, D. L., D. W. Hondorp, L. A. Davias, and R. J. Diaz. 2009. Hypoxia, Nitrogen, and Fisheries: Integrating Effects Across Local and Global Landscapes. Annu. Rev. Mar. Sci. **1:** 329–349

Canfield, D. E., E. Kristensen, and B. Thamdrup. 2005. Aquatic Geomicrobiology. Elsevier.

Capone, D. G. 2001. Marine nitrogen fixation: what's the fuss? Current Opinion in Microbiol. **4:** 341-348

Codispoti, L. A., J. A. Brandes, J. P. Christensen, A. H. Devol, S. W. A. Naqvi, H. W. Paerl, and T. Yoshinari. 2001. The oceanic fixed nitrogen and nitrous oxide budgets: Moving targets as we enter the anthropocene? Sci. Mar. **65:** 85-105

Codispoti, L. A. 2007. An oceanic fixed nitrogen sink exceeding 400 TgNa−1 vs the concept of homeostasis in the fixed-nitrogen inventory. Biogeosciences. **4:** 233-253

Common Wadden Sea Secretariat. 2008. Nomination of the Dutch-German Wadden Sea as world heritage site -volume one. **pp.** 19-30. Wilhelmshaven, Germany

Cook, P. L. M., F. Wenzhofer, S. Rysgaard, O. S. Galaktionov, F. J. R. Meysman, B. D. Eyre, J. Cornwell, M. Huettel, and R. N. Glud. 2006. Quantification of denitrification in permeable sediments: Insights from a two-dimensional simulation analysis and experimental data. Limnol. Oceanogr-Meth. **4:** 294-307

Cook, P. L. M., B. Veuger, S. I. Böer, and J. J. Middelburg. 2007. Effect of nutrient availability on carbon and nitrogen incorporation and flows through benthic algae and bacteria in near shore sandy sediment. Aquat. Microb. Ecol. **49:** 165-180

Dalsgaard, T., D. E. Canfield, J. Petersen, B. Thamdrup, and J. Acuña-González. 2003. N2 production by the anammox reaction in the anoxic water column of Golfo Dulce, Costa Rica. Nature **422:** 606-608

Dalsgaard, T., B. Thamdrup, and D. E. Canfield. 2005. Anaerobic ammonium oxidation (anammox) in the marine environment. I : Research in Microbiology. Vol. 156, **pp.** 457-464

Davis, C. S., and D. J. Mcgillicuddy. 2006. Transatlantic Abundance of the N_2-Fixing Colonial Cyanobacterium Trichodesmium. Science **312:** 1517-1520

de Beer, D., F. Wenzhofer, T. G. Ferdelman, S. E. Boehme, M. Huettel, J. E. E. van Beusekom, M. E. Boettcher, N. Musat, and N. Dubilier. 2005. Transport and

mineralization rates in North Sea sandy intertidal sediments, Sylt-Rømø Basin, Wadden Sea. Limnolo. Oceanogr. **50:** 113-127

Deutsch, C., J. L. Sarmiento, D. M. Sigman, N. Gruber, and J. P. Dunne. 2007. Spatial coupling of nitrogen inputs and losses in the ocean. Nature. **445:** 163-167

Devol, A. H. 1991. Direct measurement of nitrogen gas fluxes from continental shelf sediments. Nature. **349:** 319-321

Devol, A. H., and J. P. Christensen. 1993. Benthic fluxes and nitrogen cycling in sediments of the continental margin of the eastern North Pacific. J Mar. Res. **51:** 345-372

Devol, A. H., L. A. Codispoti, and J. P. Christensen. 1997. Summer and winter denitrification rates in western Arctic shelf sediments. Continental Shelf Res. **17:** 1029-1050

Devol, A. H. 2003. Solution to a marine mystery. Nature **422:** 575-576

Duce, R. A., J. LaRoche, K. Altieri, K. R. Arrigo, A. R. Baker, D. G. Capone, S. Cornell, F. Dentener, J. Galloway, R. S. Ganeshram, R. J. Geider, T. Jickells, M. M. Kuypers, R. Langlois, P. S. Liss, S. M. Liu, J. J. Middelburg, C. M. Moore, S. Nickovic, A. Oschlies, T. Pedersen, J. Prospero, R. Schlitzer, S. Seitzinger, L. L. Sorensen, M. Uematsu, O. Ulloa, M. Voss, B. Ward, and L. Zamora. 2008. Impacts of anthropogenic atmospheric nitrogen on the open ocean. Science. **320:** 893-897

Ehrenhauss, S., U. Witte, S. I. Buhring, and M. Huettel. 2004a. Effect of advective pore water transport on distribution and degradation of diatoms in permeable North Sea sediments. Mar. Ecol. Prog. Ser. **271:** 99-111

Ehrenhauss, S., U. Witte, S. Jansen, and M. Huettel. 2004b. Decomposition of diatoms and nutrient dynamics in permeable North Sea sediments. Continental Shelf Res. **24:** 721-737

Elser, J. J., M. E. S. Bracken, E. E. Cleland, D. S. Gruner, W. S. Harpole, H. Hillebrand, J. T. Ngai, E. W. Seabloom, J. B. Shurin, and J. E. Smith. 2007. Global analysis of nitrogen and phosphorus limitation of primary producers in freshwater, marine and terrestrial ecosystems. *Ecol. Letter*s **10:** 1135-1142

Emery, K. O. 1968. Relict sands on continental shelves of the world. Am. Assoc. Petrol. Geo. Bull. **52:** 445-464

Eppley, R. W., and B. J. Peterson. 1979. Particulate organic matter flux and planktonic new production in the deep ocean. Nature. **282:** 677– 680

Engström, P., T. Dalsgaard, S. Hulth, and R. C. Aller. 2005. Anaerobic ammonium oxidation by nitrite (anammox): Implications for N2 production in coastal marine sediments.Geochim. Cosmochim. Acta. **69:** 2057–2065.

Eyre, B. D., and A. J. P. Ferguson. 2002. Comparison of carbon production and decomposition, benthic nutrient fluxes and denitrification in seagrass, phytoplankton, benthic microalgae- and macroalgae-dominated warm-temperate Australian lagoons. Mar. Ecol. Prog. Ser. **229:** 43-59

Falkowski, P. G. 1997. Evolution of the nitrogen cycle and its influence on the biological sequestration of CO2 in the ocean. Nature. **387:** 272-275

Fossing, H., V. A. Gallardo, B. B. Jørgensen, M. Huttel, L. P. Nielsen, and H. Schulz et al. 1995. Concentration and transport of nitrate by the mat-forming sulfur bacterium Thioploca. Nature. **374:** 713–715

Franke, U., L. Polerecky, E. Precht, and M. Huettel. 2006. Wave tank study of particulate organic matter degradation in permeable sediments. Limnol. Oceanogr. **51:** 1084-1096

Galloway, J. N., E. B. Cowling, S. J. Seitzinger, and R. Socolow. 2002. Reactive nitrogen: Too much of a good thing? Ambio. **31:** 60–63

Galloway, J. N., J. D. Aber, J. W. Erisman, S. P. Seitzinger, R. W. Howarth, E. B. Cowling, and B. J. Cosby. 2003. The nitrogen cascade. BioScience. **53:**341-356

Galloway, J. N., and others. 2004. Nitrogen cycles: Past, present, and future. Biogeochemistry. **70:** 153–226

Gardner, W. S., M. J. McCarthy, S. An, D. Sobolev, K. S. Sell, and D. Brock. 2006. Nitrogen fixation and dissimilatory nitrate reduction to ammonium (DNRA) support nitrogen dynamics in Texas estuaries. Limnol. Oceanogr. **51:** 558–568

Goto, N., O. Mitamura, and H. Terai. 2001. Bidegradation of photosynthetically produced extracellular organic carbon from intertidal benthic algae. J. Exp. Mar. Biol. Ecol. **257:** 73–86

Gray, N. F. 1990. Activated sludge: theory and practice. Oxford University Press, Oxford, United Kingdom

Green, P. A., and others. 2004. Pre-industrial and contemporary fluxes of nitrogen through rivers: A global assessment based on typology. Biogeochemistry. **68:** 71–105

Gruber, N., and J. L. Sarmiento. 1997. Global patterns of marine nitrogen fixation and denitrification. Global Biogeochem. Cycles. **11:** 235–266

Gruber, N., and J. L. Sarmiento. 2002. Biogeochemical/Physical Interactions in Elemental Cycles, in THE SEA: Biological-Physical Interactions in the Oceans, edited by A. R. Robinson, J. J. McCarthy, and B. J. Rothschild, John Wiley and Sons. Volume 12, **pp.**337-399

Gruber, N. 2004. The dynamics of the marine nitrogen cycle and its influence on atmospheric CO2 variations, in The Ocean Carbon Cycle and Climate, NATO Sci. Ser. IV, vol. 40, edited by M. Follows and T. Oguz, Kluwer Acad., Dordrecht. **pp.** 97–148

Hannig, M., G. Lavik, M. M. M. Kuypers, D. Woebken, W. Martens-Habbena, and K. Juergens. 2007 .Shift from denitrification to anammox after inflow events in the central Baltic Sea, Limnol. Oceanogr. **52:** 1336-1345

Howarth, R. W., E. W. Boyer, W. J. Pabich, and J. N. Galloway. 2002. Nitrogen use in the United States from 1961–2000 and potential future trends. Ambio. **31:** 88–96.

Howarth, R. W., E. W. Boyer, R. Marino, D. Swaney, N. Jaworski, and C. Goodale. 2006. The influence of climate on average nitrogen export from large watersheds in the northeastern United States. Biogeochemistry. **79:** 163–186

Huettel, M., and G. Gust. 1992. Solute Release Mechanisms from Confined Sediment Cores in Stirred Benthic Chambers and Flume Flows, Mar. Ecol.Prog. Ser. **82:** 187-197

Huettel, M., W. Ziebis, and S. Forster. 1996. Flow-induced uptake of particulate matter in permeable sediments. Limnol. Oceanogr. **41:** 309-322

Huettel, M., and A. Rusch. 2000. Transport and degradation of phytoplankton in permeable sediment. Limnol. Oceanogr. **45:** 534-549

Huettel, M., H. Røy, E. Precht, and S. Ehrenhauss. 2003. Hydrodynamical impact on biogeochemical processes in aquatic sediments. Hydrobiologia. **494:** 231-236

Hulth, S., R. C. Aller, D. E. Canfield, T. Dalsgaard, P. Engstrom, and F. Gilbert et al. 2005 Nitrogen removal in marine environments: recent findings and future research challenges. Mar. Chem. **94:** 125-145

Jansen, S., E. Walpersdorf, U. Werner, M. Billerbeck, M. Böttcher, and D. de Beer. 2009. Functioning of intertidal flats inferred from temporal and spatial dynamics of O_2, H_2S and pH in their surface sediment. Ocean Dynam. **59:** 317-332

Jensen, K. M., M. H. Jensen, and R. P. Cox. 1996. Membrane inlet mass spectrometric analysis of N-isotope labelling for aquatic denitrification studies. FEMS Microbio. Ecol. **20:** 101-109

Johnson, H. D., and C. T. Baldwin. 1986. Shallow siliciclastic seas. In Reading, HG (Ed.) Sedimentary environments and facies (2nd ed.). Blackwell Scientific Publications, Oxford, **pp.** 229-282

Joye, S. B., and J. T. Hollibaugh. 1995. Influence of Sulfide Inhibition of Nitrification on Nitrogen Regeneration in Sediments. Science. **270:** 623-625

Joye, S. B., and I. C. Anderson. 2008. Nitrogen Cycling in Coastal Sediments. Nitrogen in the Marine Environment (2nd Edition). Academic Press. **pp.** 867-915

Kartal, B., and others. 2007. Anammox bacteria disguised as denitrifiers: nitrate reduction to dinitrogen gas via nitrite and ammonium. Environ. Microbiol. **9:** 635-642

Kieskamp, W. M., L. Lohse, E. Epping, and W. Helder. 1991. Seasonal variation in denitrification rates and nitrous oxide fluxes in intertidial sediments of the western Wadden Sea. Mar. Ecol. Prog. Ser. **72:** 145-151

Kuypers, M. M. M., A. O. Sliekers, G. Lavik, M. Schmid, B. B. Jørgensen, J. G. Kuenen, J. S. S. Damsté, M. Strous, and M. S.M. Jetten. 2003 Anaerobic ammonium oxidation by Anammox bacteria in the Black Sea. Nature **422:** 608-611

Kuypers, M. M. M., G. Lavik, D. Woebken, M. Schmid, B. M. Fuchs, R. Amann, B.B. Jorgensen, and S.M. Jetten. 2005. Massive nitrogen loss from the Benguela upwelling system through anaerobic ammonium oxidation. PNAS. **102:** 6478-6483

Kuypers, M. M. M., G. Lavik, and B. Thamdrup. 2006. Anaerobic ammonium oxidation in the marine environment, In Past and Present Marine Water Column Anoxia (ed. L. N. Neretin), Springer. **pp.** 311-336

Lam, P., M. M. Jensen, G. Lavik, D. F. McGinnis, B. Müller, C. J. Schubert, R. Amann, B. Thamdrup, and M. M. M. Kuypers. 2007. Linking crenarchaeal and bacterial nitrification to anammox in the Black Sea. PNAS. 104: 7104-7109

Lam, P., and M. M. M. Kuypers. 2011. Microbial Nitrogen Cycling Processes in Oxygen Minimum Zones. Annu. Rev. Mar. Sci. **3:** 317-345

Laursen, A. E., and S. P. Seitzinger. 2002. The role of denitrification in nitrogen removal and carbon mineralization in Mid-Atlantic Bight sediments. Continental Shelf Res. **22:** 1397-1416

Lavik, G., T. Stührmann, V. Brüchert, A. van der Plas, V. Mohrholz, P. Lam, M. Mußmann, B. M. Fuchs, R. Amann, U. Lass and M. M.M. Kuypers. 2009. Detoxification of sulphidic African shelf waters by blooming chemolithotrophs. Nature 457:581-584.

Lohse, L., H. Kloosterhuis, T. Raaphorstwv, and W. Helder. 1996. Denitrification rates as measured by the isotope pairing method and by the acetylene inhibition technique in continental shelf sediments of the North Sea. Mar. Ecol. Prog. Ser. **132:** 169-179

MacIntyre, H. L., R. J. Geider, and D. C. Miller. 1996. Microphytobenthos: The ecological role of the "secret garden" of unvegetated, shallow-water marine habitats. 1. Distribution, abundance and primary production. Estuaries. **19:** 186–201

Mehta, M. P., D. A. Butterfield, and J. A. Baross. 2003. Phylogenetic Diversity of Nitrogenase (nifH) Genes in Deep-Sea and Hydrothermal Vent Environments of the Juan de Fuca Ridge. Appl. Environ. Microbiol. **69:** 960-970

Mehta, M. P., and J. A. Baross. 2006. Nitrogen Fixation at 92Â°C by a Hydrothermal Vent Archaeon. Science. **314:** 1783-1786

Middelburg, J. J., K. Soetaert, P. M. J. Herman, and C. H. R. Heip. 1996. Marine sedimentary denitrification: a model study. Global Biogeochem Cycles. **10:** 661-673.

Middelburg, J. J., C. Barranguet, H. T. S. Boschker, P. M. T. Herman, T. Moens, and C. H. R. Heip. 2000. The fate of intertidal microphytobenthos carbon: An in situ ^{13}C-labeling study, Limnol. Oceanogr. **46:** 1224–1234

Montoya, J. P., C. M. Holl, J. P. Zehr, A. Hansen, T. A. Villareal, and D. G. Capone. 2004. High rates of N_2 fixation by unicellular diazotrophs in the oligotrophic Pacific Ocean. Nature. **430:** 1027-1032

Mulder, A., A. A. van de Graaf, L. A. Robertson, and J. G. Kuenen. 1995. Anaerobic ammonium oxidation discovered in a denitrifying fluidized bed reactor. FEMS Microbiol. Ecol. **16:** 177–184

Mulholland, P. J., and others. 2008. Stream denitrification across biomes and its response to anthropogenic nitrate loading. Nature. **452:** 202–205

Philippart, C. J. M., E G. C. Cade´, W. Vanraaphorst, and R. Riegman. 2000. Long-term phytoplankton-nutrient interactions in a shallow coastal sea: Algal community structure, nutrient budgets, and denitrification potential. Limnol. Oceanogr. **45:**131–144

Precht, E., and M. Huettel. 2004. Rapid wave-driven advective pore water exchange in a permeable coastal sediment. J. Sea Res. **51:** 93-107

Precht, E., U. Franke, L. Polerecky, and M. Huettel. 2004. Oxygen dynamics in permeable sediments with wave-driven pore water exchange. Limnol. Oceanogr. **49:** 693-705

Rao, A. M. F., M. J. McCarthy, W. S. Gardner, and R. A. Jahnke. 2007. Respiration and denitrification in permeable continental shelf deposits on the South Atlantic Bight: Rates of carbon and nitrogen cycling from sediment column experiments. Cont. Shelf Res. **27:** 1801-1819

Rao, A. M. F., M. J. Mccarthy, W. S. Gardner, and R. A. Jahnke. 2008. Respiration and denitrification in permeable continental shelf deposits on the South Atlantic Bight: N2:Ar and isotope pairing measurements in sediment column experiments. Cont. Shelf Res. **28:** 602-613

Redfield, A. C., B. H. Ketchum, and F. A. Richards. 1963. The influence of organisms on the composition of sea-water. In M.N. Hill (ed.) The Sea. Vol.2, pp.554. John Wiley & Sons, New York. **pp.** 26-77

Richards, F. A. 1965. in Chemical Oceanography, Anoxic basins and fjords, eds Riley J. P., Skirrow G. (Academic Press, London), 1, **pp**. 611–645

Robertson, L.A., and J.G. Kuenen. 1983. Thiosphaera pantotropha gen. Nov. sp. Nov., a facultatively anaerobic, facultatively autotrophic sulphur bacterium. J. Gen. Microbiol. **129:** 2847-2855.

Rusch, A., M. Huettel, C. E. Reimers, G. L. Taghon, and C. M. Fuller. 2003. Activity and distribution of bacterial populations in Middle Atlantic Bight shelf sands. FEMS Microbiol. Ecol. **44:** 89–100

Rusch, A., M. Huettel, C. Wild, and C. E. Reimers. 2006. Benthic oxygen consumption and organic matter turnover in organic-poor, permeable shelf sands. Aquatic Geochem. **12:** 1–19

Ryther, J. H., and W. M. Dunstan. 1971. Nitrogen, Phosphorus, and Eutrophication in the Coastal Marine Environment. Science. **171:** 1008-1013

Schlesinger, W. 2009. On the fate of anthropogenic nitrogen. PNAS. **106:** 203–208

Seitzinger, S. P. 1990. Denitrification in aquatic sediments. In: N.P. Revsbech and J. Sorensen, (editors), Denitrification in soil and sediment. Plenum Press. **pp.** 301-322.

Seitzinger, S. P., and others. 2002. Nitrogen retention in rivers: Model development and application to watersheds in the northeastern US. Biogeochemistry. 58: 199–237

Seitzinger, S. P., J. A. Harrison, E. Dumont, A. H. W. Beusen, and A. F. Bouwman. 2005. Sources and delivery of carbon, nitrogen and phosphorous to the coastal zone: An overview of global nutrient export from watersheds (NEWS) models and their application. Global Biogeochemical Cycles. **19:** GB4S01

Seitzinger, S. P. 2008. Nitrogen cycle: out of reach. Nature. **452:** 162-163

Shum, K. T., and B. Sundby. 1996. Organic matter processing in continental shelf sediments–the subtidal pump revisited. Mar. Chem. **53:** 81–87.

Sloth, N. P., L. P. Nielson, and T. H. Blackburn. 1992. Nitrification in sediment cores measured with acetylene inhibition. Limnol. Oceanogr. **37:** 1108–1112

Thamdrup, B., D. E. Canfield, T. G. Ferdelman, R. N. Glud, and J. K. Gundersen. 1996. A biogeochemical survey of the anoxic basin Golfo Dulce, Costa Rica, Rev. Biol. Trop., 44 Suppl. **3:** 19–33

Thamdrup, B., and T. Dalsgaard 2002. Production of N_2 through Anaerobic Ammonium Oxidation Coupled to Nitrate Reduction in Marine Sediments. Appl. Environ. Microbiol. **68:** 1312-1318

Thamdrup, B, and T. Dalsgaard. 2008. Nitrogen Cycling in Sediments. John Wiley & Sons, Inc.

Tyrrell, T. 1999. The relative influences of nitrogen and phosphorus on oceanic primary production. Nature. **400:** 525-531

Underwood, G. J. C., and J. Kromkamp. 1999. Primary production by phytoplankton and microphytobenthos in estuaries, in: Advances in Ecological Research, Vol. 29, edited by: Nedwell, D. B. and Raffaelli, D., Academic Press Inc, San Diego. **pp.** 93–153

van Beusekom, J. E. E., and V. N. de Jonge. 1998. Retention of phosphorus and nitrogen in the Ems estuary. Estuaries. **21:** 527-539

van Beusekom, J. E. E., H. Fock, F. de Jong, S. Diehl-Christiansen, and B. Christiansen. 2001. Wadden Sea Specific Eutrophication Criteria. Wadden Sea Ecosystem No. 14. Common Wadden Sea Secretariat. Wilhelmshaven, Germany.

Vance-Harris, C., and E. Ingall. 2005. Denitrification pathways and rates in the sandy sediments of the Georgia continental shelf, USA. Geochem. T. **6:** 12-18

Werner, U., M. Billerbeck, L. Polerecky, U. Franke, and M. Huettel. 2006. Spatial and temporal patterns of mineralization rates and oxygen distribution in a permeable intertidal sand flat (Sylt, Germany). Limnol. Oceanogr. **51:** 2549-2563

Zehr, J. P., M. T. Mellon, and S. Zani. 1998. New nitrogen-fixing microorganisms detected in oligotrophic oceans by amplification of nitrogenase (nifH) genes. Appl. Environ. Microbiol. **64:** 3444-3450

Zehr, J. P., E. J. Carpenter, and T. A. L. Villarea. 2000. New perspectives on nitrogen-fixing microorganisms in tropical and subtropical oceans. Trends in Microbiol. **8:** 68-73

Zehr, J. P., and B. B. Ward. 2002. Nitrogen Cycling in the Ocean: New Perspectives on Processes and Paradigms. Appl. Environ. Microbiol. **68:** 1015-1024

Overview of manuscripts

Aerobic denitrification in permeable Wadden Sea sediments (Chapter 2)

(Hang Gao, Frank Schreiber, Gavin Collins, Marlene M Jensen, Olivera Svitlica, Joel E Kostka, Gaute Lavik, Dirk de Beer, Huai-yang Zhou and Marcel MM Kuypers)

(Published in The ISME Journal, (2010) 4, 417–426; doi:10.1038/ismej.2009.127)

Intensive and extensive nitrogen loss from intertidal permeable sediments of the Wadden Sea (Chapter 3)

(Hang Gao, Maciej Matyka, Bo Liu, Arzhang Khalili, Joel E Kostka, Gavin Collins, Stefan Jansen, Moritz Holtappels, Marlene M Jensen, Thomas H Badewien, Melanie Beck, Maik Grunwald, Dirk de Beer, Gaute Lavik, and Marcel MM Kuypers)

(Resubmittion to Limnology and Oceanography)

Nitrification coupled to aerobic denitrification in the Wadden Sea intertidal permeable sediments (Chapter 4)

(Hang Gao, Stefan Jansen, Moritz Holtappels, Marlene M Jensen, Gavin Collins, Frank Schreiber, Sumei Liu, Joel Kostka, Dirk de Beer, Gaute Lavik, Marcel MM Kuypers)

(In preparation for Limnology and Oceanography)

Aerobic denitrification in permeable Wadden Sea sediments

Hang Gao[1,2,3], Frank Schreiber[1], Gavin Collins[1,4], Marlene M Jensen[1,5], Olivera Svitlica[1], Joel E Kostka1[1,6], Gaute Lavik[1], Dirk de Beer[1], Huai-yang Zhou[2,7] and Marcel MM Kuypers[1]

1Nutrient Group, Max Planck Institute for Marine Microbiology, Bremen, Germany;

2Guangzhou Institute of Geochemistry, Chinese Academy Sciences, Guangzhou, PR China and

3Graduate School of Chinese AcademySciences, Beijing, PR China

4Current address: Department of Microbiology and Environmental Change Institute, National University of Ireland, University Road,Galway, Ireland.

5Current address: Institute of Biology and Nordic Center of Earth Evolution, University of Southern Denmark, Campusvej 55, DK-5230 Odense M, Denmark.

6Current address: Department of Oceanography, Florida State University, Leroy Collins Research Lab, Tallahassee, FL, USA.

7Current address: School of Ocean and Earth Science, Tongji University, Shanghai, PR China.

Acknowledgement

We thank the Captains Ronald Monas, Ole Pfeiler and colleagues Hans Roy, Stefan Jansen and Ingrid Dohrmann for their cheerful support on the ship and shipping time; Phyllis Lam for her constructive comments; Gabriele Klockgether and Daniela Franzke for technical supports. This research was supported by German Academic Exchange Center (Deutscher Akademischer Austausch Dienst, DAAD), Max-Planck-Society (MPG) and German Research Foundation (DFG). JEK was partially supported by the Hanse-Wissenschaftskolleg and by grants from the US National Science Foundation (OCE-0424967 and OCE-0726754).

Abstract

Permeable or sandy sediments cover the majority of the seafloor on continental shelves worldwide, but little is known about their role in the coastal nitrogen cycle. We investigated the rates and controls of nitrogen loss at a sand flat (Janssand) in the central German Wadden Sea using multiple experimental approaches, including the nitrogen isotope pairing technique in intact core incubations, slurry incubations, a flow-through stirred retention reactor, and microsensor measurements. Results indicate that permeable Janssand sediments are characterized by some of the highest potential denitrification rates ($\geq$ 0.19 mmol N m^{-2} h^{-1}) in the marine environment. Moreover, several lines of evidence showed that denitrification occured under oxic conditions. In intact cores, microsensor measurements showed that the zones of nitrate/nitrite and O_2 consumption overlapped. In slurry incubations conducted with $^{15}NO_3^-$ enrichment in gas-impermeable bags, denitrification assays revealed that N_2 production occurred at initial O_2 concentrations of up to ~90 µM. Initial denitrification rates were not substantially affected by O_2 in surficial (0-4 cm) sediments, while rates increased by two fold with O_2 depletion in the at 4-6 cm depth interval. In a well mixed, flow-through stirred retention reactor, $^{29}N_2$ and $^{30}N_2$ were produced and O_2 was consumed simultaneously, as measured on-line using membrane inlet mass spectrometry. We hypothesize that the observed high denitrification rates in the presence of O_2 may result from the adaptation of denitrifying bacteria to recurrent tidally-induced redox oscillations in permeable sediments at Janssand.

Keywords: aerobic dentrification / nitrogen loss / permeable sediments / simultaneously NO_x^- and O_2 respiration

Introduction

Nitrogen (N) is primarily removed from coastal ecosystems by microbially-mediated denitrification that occurs on the seafloor (Hulth et al., 2005). Continental shelf sediments are important sites of N-removal, which may account for 50-70% of oceanic N-loss (Codispoti et al., 2001). Although the majority of continental margins is covered by coarsed-grained relict sediments (Emery, 1968; Johnson and Baldwin, 1986), most previous biogeochemical research has focused on muddy or fine-grained sediments. Pore-water advection, driven mainly by pressure gradients from wave action and bottom currents interacting with surface topography, causes rapid solute exchange and allows direct transfer of suspended particles into permeable sediment strata. Recent studies indicate that advective transport leads to an acceleration of organic matter mineralization and a stimulation of biogeochemical cycling proportional to the extent of pore-water exchange (Huettel and Rusch, 2000; de Beer et al., 2005; Werner et al., 2006). Up- and downward flow of pore-water associated with migrating sandy sediment ripples generates vertical oscillations in oxic and anoxic conditions as redox zones move horizontally through the surface layer of the bed. The dynamic redox conditions found in permeable marine sediments resemble those found in wastewater treatment plants (Gray, 1990). In other words, high transport rates of organic matter and electron acceptors from the water column into the seafloor and the presence of oscillating oxic / anoxic conditions allow marine sands to act as an efficient nutrient filter that may facilitate N removal. However, few studies have investigated N-loss by denitrification in coastal permeable sediments; of these studies, fewer still have considered the effects of advective pore water flows on the rates of denitrification (Cook et al., 2006; Hunter et al., 2006; Rao et al., 2007; 2008). Further research is needed to determine the rates and controls of N-removal from permeable marine sediments.

The current paradigm is that denitrification is an anaerobic process in marine sediments, and oxygen is believed to act as a major control of the process (Brandes et al., 2007). Denitrification is considered to require completely anoxic conditions due to the fact that O_2 acts as a competing electron acceptor for NO_3^- respiration and key enzymes of the denitrification pathways are inhibited by relatively small amounts of O_2 (Tiedje et al., 1982; Zumft, 1997; Shapleigh, 2006). However, in contrast to the observations made in natural environments, a large number of laboratory studies have reported that

denitrification occurs under aerobic conditions in pure cultures of bacteria (Robertson and Kuenen, 1984; Ronner and Sorensson, 1985; Trevors and Starodub, 1987; Robertson et al., 1995). Such findings suggest that denitrification may not always be so effectively inhibited by O_2. Microbiologists have defined aerobic denitrification as the co-respiration or co-metabolism of O_2 and NO_3^-. Physiological studies show that microorganisms are able to use branches of their electron transport chain to direct electron flow simultaneously to denitrifying enzymes as well as to O_2 (Robertson and Kuenen, 1988; Huang and Tseng, 2001; Chen et al., 2003). Although some environmental studies suggest that denitrification can occur in the presence of O_2 (Carter et al., 1995; Bateman and Baggs, 2005; Rao et al., 2007), substantial rates of aerobic denitrification have not yet been verified in the natural marine environment. Through a combination of new techniques employing stable N isotopes for the direct determination of denitrification rates as well as the rapid quantification of aqueous gases over short time scales, the study of aerobic denitrification becomes more feasible.

The main objective of this study was to investigate the impact of O_2 dynamics on N-loss by denitrification in permeable marine sediments of the Wadden Sea. Taking advective transport into account, we investigated denitrification rates in permeable sediments under near *in situ* conditions using a variety of experimental approaches. Surprisingly, multiple lines of evidence indicated that denitrification was not inhibited in the presence of substantial oxygen concentrations but rather the co-respiration of O_2 and NO_x^- occurred. Therefore, we hypothesized that where NO_x^- and O_2 cooccur, O_2 may not act as the primary or exclusive control of N_2 production in permeable sediment environments.

Materials and Methods

Site description

The Janssand sand flat (13 km^2) is in the back barrier area of Spiekeroog Island in the German Wadden Sea. The western edge of the flat faces the 17 m-deep, tidal channel separating the barrier islands Spiekeroog and Langeroog. The entire Janssand flat is inundated with ~2 m of seawater for 6-8 h during each semi-diurnal tidal cycle, becoming exposed to air for 6-8 h during low tide, depending on the tidal range.

The central region of Janssand comprises the main area of the sand flat and is termed the upper flat due to the sloping margin downwards to the low water line. The upper flat is itself almost level and the physical appearance is homogeneous, consisting mainly of well-sorted silica sand with a mean grain size of 176 μm (Billerbeck et al., 2006a). The mean permeability of 7.2 – 9.5 × 10^{-12} m^2 (upper 15 cm of sediment; (Billerbeck et al., 2006a) permits advective pore water flows (Huettel and Gust, 1992). Detailed descriptions of the Janssand flat are available in Billerbeck et al. (2006a; 2006b), Røy et al. (2008) and Jansen et al. (2009).

The sampling site (53°44.11'N, 7°41.95'E) is situated on the northeastern margin of the upper flat, about 80 m upslope from the mean low water line. Flat-bottom ships, the Spes Mea and Doris von Ochtum, were used to investigate the site in March 2007 and April 2008, respectively. All sediment core and seawater sampling was conducted at the upper Janssand tidal flat in March, 2007, unless otherwise indicated.

Dissolved inorganic nitrogen (DIN) in sediment pore water

Rhizon samplers (Seeberg-Elverfeldt et al., 2005) were utilized to extract pore water directly from sediment cores on the deck of the ship. Cores were sampled by pushing Plexiglas core liners (I.D., 9.5 cm) with side ports into the sediment, and Rhizons were then inserted horizontally into the ports at 1 cm intervals to 10 cm depth. Site seawater was also collected during low tide and filtered through a 0.2 um syringe filter. All samples were immediately frozen onboard ship at -20 °C for later analysis. Dissolved ammonium (NH_4^+) concentrations were determined using a flow injection analyzer (Hall and Aller, 1992). Nitrate + nitrite (NO_x^-) was determined by chemiluminescence after reduction to NO with acidic vanadium(II) chloride (Braman and Hendrix, 1989).

Intact core incubations

Denitrification rates were determined by the isotope pairing technique (Nielsen, 1992) in intact core incubations modified according to De Beer et al. (2005) to simulate *in situ* pore water advection in the permeable sediments. A set of 15 sediment cores were collected in parallel to obtain 15 cm of sediment and 15 cm of overlying water each from a 1-m^2 area using Plexiglas push-cores (I.D., 3.5 cm; height, 28 cm). Seawater was also collected in parallel from the site. Water overlying the sediment was removed and

replaced with $^{15}NO_3^-$-amended site seawater (final concentration of 50 μM). Rubber bottom stoppers were fitted with valves to allow for pore water perfusion over the upper 5 cm depth, and each core was percolated by 20 ml $^{15}NO_3^-$-amended aerated seawater at the perfusion speed of 12 ml/min. Cores were immediately sealed without any headspace by rubber stoppers after percolation, incubated at *in situ* temperature (8-10°C) and were destructively sampled in triplicate at regular intervals between 0 and 6 hours. The overlying water of all cores was mixed continuously at approximately 60 rpm during the incubations by externally-driven magnetic stirring bars. Cores were sacrificed in reverse order of percolation. Briefly, 1 ml of zinc chloride (50% w/v) $ZnCl_2$ was added to the sediment surface. The cores were resealed with no headspace prior to mixing by inversion. After allowing the sediment particles to settle, an aliquot of water was removed from each core and transferred to a 12 ml Exetainer ™ (Labco, UK) pre-filled with 200 μl saturated $HgCl_2$ for $^{29}N_2$ and $^{30}N_2$ determinations. The concentrations of excess $^{29}N_2$ and $^{30}N_2$ were calculated from $^{29}N_2$:$^{28}N_2$ and $^{30}N_2$:$^{28}N_2$ ratios of He-equilibrated headspace in Exetainers determined by gas chromatography-isotope ratio mass spectrometry (GC-IRMS; VG Optima). Denitrification rates were calculated based on the linear production of excess $^{29}N_2$ and $^{30}N_2$ according to Nielsen (1992).

Another set of intact core incubations was conducted to provide direct evidence for the co-respiration of O_2 and NO_x^- using multiple microsensors. An O_2 microsensor and a NO_x^- biosensor were simultaneously applied to freshly sampled sediment cores. Advective transport in sediments cores was simulated by percolation as described above.

Oxygen microsensors were constructed as described previously (Revsbech, 1989). A 2-point calibration method for the O_2 sensor was performed using the signal in saturated overlying site seawater and anoxic sediments, and the O_2 solubility was corrected for the ambient water temperature (18 °C) and salinity (32 ‰) using the spreadsheet supplied by Unisense (www.unisense.dk). The NO_x biosensor was constructed, according to Larsen et al. (1997), with a tip diameter of 100 μm and was calibrated in seawater with additions of increasing amounts of NO_3^- to confirm linearity of the response (0-500 μM). For the calculation of pore water concentrations, the slope and offset were corrected for NO_3^- concentrations in the overlying water determined as described above.

For simultaneous measurements of vertical concentration profiles, the O_2 and NO_x sensors were mounted on a 3-axis micromanipulator (MM 33; Märzhäuser, Wetzlar, Germany). The vertical axis was motorized for µ-positioning and controlled by µ-Profiler software described in Polerecky et al. (2005). The microsensor tips were aligned carefully to the same horizontal axis. The even sediment topography allowed alignment of both sensor profiles to the sediment surface with a precision of 1 mm, using the initial decrease of O_2 in the diffuse boundary layer. Microsensor measurements were made at 0.5 cm and 1 cm below the sediment surface during each percolation. Data were recorded over a time series to determine rates of potential O_2 uptake and NO_x^- consumption under oxic and anoxic conditions.

Slurry incubations in gas-tight bags

The depth-specific response of denitrification to O_2 was initially examined in bag incubations using the ^{15}N tracer isotope pairing technique according to Thamdrup and Dalsgaard (2002). Sediments were sampled using Plexiglas push-cores (I.D., 9.5 cm; height, 60 cm) and sectioned into 2-cm depth intervals to a depth of 6 cm. Afterward, sediment and air-saturated, site seawater were mixed at a ratio of 1:1 in the gas-tight bag while expelling all air bubbles. The slurries were amended with $^{15}NO_3^-$ to a final concentration of 200 µM, and the bags were incubated at *in situ* temperature (same as for intact core incubations). During the incubation, the bags were periodically shaken to ensure that the labeled N species were homogenously distributed. Sub-samples of the interstitial water were withdrawn from the bags at regular intervals and preserved in 6 ml Exetainer ^{TM} vials (Labco, UK) pre-filled with 100 µl saturated $HgCl_2$. An initial subsample was taken immediately after the addition of the tracer and at regular intervals to 16 hours.

The aqueous O_2 concentration of the subsamples was determined using an O_2 microelectrode (MPI, Bremen) as described above. The 6 ml Exetainer vials were opened only briefly during the measurement, and were afterwards stored with no headspace for further analysis of dissolved N_2 by GC-IRMS as described above.

Flow-through stirred retention reactor (FTSRR) incubation experiment

To provide further corroboration for the co-respiration of O_2 and NO_3^- in a sediment slurry, aqueous gases (O_2 and N_2) were directly determined in line by membrane inlet mass spectrometry (MIMS; GAM200, IPI) in a FTSRR system. Surface sediments (0-3 cm) and site seawater were collected from the upper flat in April 2008, and stored at 4°C during transport to the laboratory. Sediments and site seawater were mixed at a ratio of 1:3 in the gas-tight FTSRR without headspace. The slurry was vigorously mixed at 200 rpm by a magnetic stir bar, and the incubation was carried out in the dark at room temperature. The FTSRR system consisted of a sealed cylinder chamber (Plexiglas, inner diameter 9 cm, height 6cm) fitted with three ports for the input and output of water. The effluent pumped through a filter by one port from the chamber was injected directly into the membrane inlet using a peristaltic pump with the pumping speed of 0.5 ml/min. Gas-tight syringes connected to the chamber by the other two ports, each filled with 50 ml of air-saturated site sea water, provided replacement water during pumping.

Simultaneous online measurements of mass 28 ($^{14}N^{14}N$), 29 ($^{14}N^{15}N$), 30 ($^{15}N^{15}N$), 40 (Ar), 31 (^{15}NO), 32 (O_2), 44 ($^{14+14}N_2O/CO_2$), 45 ($^{14}N^{15}NO$) and 46 ($^{15}N^{15}NO$) were obtained by MIMS. A standard calibration curve was constructed, based on measurements obtained under both air-saturated and anoxic conditions using a two-point calibration for each. The slurry in the incubator was amended with $^{15}NO_3^-$ to a final concentration of ~150 μM. Mass abundance signals were recorded by MIMS at one second time intervals and the flow-through samples were collected in 2-ml vials and stored at -20°C for DIN analysis as described above (***2.2***).

Results

DIN and O_2 penetration in permeable sediments

Zones of O_2 penetration and NO_x^- depletion largely overlapped in the upper 2 to 3 cm of tidal flat sediments. During the winter-spring, NO_x^- concentrations with a mean value of ~67 μM were observed in the overlying seawater, while NH_4^+ concentrations were comparably 10 times lower (< 7 μM) (Fig. 1A). In surficial sediments, pore water NO_x^- decreased rapidly with depth to ~40 μM at 1 cm depth, and a minimum concentration was observed below 3 cm depth. Concomitantly, pore water NH_4^+ increased to ~70 μM from the surface to 3 cm depth and remained consistently high (70-

105 µM) below that depth (Fig. 1A). *In situ* O_2 measurements in the upper flat from March 2006, showed that, O_2 penetrated to ~3 cm during tidal inundation (Fig. 1B) and O_2 penetration depths of up to 5 cm were observed at other locations on Janssand tidal flat (Billerbeck et al., 2006b; Jansen et al., 2009). The decrease in NO_x^- was equivalent to approximately half of the observed increase of NH_4^+ with depth (Figure 1A).

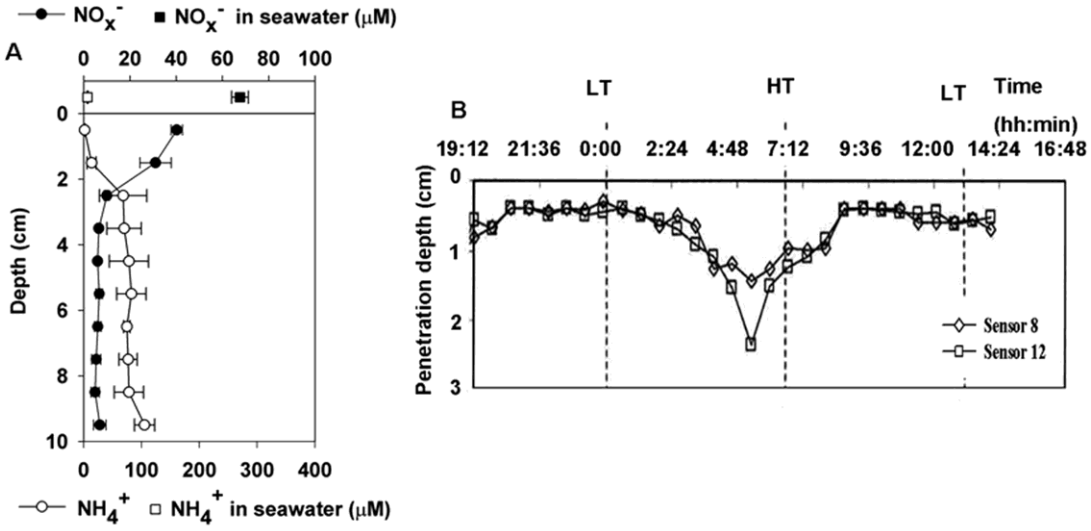

Figure 1: Distribution of dissolved inorganic nitrogen species [NH_4^+ and NO_x^- (NO_3^- + NO_2^-)] and O_2 penetration in sediments from the upper flat at Janssand. (A) NO_x^- (closed circles) and NH_4^+ (open circles) concentration profiles in permeable sediments in March 2007 during exposure. The daily mean values of NO_x^- and NH_4^+ concentrations in overlying seawater are depicted as closed and open squares, respectively. (B) O_2 penetration depth during a tidal cycle measured by two oxygen sensors in March 2006 (modified from Jansen *et al*., 2009).

Denitrification potential in intact cores and gas-tight bag incubations

Following with the overlap in O_2 penetration and NO_x depletion, we observed the immediate and rapid production of ^{15}N-labeled N_2 in both incubations amended with $^{15}NO_3^-$ throughout the first 4 hours of incubation under oxic conditions (Fig. 2). Our study of the intact core incubations was motivated by a previous study of O_2 consumption using the same pore water percolation method that observed substantial O_2 was present during the first 1-2 hours of intact core incubations in March (Polerecky et al., 2005; Billerbeck et al., 2006b). In the present study, $^{29}N_2$ and $^{30}N_2$ were produced linearly (r^2_{29N2} = 0.93 and r^2_{30N2} = 0.91, respectively) without any lag during the first 2

hours of incubation in the presence of O_2 (Fig 2A). In bag incubation experiments conducted in parallel, high potential denitrification rates were observed in sediment slurries from the 0-2 cm, 2-4 cm and 4-6 cm depth intervals in which initial O_2 concentrations of ~95, 30 and 35 µM were observed, respectively. Higher $^{29}N_2$ and $^{30}N_2$ production rates were observed in incubations from the 0 to 4 cm depth intervals where higher NO_x^- concentrations are observed in sediment pore waters (Fig. 1A, Fig. 2B - D). No significant change in the denitrification rates was observed in the incubations under oxic conditions (during the first 4 h) in comparison to anoxic conditions (during the last 12 h) (Table 1). In the incubation from the deepest depth interval (4-6 cm) where NO_x^- was depleted, the lowest denitrification rates were observed while O_2 depleted earliest (~2 h) (Table 1). Moreover at 4 to 6 cm depth, the rate under anoxic conditions was 2.3 times higher as that under oxic conditions (Fig. 2D and Table 1). When extrapolated over the 0-5 cm depth interval, potential denitrification rates measured in percolated intact cores and bag incubations were in the same range (Table 1).

Microelectrode and biosensor measurements

Similar to the observations in the bag incubations, time series measurements by microsensors upon percolation of air-saturated and NO_3^--rich sea water showed that NO_x^- and O_2 were consumed simultaneously at 0.5 to 1 cm depth in intact sediment cores (Fig. 3; Table 1). O_2 and NO_x^- - rich seawater was transported downward into the sediment by percolation, which increased concentrations at 0.5 cm to ~240 µM O_2 and 50 µM NO_x^-, and at 1 cm to ~230 µmol l^{-1} O_2 and 40 µM NO_x^-. Under those high initial O_2 concentrations, a slight accumulation of 3-6 µM NO_x^- was detected after 2-3 min, followed by a substantial linear decrease in NO_x^- over the next 0.5 to 1.0 hour of incubation in the presence of O_2. NO_x^- was consumed at a higher rate at 1 cm than at 0.5 cm under oxic conditions (Table 1). After O_2 was completely consumed, the NO_x^- reduction rate increased slightly at 0.5 cm depth, however, NO_x^- consumption rates showed no significant difference under oxic and anoxic conditions at 1 cm depth (Table 1), which corresponded to the results observed in the bag incubations with sediments from 0-4 cm depth.

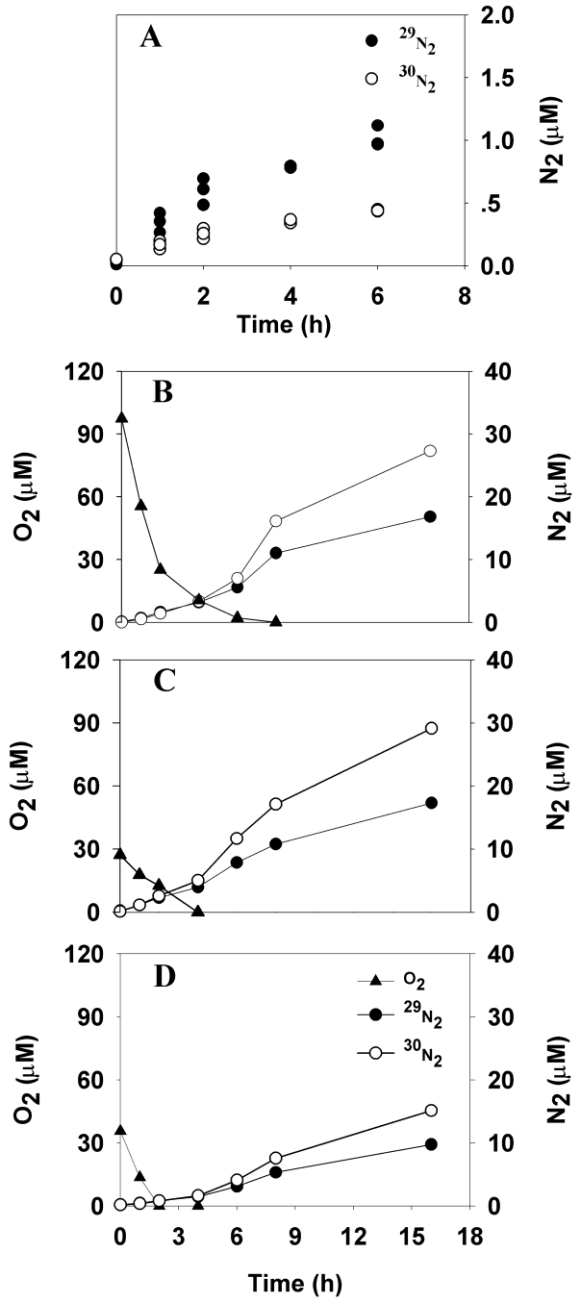

Figure 2: ^{15}N-labeled N_2 production and oxygen consumption in whole-core and bag incubations. **(A)** $^{29}N_2$ (black circles) and $^{30}N_2$ (open circles) production from $^{15}NO_3$ amendments in percolated whole-core incubations. O_2 consumption and ^{15}N-labeled N_2 production versus time in $^{15}NO_3^-$ - amended, oxic, gas-tight bag incubations with sediment from **(B)** 0-2 cm, **(C)** 2-4 cm and **(D)** 4-6 cm depth intervals.

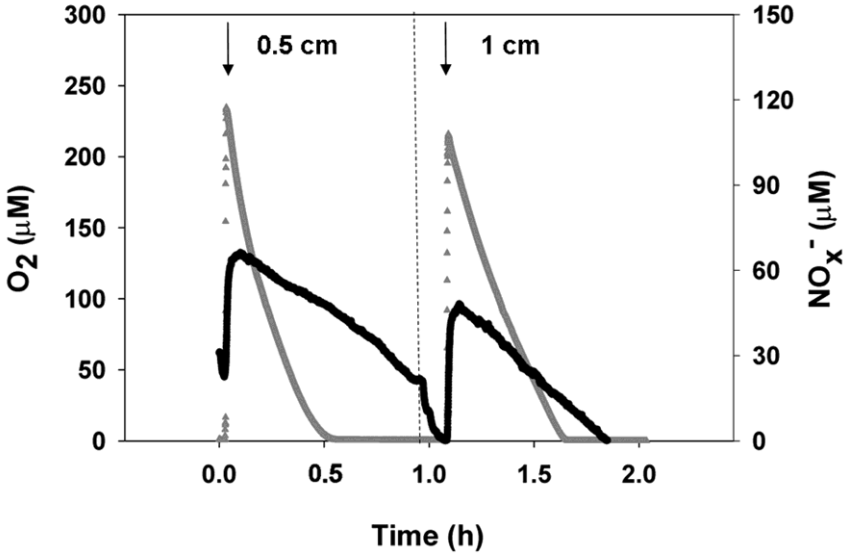

Figure 3: Time series of O_2 (grey) and NO_x^- (black) concentrations in an intact sediment core after percolation (indicated by arrows) with air-saturated overlying seawater containing ~60 µM NO_x^-. O_2 and NO_x^- microsensor tips were adjusted on a horizontal axis and measurements were carried out simultaneously. The first percolation treatment started at 0 h when sensors were positioned at 0.5 cm depth. The sensors were moved from 0.5 cm to 1 cm after 0.9 h and the second percolation began at 1.1 h when sensors were positioned at 1 cm depth.

Aerobic denitrification in a FTSRR

To provide further evidence for the simultaneous consumption of NO_x^- and O_2 in permeable sediments, an incubation was conducted in a stirred retention reactor, in which the slurry was vigorously and continuously mixed. Under constant mixing, substantial $^{30}N_2$ production was again observed by real-time MIMS measurements in the presence of 32 µM O_2 (Fig. 4). $^{15}NO_3^-$ was amended to the continuously stirred chamber 20 minutes after the start of the incubation in the presence of 128 µM O_2. Online MIMS analyses indicated that after an initial lag period of 1.1 hours, significant $^{30}N_2$ production occurred in the presence of 40 µM O_2. Concomitantly, O_2 consumption slowed below that concentration. Simultaneously, there was a slight accumulation of NO_x^- (data not shown) during $^{30}N_2$ production. However, during that period, $^{29}N_2$ production was not concurrent with $^{30}N_2$ production and the increase of NO_x^-. In contrast, $^{29}N_2$ began to accumulate

only when NO_x^- decreased at 1.5 hours of incubation in parallel with a 7-fold higher rate of $^{30}N_2$ production (Fig. 4).

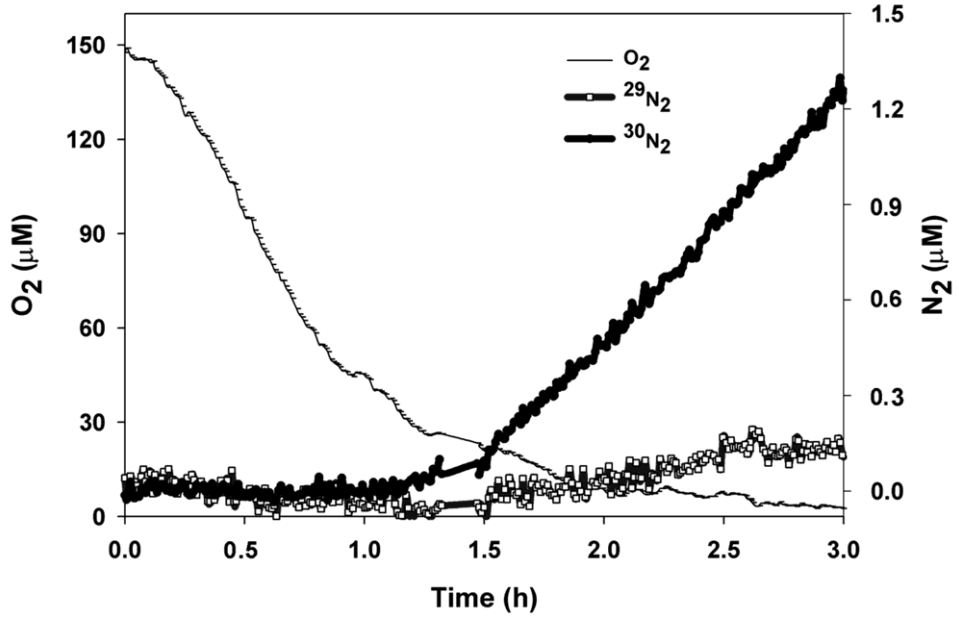

Figure 4: ^{15}N-labeled N_2 production and oxygen concentration versus time during the incubation of permeable sediments in the flow-through stirred retention reactor (FTSRR). Sediments were sampled from the 0-3 cm depth interval of the upper flat during April 2008. $^{29}N_2$, $^{30}N_2$ and O_2 concentrations are depicted as open circles, black squares and open triangles, respectively.

Table 1. Summary of denitrification rates measured in all incubations

Measurement	Investigated depth (cm)	Denitrification / NOx – consumption (mmol N $m^{-3}_{sediment}$ h^{-1})	
		Oxic	Anoxic
Intact core incubation	5	4.60 ± 0.46	
	Integrated to 5	0.23 ± 0.02*	
Intact core by multi – microsensors	0.5	15.5 ± 0.04	21.9 ± 0.05
	1	22.0 ± 0.04	21.5 ± 0.04
Slurry incubation	0 – 2	6.40 ± 0.37	10.57 ± 3.20
	2 – 4	8.27 ± 0.32	9.63 ± 1.15
	4 – 6	2.72 ± 0.16	6.28 ± 0.84
	Extrapolated to 5	0.32 ± 0.01*	0.47 ± 0.07*
Constant mixing, flow-through retention reactor incubation	0 - 3	6.23 ± 0.07	
	Extrapolated to 3	0.187 ± 0.002*	

The mean porosity of sediments in upper flat is 35% (Billerbeck et al., 2006b)
* the unit is mmol N $m^{-2}_{sediment}$ h^{-1}

Discussion

In permeable marine sediments of the Wadden Sea, zones of NO_x^- and O_2 penetration often overlap to several centimeters depth due to pore water advection (Fig 1) (Werner et al., 2006; Billerbeck et al., 2006a; 2006b; Jansen et al., 2009). Further, previous O_2 percolation experiments that incorporated pore water advection, showed that during the spring season when NO_x^- is at high concentration in the overlying seawater, O_2 persisted in the bulk pore water over the first 1 to 2 hours of incubation in intact cores of Wadden Sea sediments (Polerecky et al., 2005; Billerbeck et al., 2006b). From these observations, it could be inferred that where NO_x^- and O_2 cooccur, O_2 may not act as the primary or exclusive control of N_2 production in permeable sediment environments. To test this assumption, we investigated N-loss by denitrification in relation to O_2 dynamics. Several lines of independent evidence collected with multiple experimental approaches under near *in situ* conditions showed that denitrification occurs in the presence of oxygen. We observed the immediate and rapid consumption of NO_x^- under air saturated pore water in the intact core, and the directly determined production of ^{15}N-labeled N_2 in the presence of up to 90 µM O_2 in slurry incubations. Further, the rapid production of labeled N_2 was not diminished in a vigorously stirred, flow-through retention reactor. Thus, our results strongly suggest that aerobic denitrification makes a substantial contribution to N-loss in permeable marine sediments.

The rates and mechanisms of N-removal in permeable marine sediments remain in question. Few studies have quantified N_2 production in coastal permeable sediments, and the rate measurements in this small but growing database vary widely, ranging from 0.1 to 3 mmol m^{-2} d^{-1} (Laursen and Seitzinger, 2002; Vance-Harris and Ingall, 2005; Cook et al., 2006; Rao et al., 2007; 2008). However, researchers have now become aware of the fact that in experiments where pore water advection is absent or impeded, a realistic determination of diagenetic processes is not achieved (Jahnke et al., 2000; Cook et al., 2006). At present, at least two mechanisms have been proposed to explain denitrification in the presence of oxygen: 1) co-respiration of NO_x^- and O_2 (Bateman and Baggs, 2005), and 2) closely coupled nitrification-denitrification in microenvironments isolated from bulk sediment pore water (Rao et al., 2007). Bateman and Baggs (2005) provided one of the few observations of the contribution of aerobic denitrifying bacteria to denitrification potential in the environment. Using a combined stable isotope and acetylene inhibition

approach, they were able to distinguish the relative contribution of nitrification and denitrification to N_2O production in arable soil. The results suggested that aerobic denitrification occurred at 20% water-filled pore space.

Although biogeochemical evidence exists for denitrification in the presence of oxygen in the marine environment (Hulth et al., 2005; Hunter et al., 2006; Brandes et al., 2007; Rao et al., 2007), significant rates of aerobic denitrification have not been verified until now. New techniques such as NO_x biosensors and stable N isotope tracers applied in conjunction with MIMS allowed for the further confirmation of aerobic denitrification. Rao et al. (2007; 2008) incorporated the effects of pore water advection, and in corroboration with our results, observed high rates of N_2 production in flow-through columns of oxic permeable sediments. In oligotrophic continental shelf sediments of the South Atlantic Bight, Rao et al. (2007) observed that pore water nitrate was only above detection in the oxic zone. Nitrogen released as N_2 accounted from 80 to 100 % of remineralized N, and the C:N ratio of regeneration supported the interpretation of N_2 produced by denitrification. In the Rao et al. study, the addition of ^{15}N-nitrate caused only a small and gradual rise in $^{29}N_2$ and $^{30}N_2$ production in sediment columns over up to 12 days of incubation. Only columns with anoxic outflow showed substantial $^{29}N_2$ or $^{30}N_2$ production. Thus, Rao et al. (2007) concluded that their evidence for aerobic denitrification was equivocal, and N_2 production more likely occurred from coupled nitrification-denitrification in microenvironments.

In the present study, we observed the rapid and immediate production of ^{15}N-labelled N_2 in the presence of O_2 under a variety of experimental conditions. Oxygen and NO_x^- dynamics were directly determined in real time under well mixed conditions in sediment slurries and intact core incubations. Microsensor measurements showed that NO_x^- and O_2 consumption occurred simultaneously in intact cores (Fig. 3). Further direct evidence for the co-respiration of O_2 and NO_x^- was provided using ^{15}N tracer experiments in slurries which were constructed with sediments from different depths. Successive incubation experiments showed the reliability and uniformity of aerobic denitrification rates, despite the fact that the experimental setup differed (including the amount of sediments, volume of associated water, and starting concentration of labeled nitrate; Supplementary Table 1). Although the concentrations of $^{29}N_2$ and $^{30}N_2$ in the associated water varied, the denitrification rates normalized to sediment volume were in

the same range, with the exception of the higher rate measured by the microsensor, which incorporated NO_3^- assimilation as well as denitrification (Table 1). Under the experimental conditions used, $^{29}N_2$ could be attributed to coupled nitrification-denitrification or anammox in the slurry (Thamdrup and Dalsgaard, 2002). In contrast, $^{30}N_2$ would only be produced by complete denitrification. Anammox was shown to comprise only a small percentage of N_2 production in parallel slurry experiments conducted in gas-tight bags (Gao et al., in preparation). Therefore, we conclude that the ^{15}N-labeled N_2 production is mainly contributed by denitrification, and the occurrence in the presence of O_2 provided evidence for aerobic denitrification.

At each depth examined in slurry incubation, the potential denitrification rate under aerobic conditions was similar to that measured under anaerobic conditions. Moreover, the maximum denitrification rate was not observed in the deepest depth interval with the lowest initial O_2 concentration, but rather in the surface 0 to 4 cm depth. This suggests that the overlapping NO_x^- concentration may act together with O_2 to control the denitrification rate. On the Janssand tidal flat during winter/spring, rapid denitrification is likely to be supported by the constant supply of NO_x^- advected from the overlying seawater (Gao et al., in preparation). In short, O_2 dynamics did not strongly affect N-loss by denitrification in the presence of abundant NO_x^-, but rather denitrification co-existed with O_2 respiration in permeable Wadden Sea sediments affected by advection.

In order to further exclude the possibility of anoxic microniches forming in our sediment incubations, we conducted an experiment in a vigorously mixed FTSRR. The initial production of $^{30}N_2$ in the presence of 40 µM O_2 (Fig. 4) provided evidence for the process of aerobic denitrification. The concomitantly suppressed O_2 consumption may indicate that nitrate acts as a competitive electron acceptor to facultatively aerobic denitrifying bacteria. Whereas at lower O_2 concentrations later in the incubation (where an increased ratio of unlabeled NO_3^- was observed), the production of $^{29}N_2$ indicated denitrification coupled to nitrification. Due to the variability in the mass abundance signals, we cannot exclude the possibility that some $^{29}N_2$ was also produced in the early stages of the FTSRR incubation. Thus, we observed the mechanism for rapid denitrification under oxic conditions depended on two pathways- aerobic denitrification and dentrification coupled to nitrification.

During the FTSRR incubation, the bulk porewater was vigorously flushed by aerated seawater and the labeled isotope ratio was kept constant. Thus, the possibility that denitrification occurred in anoxic microzones can be completely excluded. In corroboration with our results, previous studies on the formation of anoxic microzones in particles and aggregates showed that the respiration capacity is simply not sufficient to create anoxia under high ambient O_2 concentration, and anoxic microzones more likely form at around 10 % of air saturation (under ~ 25 µM O_2 in the bulk phase; (Schramm et al., 1999; Ploug, 2001). In our study, at O_2 concentrations of ~20 % air saturation and above, the establishment of anoxic microzones would be unlikely. Given the larger grain sizes present in marine sands, O_2 transport is enhanced by advection / interstitial fluid flow, which produces less steep O_2 gradients at the sediment-water interface and within particles / aggregates compared with those that develop under pure diffusion conditions (Ploug, 2001). The abovementioned experiments were conducted in a vertical flow system under non-turbulent uniform flow conditions. Thus, for the coarse-grained sediments in our well-mixed retention reactor experiments where the sediment slurry is exposed to turbulent aerated flow, anoxic microzones would not form. Therefore, we conclude that substantial N-loss occurs by aerobic denitrification in the permeable Wadden sediments.

Denitrification has long been considered as an anoxic biogeochemical process in marine and aquatic environments, and oxygen has been shown to inhibit denitrifying enzyme activity (Tiedje et al., 1982; Hulth et al., 2005; Brandes et al., 2007). However, a phylogenetically and physiologically diverse group of microorganisms has been shown to denitrify in the presence of oxygen in laboratory studies (Zehr and Ward, 2002; Hayatsu et al., 2008). Bacteria capable of aerobic nitrate respiration were cultured in abundance from freshwater soils and sediments (Carter et al., 1995). Aerobic denitrifiers were further isolated from a variety of managed and natural ecosystems (Patureau et al., 2000). Thus, the influence of oxygen on nitrate respiration activity appears to vary between microorganisms, with some strains able to respire nitrate at or above air saturation (Lloyd et al., 1987; Hayatsu et al., 2008). Microbiological studies have gone so far as to suggest that the capacity for denitrification under aerobic conditions is the rule rather than the exception amongst ecologically important denitrifying microbial communities (Lloyd et al., 1987).

Previous studies indicate that the diversity, as well as the metabolic activity, of bacterial communities is high in permeable sediment environments, likely due to increased transport of growth substrates and the removal of metabolites by advective exchange with the overlying water column (Hunter et al., 2006; Mills et al., 2008; Boer et al., 2009). Denitrification in the marine environment is believed to be mediated by a group of facultative anaerobes that display a wide range in phylogenetic affiliation and metabolic capabilities (Zehr and Ward, 2002). In pristine ecosystems, nitrate concentrations are typically too low to select for large populations of denitrifying organisms, and denitrifiers are thought to rely on aerobic heterotrophy in conjunction with their denitrification capacity (Tiedje, 1988). In permeable marine sediments, up- and downwelling of pore water associated with sandy sediment ripples generates redox oscillations that may promote the microbially-mediated oxidation and reduction of N species.

Although the consensus is that low or no O_2 is required for the initiation of denitrification, most information on the O_2 level at which denitrification starts comes from pure cultures. Denitrification has been observed in the laboratory at O_2 concentrations approaching air saturation (Zehr and Ward, 2002), but previous environmental studies are equivocal with regard to the impact of O_2 dynamics on denitrification. Large differences are observed in the expression and regulation of denitrification genes between species studied in pure culture (Shapleigh, 2006). The expression of denitification genes was shown to require O_2 in some cases, and the presence of denitrification intermediates may impact the denitrification rate in the presence of O_2. A possible explanation is that the accumulation of intermediates slows O_2 respiration, particularly at low O_2 levels, thereby slowing down the aerobic-anaerobic transition and allowing the expression of O_2-requiring denitrification genes (Bergaust et al., 2008).

We hypothesize that the co-respiration of nitrate and O_2 represents an adaptation of denitrifiers to recurrent tidally-induced redox oscillations in permeable sediments of the Wadden Sea. Some evidence from pure cultures of denitrifying bacteria supports this hypothesis. For example, when the selective pressure of environmental redox changes was removed, the aerobic denitrification ability of *Paracoccus denitrificans* decayed (Dalsgaard et al., 1995; Robertson et al., 1995). Further, Bergaust et al. (2008) proposed

that denitrifiers adapt to recurrent oscillations in oxygen concentrations through a protection mechanism, which consists of the coordinated expression and activity of the denitrification enzymes for survival during the rapid transition from oxic to anoxic conditions. A "bottle neck effect" was also proposed, whereby nitrifying and denitrifying bacteria react to oxygen and nitrate in the environment by coordinating their respective activities. Schmidt et al. (2003) observed that the onset of the aerobic denitrification did not depend on oxygen sensitivity of the corresponding enzymes, but rather on regulation of redox-sensing factors at the transcriptional level. Our biogeochemical evidence corroborates microbiological studies to indicate a clear need to elucidate the significance and the controls of aerobic denitrification in permeable marine sediments.

In contrast to the paradigm that denitrification is an exclusively anaerobic process, our experiments point to aerobic denitrification and indicate that O_2 may not act as a primary or exclusive control of N_2 production in permeable marine sediments. We propose that the availability of NO_x^- as well as O_2 limit the denitrification rate at depths of marine sands that are impacted by pore water advection. We can only speculate on the mechanism of aerobic denitrification at this time. Co-metabolism would imply that both NO_x^- and O_2 are used simultaneously as electron acceptor in a single organism. Alternatively, separated denitrifying and oxygen respiring populations may be active within the community. In the first case one would expect a competition for electrons within the electron transport chain, thus an enhanced denitrification upon oxygen depletion. In the second case, denitrification would be uncoupled entirely from the presence of oxygen, as denitrification is not kinetically inhibited by oxygen, nor can oxygen compete for electrons. In the FTSRR, we observed a pronounced effect of oxygen on denitrification rate whereas in other incubations less of an effect was found, indicating that both mechanisms may be present. Further research is needed to elucidate the true mechanisms of aerobic denitrification in permeable marine sediments.

References

Bateman, E. J., and E. M. Baggs. 2005. Contributions of nitrification and denitrification to N2O emissions from soils at different water-filled pore space. Biol. Fert. Soils. **41:** 379-388

Bergaust, L., J. Shapleigh, Å. Frostegård, and L. Bakken. 2008. Transcription and activities of NOx reductases in *Agrobacterium tumefaciens:* the influence of nitrate, nitrite and oxygen availability. Environ. Microbiol. **10:** 3070-3081

Billerbeck. M, U. Werner, K. Bosselmann, E. Walpersdorf, and M. Huettel. 2006a. Nutrient release from an exposed intertidal sand flat. Mar. Ecol-Prog. Ser. **316:** 35-51

Billerbeck, M, U. Werner, L. Polerecky, E. Walpersdorf, D. de Beer, and M. Huettel. 2006b. Surficial and deep pore water circulation governs spatial and temporal scales of nutrient recycling in intertidal sand flat sediment. Mar. Ecol-Prog. Ser. **326:** 61-76

Bøer, S. I., S.I.C. Hedtkamp, J.E.E. Beusekom, J.A. Fuhrman, A. Boetius, and A. Ramette. 2009. Time- and sediment depth-related variations in bacterial diversity and community structure in subtidal sands. The ISME Journal. 3: 780-791.

Braman, R. S., and S. A. Hendrix. 1989. Nanogram Nitrite and Nitrate Determination in Environmental and Biological-Materials by Vanadium(Iii) Reduction with Chemi-Luminescence Detection. Anal. Chem. **61:** 2715-2718

Brandes, J. A., A. H. Devol, and C. Deutsch. 2007. New developments in the marine nitrogen cycle. Chem. Rev. **107:** 577-589

Carter, J., Y. Hsaio, S. Spiro, D. Richardson. 1995. Soil and sediment bacteria capable of aerobic nitrate respiration. Appl. Environ. Microb. **61:** 2852-2858

Chen, F., Q Xia., L. K. Ju. 2003. Aerobic Denitrification of Pseudomonas aeruginosa Monitored by Online NAD(P)H Fluorescence. Appl. Environ. Microb. **69:** 6715-6722

Codispoti, L. A., J. A. Brandes, J. P. Christensen, A. H. Devol, S. W. A. Naqvi, H. W. Paerl, and T. Yoshinari. 2001. The oceanic fixed nitrogen and nitrous oxide budgets: Moving targets as we enter the anthropocene? Sci. Mar. **65:** 85-105

Cook, P. L. M., F. Wenzhofer, S. Rysgaard, O. S. Galaktionov, F. J. R. Meysman, B. D. Eyre et al. 2006. Quantification of denitrification in permeable sediments:

Insights from a two-dimensional simulation analysis and experimental data. Limnol. Oceanogr-Meth. **4:** 294-307

Dalsgaard, T., J. D. Zwart, L. A. Robertson, J. Kuenen and G., and N. P. Revsbech. 1995 Nitrification, denitrification and growth in artificial Th*iosphaera pantotropha b*iofilms as measured with a combined microsensor for oxygen and nitrous oxide. FEMS Microbiol. Ecol. **17:** 137-148

de Beer, D., F. Wenzhofer, T. G. Ferdelman, S. E. Boehme, M. Huettel, J. E. E. van Beusekom et al. 2005 Transport and mineralization rates in North Sea sandy intertidal sediments, Sylt-Rømø Basin, Wadden Sea. Limnolo. Oceanogr. **50:** 113-127

Emery, K. O. 1968. Relict sands on continental shelves of the world. Am. Assoc. Petrol.Geo. Bull. **52:** 445-464

Gray, N. F. 1990. *Activated sludge : theory and practice*. Oxford University Press, Oxford, United Kingdom

Hall, P. J., and R. C. Aller. 1992. Rapid, small-volume, flow injection analysis for $\sum CO_2$, and NH_4^+ in marine and freshwaters. Limnol. Oceanogr. **37:** 1113-1119

Hayatsu, M., K. Tago, and M. Saito. 2008. Various players in the nitrogen cycle: Diversity and functions of the microorganisms involved in nitrification and denitrification. Soil Sci. Plant Nutr. **54:** 33-45

Huang, H. K., and S. K. Tseng. 2001. Nitrate reduction by Citrobacter diversus under aerobic environment. Appl. Microbiol. Biot. **55: 9**0-94

Huettel, M., and A. Rusch (2000) Transport and degradation of phytoplankton in permeable sediment. Limnol. Oceanogr. **45:** 534-549

Huettle, M., and G. Gust. 1992. Impact of bioroughness on interfacial solute exchange in permeable sediments. Mar. Ecol-Prog, Ser. **89:** 253-267

Hulth, S., R. C. Aller, D. E. Canfield, T. Dalsgaard, P. Engstrom, F. Gilbert et al. 2005. Nitrogen removal in marine environments: recent findings and future research challenges. Mar. Chem. **94:** 125-145

Hunter, E. M., H. J. Mills, and J. E. Kostka. 2006. Microbial community diversity associated with carbon and nitrogen cycling in permeable shelf sediments. Appl. Environ. Microb. **72:** 5689-5701

Jahnke, R. A., J. R. Nelson, R. L. Marinelli, and J. E.Eckman. 2000. Benthic flux of biogenic elements on the Southeastern US continental shelf: influence of pore water advective transport and benthic microalgae. Cont. Shelf Res. **20:** 109-127

Jansen, S., E. Walpersdorf, U. Werner, M. Billerbeck, M. Böttcher, D. de Beer. 2009. Functioning of intertidal flats inferred from temporal and spatial dynamics of O_2, H_2S and pH in their surface sediment. Ocean Dynam. **59:** 317-332

Johnson, H. D., and C. T. Baldwin1986. Shallow siliciclastic seas. In Reading, HG (Ed.) *Sedimentary environments and facies (2nd ed.).* Blackwell Scientific Publications, Oxford, **pp 229-282.**

Larsen, L. H., T. Kjaer, and N. P. Revsbech. 1997. A microscale NO_3^- biosensor for environmental applications. Anal. Chem. **69:** 3527-3531

Laursen, A. E., and S. P. Seitzinger. 2002. The role of denitrification in nitrogen removal and carbon mineralization in Mid-Atlantic Bight sediments. Cont. Shelf Res. **22:** 1397-1416

Lloyd, D., L. Boddy, K. J. P Davies. 1987. Persistence of Bacterial Denitrification Capacity under Aerobic Conditions - the Rule Rather Than the Exception. FEMS Microbiol. Ecol. **45:** 185-190

Mills, H. J., E. Hunter, M. Humphrys, L. Kerkhof, L. McGuinness, M. Huettel, J. E Kostka. 2008. Characterization of nitrifying, denitrifying, and overall bacterial communities in permeable marine sediments of the northeastern Gulf of Mexico. Appl. Environ. Microb. **74:** 4440-4453

Nielsen, L. P. 1992. Denitrification in sediment determined from nitrogen isotope pairing. FEMS Microbiol. Ecol. **86:** 357-362

Patureau, D., E. Zumstein, J. P. Delgenes, and R. Moletta. 2000. Aerobic denitrifiers isolated from diverse natural and managed ecosystems. Microbial Ecol. **39:** 145-152

Ploug, H. 2001 Small-scale oxygen fluxes and remineralization in sinking aggregates. Limnol. Oceanogr. **46:** 1624-1631

Polerecky, L., U. Franke, U. Werner, B. Grunwald, D. de Beer. 2005. High spatial resolution measurement of oxygen consumption rates in permeable sediments. Limnol. Oceanogr-Meth. **3:** 75-85

Rao, A. M. F., M. J. McCarthy, W. S. Gardner, and R. A. Jahnke. 2007. Respiration and denitrification in permeable continental shelf deposits on the South Atlantic Bight: Rates of carbon and nitrogen cycling from sediment column experiments. Cont. Shelf Res. **27:** 1801-1819

Rao, A. M. F., M. J. Mccarthy, W. S. Gardner, and R. A. Jahnke 2008. Respiration and denitrification in permeable continental shelf deposits on the South Atlantic Bight: N2:Ar and isotope pairing measurements in sediment column experiments. Cont. Shelf Res. **28:** 602-613

Revsbech, N. P. 1989. An oxygen microsensor with a guard cathode. Limnol. Oceanogr. **34:** 474-478

Robertson, LA, and J. G. Kuenen. (1984) Aerobic Denitrification - a Controversy Revived. *Arch Microbiol.* **139:** 351-354

Robertson, L. A., and J. G. Kuenen. 1988. Heterotrophic Nitrification in Thiosphaera-Pantotropha - Oxygen-Uptake and Enzyme Studies. J. Gen. Microbiol. **134:** 857-863

Robertson, L. A., T. Dalsgaard, N. P. Revsbech, and J. G. Kuenen. 1995. Confirmation of 'aerobic denitrification' in batch cultures, using gas chromatography and 15N mass spectrometry. FEMS Microbiol. Ecol. **18:** 113-119

Ronner, U., and F. Sorensson. 1985. Denitrification Rates in the Low-Oxygen Waters of the Stratified Baltic Proper. Appl. Environ. Microbiol. **50:** 801-806

Røy, H., J. S. Lee, S. Jansen, and D. de Beer. 2008. Tide-driven deep pore-water flow in intertidal sand flats. Limnol. Oceanogr. **53:** 1521-1530

Schmidt, I., O. Sliekers, M. Schmid, E. Bock, J. Fuerst, J. G. Kuenen et al. 2003. New concepts of microbial treatment processes for the nitrogen removal in wastewater. FEMS Microbiol. Rev. **27:** 481-492

Schramm, A., C. M. Santegoeds, H. K. Nielsen, H. Ploug, M. Wagner, and M. Pribylet al. 1999. On the occurrence of anoxic microniches, denitrification, and sulfate reduction in aerated activated sludge. Appl. Environ. Microb. **65:** 4189-4196

Seeberg-Elverfeldt, J., M. Schlüter, T. Feseker, and M. Kölling. 2005. Rhizon sampling of porewaters near the sediment-water interface of aquatic systems. Limnol. Oceanogr-Meth. **3:** 361-371

Shapleigh, J. 2006. The Denitrifying Prokaryotes. *In the Prokaryotes.* Springer New York, New York, **pp** 769-792

Thamdrup, B., and T. Dalsgaard 2002. Production of N_2 through Anaerobic Ammonium Oxidation Coupled to Nitrate Reduction in Marine Sediments. Appl. Environ. Microbiol. **68:** 1312-1318

Tiedje, J. M. 1988. Ecology of denitrification and dissimilatory nitrate reduction to ammonium. In: Zehnder, AJB (Ed.) *Environmental Microbiology of Anaerobes.* John Wiley and Sons, New York, **pp** 179-244

Tiedje, J. M., A. J. Sexstone, D. D. Myrold, and J. A. Robinson. 1982. Denitrification: ecological niches, competition and survival. Antonie Van Leeuwenhoek **48:** 569-583

Trevors, J. T., and M. E. Starodub. 1987. Effect of oxygen concentration on denitrification in freshwater sediment. J. Basic Microb. **27:** 387-391

Vance-Harris, C., and E. Ingall 2005. Denitrification pathways and rates in the sandy sediments of the Georgia continental shelf. Geochim. Cosmochim. Ac. **69:** A578-A578

Werner, U., M. Billerbeck, L. Polerecky, U. Franke, and M. Huettel. 2006. Spatial and temporal patterns of mineralization rates and oxygen distribution in a permeable intertidal sand flat (Sylt, Germany). Limnol. Oceanogr. **51:** 2549-2563

Zehr, J. P., and B. B.Ward. 2002. Nitrogen cycling in the ocean: New perspectives on processes and paradigms. Appl. Environ. Microb. **68:** 1015-1024

Zumft, W. 1997. Cell biology and molecular basis of denitrification. Microbiol. Mol. Biol. R. **61:** 533-616

Supplementary information:

Supplementary Table 1. Summary of the experimental conditions in the incubations.

Experiment	Sampling date	Depth (cm)	Tracer additions (µM)
Intact whole core incubation	Mar 17 2007	0 – 5	$^{15}NO_3^-$ (final concentration: 50µM) ($^{15}NH_4^+/^{14}NO_3^-$ +ATU*) (final concentration: 50, 50, 86µM)
Intact core by multi – microsensors	Mar 22 2007	0.5 1	NO_3^- in site sea water (~ 60µM)
Slurry incubation	Mar 22 2007	0 – 2 2 – 4 4 – 6	$^{15}NO_3^-$ (final concentration: 200µM) ($^{15}NH_4^+/^{14}NO_3^-$ +ATU*) (final concentration: 200, 200, 86µM)
Constant mixing, flow-through retention reactor incubation	April 28 2008	0 – 3	$^{15}NO_3^-$ (final concentration: 147µM)

Intensive and extensive nitrogen loss from intertidal permeable sediments of the Wadden Sea

Hang Gao,[a] Maciej Matyka,[a,1] Bo Liu,[a] Arzhang Khalili,[a,2] Joel E Kostka,[a,3] Gavin Collins,[a,4] Stefan Jansen,[a,5] Moritz Holtappels,[a,*] Marlene M Jensen,[a,6] Thomas H Badewien,[b] Melanie Beck,[b] Maik Grunwald,[c] Dirk de Beer,[a] Gaute Lavik,[a] and Marcel M M Kuypers[a]

[a]Max Planck Institute for Marine Microbiology, Bremen, Germany

[b]Institute of Chemistry and Biology of the Marine Environment, University Oldenburg, Oldenburg, Germany

[c]Helmholtz-Zentrum Geesthacht, Geesthacht, Germany

Current Addresses:

[1]Institute for Theoretical Physics, University of Wrocław, Wrocław, Poland

[2]Department of Earth and Environmental Sciences, Jacobs University Bremen, Bremen, Germany

[3]Department of Oceanography, Florida State University, Tallahassee, Florida, the United States

[4]Infrastructure and Environment, School of Engineering, University of Glasgow, Glasgow, Scotland, the United Kingdom

[5]Deltares, Princetonlaan 6, 3584 CB, Utrecht, The Netherlands

[6] Nordic Center of Earth Evolution (NordCEE) and Institute of Biology, University of Southern Denmark, Odense, Denmark

Acknowledgements

We thank Hans Roy, Frank Schreiber, Ingrid Dohrmann, and Hani Tahsk for their field support, and Gabriele Klockgether and Daniela Franzke for their technical support in the lab. We are grateful to Ronald Monas and Ole Pfeiler for the ship time and excellent collaboration. This research was funded by the Max Planck Society (MPG) and the German Research Foundation (DFG). HG was supported by the scholarships from German Academic Exchange Center (DAAD) and MPG.

Abstract

Nitrogen (N) loss rates were determined in permeable sediments of the Wadden Sea using a combination of stable N isotope incubation experiments and model simulation approaches during three seasons. Three different incubation methods that employed the isotope pairing technique (IPT) were used: intact core incubations simulating either 1) diffusive or 2) advective transport conditions and 3) slurry incubations. N-loss rates from core incubations under simulated advective transport conditions exceeded those rates measured under diffusive transport conditions by 1-2 orders of magnitude, but were comparable to those observed in slurry incubations. N-loss rates generally showed little seasonal and spatial variation (207 ± 30 μmol m^{-2} h^{-1}) in autumn 2006 and spring and summer 2007. Utilizing an extensive time series of nutrient concentrations and current velocities obtained from a continuous monitoring station, Nitrate and nitrite (i.e. NO_x^-) flux into the sediment was modeled over a full annual cycle. Fluxes were sufficient to support the experimentally derived N-loss rates. Combining the measured rates with the modeled results, an annual N-removal rate of 745 ± 109 mmol N m^{-2} yr^{-1} was estimated for permeable sediments of the Wadden Sea. This rate agrees well with previous N-loss estimates for the Wadden Sea based on N-budget calculations. Permeable sediments, accounting for 58-70% of the continental shelf area, are an important N-sink and their contribution to the global N-loss budget should be re-evaluated.

Keywords: nitrogen, permeable sediments, N-loss, denitrification, pore water advection
Running head: Nitrogen loss in the Wadden Sea permeable sediments

Introduction

Continental margin sediments represent a major sink of fixed nitrogen (N) in the oceanic N cycle (Gruber 2008; Thamdrup and Dalsgaard 2008). Benthic N_2 production in shelf sediments, derived from denitrification and anammox processes, accounts for 50-70% of fixed oceanic sedimentary N-loss in current budgets (Codispoti et al. 2001; Gruber et al. 2004; Codispoti 2007). Although the majority (58-70%) of continental margins is covered by coarse-grained relict sediments (Emery 1968; Johnson and Baldwin 1986), most previous biogeochemical research has focused on muddy or fine-grained shelf sediments, and the role of sandy sediments in N-loss has been largely ignored.

The seafloor of the Wadden Sea, one of the largest tidal systems in the world, is dominated by permeable or sandy sediments. Recent studies showed that porewater advection dominates chemical exchange at the sediment-water interface of the sandy seafloor, with advective transport exceeding the rate of molecular diffusion by several orders of magnitude (Precht and Huettel 2004; and references therein). Pressure gradients driven by waves and currents interact with sediment topography (Huettel and Gust 1992; Ziebis et al. 1996; Precht and Huettel 2003), and pump solutes and particles from the overlying water into the sediment (Rusch and Huettel 2000; Reimers et al. 2004; Werner et al. 2006). Advective transport leads to an acceleration of organic matter mineralization and a stimulation of biogeochemical cycling proportional to the extent of porewater exchange (Precht et al. 2004; de Beer et al. 2005; Franke et al. 2006). The high transport rates of organic matter and electron acceptors from the water column into the seafloor allow marine sands to act as an efficient filter for organic matter that may also facilitate N removal by denitrification. However, few studies have investigated N-loss by denitrification in coastal permeable sediments (Lohes et al. 1996; Eyre and Ferguson 2002; Vance-Harris and Ingall 2005); and of these studies, few have incorporated advective transport processes.

Recent laboratory studies using ^{15}N-labeling experiments showed that denitrification rates in marine sands under simulated advective conditions are substantially enhanced relative to diffusive conditions (Cook et al. 2006; Rao et al. 2007, 2008; Gihring et al. 2010). Furthermore, rapid rates of denitrification (> 50 μmol m^{-2} h^{-1})

were measured under oxic conditions in permeable sediments affected by advection (Rao et al. 2007, 2008; Gao et al. 2010). These studies suggest that N-loss in permeable sediments with advective pore water flow is much higher than previously perceived. However, temporally and spatially resolved sedimentary N_2-production rates as well as estimates for the benthic NO_x porewater flux have so far been missing.

In this study, we use a combination of ^{15}N-labeling experiments and a flux model based on annual monitoring data of NO_x concentrations and bottom current velocities to determine N-loss from permeable sediments of the worlds largest tidal system, the Wadden Sea. The consistency of measured N-loss rates at different sites and during different seasons allows extrapolating the results to the entire Wadden Sea area. This study provides to our knowledge the first regional estimates of N-loss from permeable sediments based on experimental data. Our results are comparable with N-loss estimates for the Wadden Sea based on N budget calculations.

Methods

Study sites—The Wadden Sea, located in the southeastern part of the North Sea, stretches from Den Helder in the Netherlands in the southwest, past the great river estuaries of Germany, to its northern boundary at Skallingen north of Esbjerg in Denmark. The Wadden Sea covers 500 km of coastline, and encompasses a total area of about 14,700 km^2 (Fig. 1a). One third of it is mainly composed of intertidal flats, and approximately 93% of the seafloor is covered by coarse, sandy or mixed sediments (Common Wadden Sea Secretariat 2008).

Janssand is a typical intertidal sand flat in the central Wadden Sea that has been intensively studied as a hotspot of biogeochemical cycling (Al-Raei et al. 2009; Jansen et al. 2009). The Janssand flat, located in the back barrier area of Spiekeroog Island in the German Wadden Sea (Fig. 1b), consists mainly of well-sorted sands with a mean grain size of 176 μm, porosities of 35% to 40% , and permeabilities ranging from 0.5 to 9.5 × 10^{-12} m^2 (Billerbeck et al. 2006). The western edge of the flat faces a 17 m-deep tidal channel separating the barrier islands Spiekeroog and Langeoog. The entire Janssand flat is inundated with ~ 2 m of seawater for 4-6 h during each semi-diurnal tidal cycle and exposed to air for 6-8 h during low tide. Along the sloping margin from the central flat

region to the low water line, two representative sites were visited for detailed investigations of N-loss processes using slurry incubations and intact core incubations simulating either diffusive or advective transport conditions (Table 1). An 'upper flat' site (UF) is located approximately 80 m upslope, and a 'middle flat' site (MF) lies in between the low water line and UF (Fig. 1c). UF was chosen as a proxy for the central region, composed mainly of sandy sediments. The central tidal flat exhibits little to no incline, and its physical appearance is homogeneous. MF is along the edge of the tidal flat and in general entirely exposed during low tide. These two sites were investigated using the flat-bottom ships *Spes Mea* in October 2006 and *Doris von Ochtum* in March and August 2007.

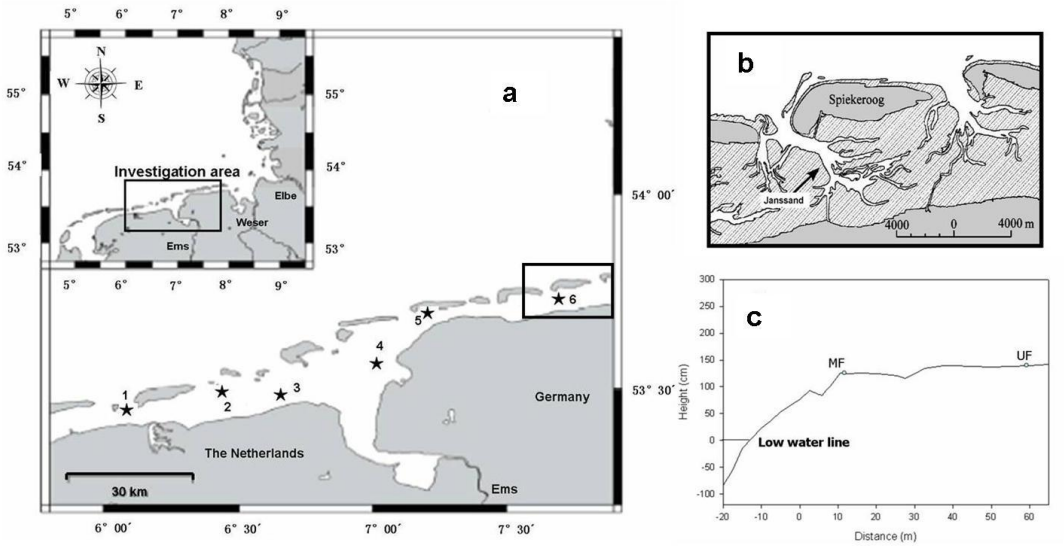

Figure 1: (a) Intertidal sand flats sampled in 2006 along a transect in the East Frisian Wadden Sea. Stations labeled from 1 to 6 are Engelsmanplaat, Simonszand, Horsbornzand, Kopersand, Hohes Riff and Janssand, respectively. (b) Location of Janssand (arrow), the primary sand flat studied. (c) The topography and the sampling sites 'middle flat' (MF) and 'upper flat' (UF) at Janssand. The average water level at low tide (low water line) is used as reference point for the height.

To address the spatial variation of N-loss processes throughout the Wadden Sea, we investigated additional five intertidal sand flats between the island Ameland (The Netherlands) and the island Spiekeroog (Germany) in October 2006 (Fig. 1a, Table 1). At all sites, sampling was conducted in the central region of the respective flats, and N-loss

rates were investigated using intact core incubation simulating advective transport conditions (*see* below).

Physical and chemical analysis—Time series measurements were performed at a station nearby the Janssand flat in the tidal inlet between the Islands Spiekeroog and Langeoog (Table 1). In situ temperature was determined from October 2006 to October 2007 using a temperature sensor (Pt100) mounted at the time series station. For validation, conductivity, temperature, and depth (CTD)-measurements were conducted at regular intervals (Reuter et al. 2009). Bottom water current velocities were measured using an in situ acoustic doppler current profiler (ADCP, 1200 KHz, workhorse sentinal, Teledyne RD Instruments) in July 2009 and April 2010. In July 2009, current velocities were monitored by a downward looking ADCP mounted on a boat nearby the central Janssand. Flow velocities were measured from 80 cm above the sediment surface with a vertical resolution of 25 cm every 5 seconds for each ping. The same instrument was mounted upward looking on a bottom metal frame at the central Janssand flat over four tidal cycles in April 2010. For the upward deployments, the ADCP was mounted 9 cm above the sea floor and measured with a vertical resolution of 10 cm and a measuring interval of 10 sec for 60 pings.

In parallel, real-time monitoring of NO_x^- concentration of near surface water was conducted with an in situ automated nutrient analyzer (Systea, μMac1000, Grunwald et al. 2010) at the time series station. Concentrations of dissolved NO_3^- and NO_2^- were determined hourly after automated filtration using a loop-flow reactor and loop-flow analysis technology combined with conventional photometry (Grunwald et al. 2007). The detection limit for NO_x^- is approximately 0.2 μmol L^{-1} (Grunwald et al. 2010). For this study, a time series of NO_x^- data from October 2006 to October 2007 was used.

NO_x^- samples were also taken in parallel to the incubation experiments. At the sites and time periods when cores were collected for rate measurements, seawater was collected during low tide and filtered through a 0.2 μm syringe filter. Seawater was sampled before and after amendment with N isotope tracer. Porewater sampling was performed in sediments during exposure, using a Rhizon method modified from Seeberg-Elverfeldt et al. (2005). A metal plate with holes at 1-1.4 cm intervals down to 15 cm was pushed into sediments. Rhizon samplers were inserted into the undisturbed sediments and

Table 1. Summary of measurements at different study sites and seasons

Sampling season	Sampling sites	Measurements					
		DIN (NO_2^-, NO_3^-)	O_2	Current velocity	Intact core incubations		Slurry incubations
					tracer	method	tracer
Oct 2006	Engelsmanplaat, Simonszand, Horsbornzand, Kopersand, Hohes Riff	Site sea water and Seawater amendment with tracer			$^{15}NO_3^-$	percolation	
	Janssand upper flat			from current velocity data in Billerbeck et al. (2006)	$^{15}NO_3^-$	percolation	
	Janssand middle flat		O_2 microsensor		$^{15}NO_3^-$	percolation and diffusion	
Mar 2007	Janssand upper flat	Site sea water and Seawater amended with tracer	O_2 microsensor	ADCP measurement in Apr 2010	$^{15}NO_3^-$	percolation and diffusion	$^{15}NO_3^-$ with aerated seawater
	Janssand middle flat						
Aug 2007	Janssand upper flat	Site sea water and Seawater amended with tracer	O_2 microsensor	ADCP measurement in Jul 2009	$^{15}NO_3^-$	percolation and diffusion	$^{15}NO_3^-$ with aerated seawater
	Janssand middle flat						

mounted through the holes on the metal plate with only the sampling ports protruding from the sediments. In situ pore water samples were directly extracted from these ports with sterile hypodermic syringes. All nutrient samples were frozen at -20 °C immediately after sampling. NO_x^- was determined by chemiluminescence after reduction to NO with acidic vanadium(II) chloride (Braman and Hendrix, 1989).

^{15}N labeling experiments— To investigate the N-loss in permeable sediments of the Wadden Sea, the isotope pairing technique (IPT) (Hauck et al. 1958) has been applied in slurry incubations as well as in intact core incubations, simulating either diffusive or advective flow conditions.

The diffusive approach follows the protocol described by Nielsen (1992). For each experiment, 15 sediment cores were collected with Plexiglas push-cores (inner diameter (i.d.), 3.5 cm; height, 28 cm). The water overlying the 10 cm thick sediment cores was replaced with site sea water amended with $^{15}NO_3^-$- to a final concentration of 50 μmol L^{-1}. The labeling percentages ranged from 41 to 99 %. The cores were immediately sealed without any headspace by rubber stoppers and pre-incubated for 2 h at in situ temperature. The overlying water was continuously mixed by externally driven magnetic stirring bars at approximately 60 revolutions per minute (rpm) during the incubations. After pre-incubation, triplicate cores were destructively sampled at regular intervals (0 h, 1 h, 2 h, 4 h and 6 h). Before sampling, 1 mL of zinc chloride ($ZnCl_2$) (50% w:v) was added to the sediment surface by opening each core lid stopper. The cores were immediately resealed without any headspace and mixed by inversion. After allowing sediment particles to settle, an aliquot of water for N_2 gas analysis was removed from each core and transferred to a 12 mL Exetainer ^{TM} (Labco), pre-filled with 200 μL saturated $HgCl_2$. The advective approach is described by Gao et al. (2010) and de Beer et al. (2005). In detail, fifteen sediment cores were collected in parallel to those used for the diffusive approach. The overlying water in each core was replaced with aerated site sea water amended with $^{15}NO_3^-$- to a final concentration of 50 μmol L^{-1} (labeling percentages as described above). Rubber bottom and top stoppers of the cores were equipped with valves to allow the percolation of the overlying water through the sediment column. De Beer et al. (2005) used this method to continuously percolate water through the sediment column. In this study, the percolation was performed only once at the beginning of the

experiment. Each core was rapidly percolated from top to bottom with 20 mL labeled seawater, thus exchanging the porewater of the upper 5 cm of the sediment. The percolation of all 15 intact cores was performed within 25 min at an average flow of 12 mL min^{-1}. Cores were immediately sealed without any headspace by rubber stoppers after percolation, incubated at in situ temperature (~13°C in October 2006, ~9°C in March 2007 and ~20°C in August 2007) and were destructively sampled in triplicate at regular intervals between 0 and 6 hours (0 h, 1 h, 2 h, 3 h, and 4 h in summer and 0 h, 1 h, 2 h, 4 h, and 6 h in winter). The overlying water of all cores was mixed continuously at approximately 60 rpm during the incubations by externally-driven magnetic stirring bars. Cores were sacrificed in reverse order of percolation. Subsamples for rate determination were obtained in the same way as described in the diffusive approach.

Slurry incubations were performed at the Janssand sites as described by Gao et al. (2010) and N_2 productions were examined in gas impermeable bags using ^{15}N tracer isotope pairing technique according to Thamdrup and Dalsgaard (2002). Sediments were sampled using Plexiglas push-cores (i.d., 9.5 cm; height, 60 cm). The sediment core was sectioned into 2 cm depth intervals to a depth of 6 cm. The sectioned sediment was transferred into gas-tight bags and mixed with air-saturated seawater from the study site at a volume ratio of 1:1.4. After removing the entire gas phase, the bags were sealed and $^{15}NO_3^-$ was injected through the rubber stopper into the bags to a final concentration of 200 μmol L^{-1} (labeling percentages ranged from ~70% to ~99%). Bags were mixed well and incubated at in situ temperature. During the incubation, the bags were periodically shaken to ensure a homogenous distribution of labeled N_2. Subsamples of the interstitial water were collected from the bags immediately before and after the addition of the tracer and at regular time intervals up to 16 hours. The withdrawn subsamples were preserved in 6 mL Exetainer ™ vials (Labco) without any headspace, each of which was pre-filled with 100 μL saturated $HgCl_2$.

Oxygen concentrations in slurry subsample were measured as described by Gao et al. (2010). Oxygen concentrations were measured directly after subsampling from the bags using oxygen microsensors. The sample vials were uncapped and a calibrated O_2 microsensor was inserted into the bottom of each vial for ~10 seconds until the sensor

signal stabilized. Sample vials were recapped immediately to avoid significant gas exchange.

^{15}N-N_2 measurements and rate calculations— A 1 mL Helium headspace was introduced to each sample vial. The isotope ratios of dinitrogen gas ($^{29}N_2/^{28}N_2$ and $^{30}N_2/^{28}N_2$) in the headspace were determined by gas chromatography-isotope ratio mass spectrometry (GC-IRMS; VG Optima) by direct injection of the sample headspace. Concentrations of $^{30}N_2$ and $^{29}N_2$ were calculated from the excess relative to air according to Holtappels et al. (2011). Incubations without a significant linear trend in concentration over time ($p > 0.05$) were discarded. For further calculations we do not consider N-loss via anammox since $^{29}N_2$ production in slurry incubations with added $^{15}NH_4^+$, $^{14}NO_3^-$ and allylthiourea (ATU) was insignificant (data not shown here). It can be assumed that denitrification is the sole N-loss process.

For intact core incubations using either the diffusive or advective approach, denitrification of $^{14}NO_3^-$ and $^{15}NO_3^-$ (D_{14} and D_{15}) is calculated from the production of $^{29}N_2$ ($p^{29}N_2$) and $^{30}N_2$ ($p^{30}N_2$) over the first 4 (March) and 2 (August) hours according to Nielsen (1992):

$$D_{15} = p^{29}N_2 + 2 \cdot p^{30}N_2 \quad (1)$$

$$D_{14} = \left(p^{29}N_2 / \left(2 \cdot p^{30}N_2\right)\right) \cdot \left(p^{29}N_2 + 2 \cdot p^{30}N_2\right) \quad (2)$$

We have strong arguments to assume that the advective NO_x^- transport from bottom waters into the first centimeters of the permeable sediment is not limiting denitrification under in situ conditions (*see* discussion below). We therefore did not distinguish between D_{14} and D_{15} in the whole core incubations. Thus, total N-loss via denitrification (D_{tot}) is calculated as

$$D_{tot} = D_{14} + D_{15} \quad (3)$$

In slurry incubations, total N-loss via denitrification (D_{tot}) is calculated from the production of $^{30}N_2$ over the first 4 hours according to Thamdrup and Dalsgaard (2002):

$$D_{tot} = 2 \cdot p^{30}N_2 / (F_{^{15}NO_3})^2 \quad (4)$$

where $F_{^{15}NO_3}$ is the labeling percentage of nitrate. $F_{^{15}NO_3}$ is derived directly from the known amount of added $^{15}NO_3^-$ and the measured concentration of $^{14}NO_3^-$ in the added seawater:

$$F_{^{15}NO_3} = {}^{15}NO_3^- / \left({}^{14}NO_3^- + {}^{15}NO_3^- \right) \quad (5)$$

The initial labeling percentage ($F_{^{15}NO_3}$) may differ from the labeling percentage at a later time point ($F'_{^{15}NO_3}$) if the production of $^{14}NO_x^-$ via nitrification dilutes the initial labeling percentage. Assuming that denitrification is the only N-loss process and that random isotope pairing of $^{14}NO_x^-$ and $^{15}NO_x^-$ leads to binomially distributed N_2 species $^{28}N_2$, $^{29}N_2$ and $^{30}N_2$ (Hauck 1958, Nielsen 1992), $F'_{^{15}NO_3}$ can be calculated from the production of $^{29}N_2$ and $^{30}N_2$ according to

$$F'_{^{15}NO_3} = 2 / (p^{29}N_2 / p^{30}N_2 + 2) \quad (6)$$

Here, D_{tot} in slurry incubations (Eq. 4) was determined using $F'_{^{15}NO_3}$ instead of $F_{^{15}NO_3}$ with $p^{29}N_2$ and $p^{30}N_2$ calculated over the first 4 hours. It should be mentioned that D_{tot} derived from combining Eqs. 4+6 is essentially equal to D_{tot} derived from combining Eqs. 1-3.

In the absence of anammox $F'_{^{15}NO_3}$ represents the actual labeling percentage of the denitrified NO_x^- pool during the incubation. A decrease of $F'_{^{15}NO_3}$ from the initial $F_{^{15}NO_3}$ indicates that the ^{15}N-labeling percentage was lowered during the incubation, most probably by the oxidation of $^{14}NH_4^+$ to $^{14}NO_x$ (nitrification). If and to what extend the presence of oxygen and any nitrification activity violates the steady state assumption of the IPT method is discussed below.

Model of NOx influx—Tidal flats in the Wadden Sea are dominated by highly permeable sandy sediments with rippled topography. Two dominant forces - waves and tidal currents - interacting with bottom topography, generate pressure gradients that drive the exchange of pore water with the overlying water. To simplify the model, only the force of tidal currents was incorporated. Due to the higher permeability, advective transport in sandy sediments exceeds the diffusive transport in the muddy sediments by orders of magnitude (Precht and Huettel et al. 2004). Based on a 2-dimensional single ripple model for permeable sediments presented by Huettel et al. (1996), a multiply rippled porous domain was constructed (Fig. 2a).

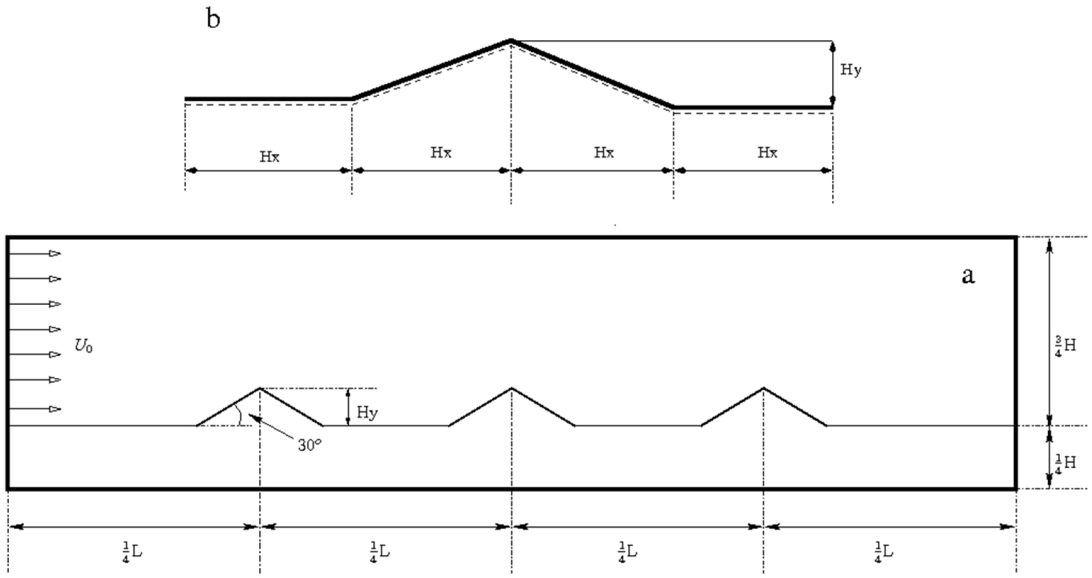

Figure 2: (a) Schematic of the multiple ripples domain. The domain was composed of three ripples, and the slope of each ripple is assumed to be 30 degrees. The center points of three triangular ripples were located at ¼L, ½L and ¾L beginning from the left. The vertical position of the interface line at the flat part was at ¼H. The inlet velocity was assumed to follow a uniform distribution U_0. (b) One ripple component. The dashed line represents the interface line. H_y is the height and $4H_x$ are the length of each ripple.

According to the topography of surface sediments at Janssand, the height of the ripple (Hy) was set to 2 cm, while the horizontal extent of a single ripple is divided into four equal lengths of Hx=3.46 cm (Fig. 2b). The permeability and porosity of the sediment was obtained in measurements as k=10^{-12} m^2 and φ=0.39, respectively. The inlet velocity (U_0) was taken in the range from 5 × 10^{-3} to 5 × 10^{-2} m s^{-1}. The fluid flow calculation in and above the sediment is based on the lattice Boltzmann method (LBM). Moreover, the velocity and pressure field were calculated from an extended Darcy equation (Guo and Zhao 2002).

For the computation of the velocity and pressure field, the hydrodynamics of percolation is characterized by the Reynolds number Re, here defined by the equation:

$$\mathrm{Re} = U_0 \cdot Hy \cdot \nu^{-1} \qquad (7)$$

The symbol v in Eq. 7 denotes the kinematic viscosity of the seawater, which is a function of temperature T (in °C). The relationship between v and T can be expressed by the following equation (Kampmeyer 1952; Perry and Green 1984):

$$\nu = 1.35 \cdot 2.5^{(-0.047T)} + 0.435 \quad (8)$$

where v has the unit of 10^{-6} m^2 s^{-1}. Revealed from the computation results, the flow shows an unsteady nature when Re is more than 100 ($U_0 > 5 \times 10^{-3}$ m s^{-1}). Therefore, an averaging procedure for velocity fields was performed over approximately 10^7 time steps, equivalent to one hour. The convergence criterion is the time-independent average inward flow velocity (U_{in}), which was defined as a sum of velocity components normal to the interface line. In order to avoid overestimation of the flux due to high velocities close to the interface line, U_{in} was calculated a few lattice nodes below the interface (dashed line in Fig. 2). Calculations were carried out for a range of Reynolds numbers, Re=100, 200, 400, 600 and 1000 with the corresponding U_0 = 0.5, 1, 2, 3, 5 × 10^{-2} m s^{-1}. For a given range of parameters it was found that U_{in} can be expressed as an exponential function of the Reynolds number using the equation:

$$U_{in} = a \cdot \mathrm{Re}^b \quad (9)$$

The fitting procedure gave a=2.57×10^{-10} [m h^{-1}] and b=2.62 [-] and a similar equation was also reported to confirm our modeled results (Cardenas and Wilson 2007). This relation was used to extrapolate U_{in} to higher Reynolds numbers in order to cover the full range of current velocities measured at Janssand.

Assuming advective transport from the water column into the sediment (U_{in}) and a constant NO_x^- concentration in the overlying water (C_N), the inward advective NO_x^- flux (F_N) across the water-sediment interface is expressed by:

$$F_N = U_{in} \cdot C_N \quad (10)$$

Results

NO_x porewater profiles—Representative results of NO_x^- concentrations in the porewater during the first 1-2 hours of exposure are shown in figure 3a and 3b. In October 2006, NO_x^- concentrations in the porewater decrease from 7 μmol L^{-1} at the surface to 1 μmol L^{-1} at 3.5 cm depth (Fig. 3a). In March 2007, NO_x^- concentrations

decrease from 42 μmol L^{-1} at the surface to 5 μmol L^{-1} at 5.8 cm depth (Fig. 3a). The dynamic change of NO_x^- concentration over time is exemplified by consecutive porewater measurements (Fig. 3b). Because porewater is stagnant during times of exposure, the NOx supply from the bottom water ceased and NOx consuming processes cause the rapid decrease of NO_x^- concentrations during the first 80 minutes of exposure. NO_x^- consumption calculated from these porewater profiles was 1.2 mmol N m^{-2} h^{-1}.

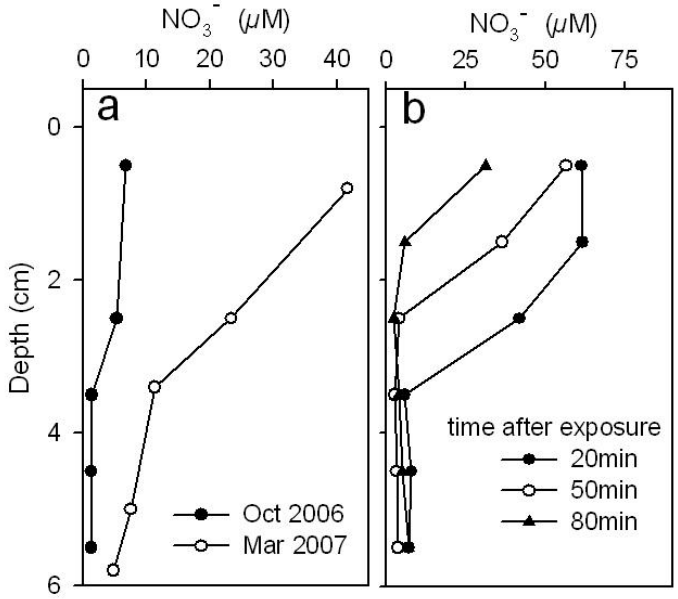

Figure 3: (a) NO_x^- concentrations in the porewater during the first hour of exposure in October 2006 and March 2007. (b) Consecutive NO_x^- porewater measurements during the first 1.5 hours of exposure in March 2007. The measurements in March 2007 shown in panel (a) and (b) were made at different days. The measurement site is Janssand, middle flat.

N-loss from sediment core and slurry incubations—Constant production of $^{29}N_2$ and $^{30}N_2$ over the first 4 hours was observed in core incubations under simulated diffusive as well as advective transport conditions (representative results shown in Fig. 4a+b). Under diffusive transport conditions, the observed total N-loss rates (D_{tot}) ranged from below detection to 19 ± 7 μmol N m^{-2} h^{-1}. Under simulated advective transport conditions, N-loss rates were consistently 1-2 orders of magnitude higher (169 - 238 μmol N m^{-2} h^{-1}) (Table 2). In slurry incubations, oxygen was present during the first 4-6 hours in March and during the first 1-2 hours in August (representative results shown in Fig. 4 c+d). Despite the initial presence of O_2, a constant production of $^{29}N_2$ and $^{30}N_2$ was observed

during all seasons, consistent with the previous findings of Gao et al. (2010). N-loss rates obtained from slurry incubations ranged between 144 and 303 μmol N m^{-2} h^{-1} when integrated over the upper 5 cm depth, and largely agreed with rates measured in percolated sediment cores (Table 2).

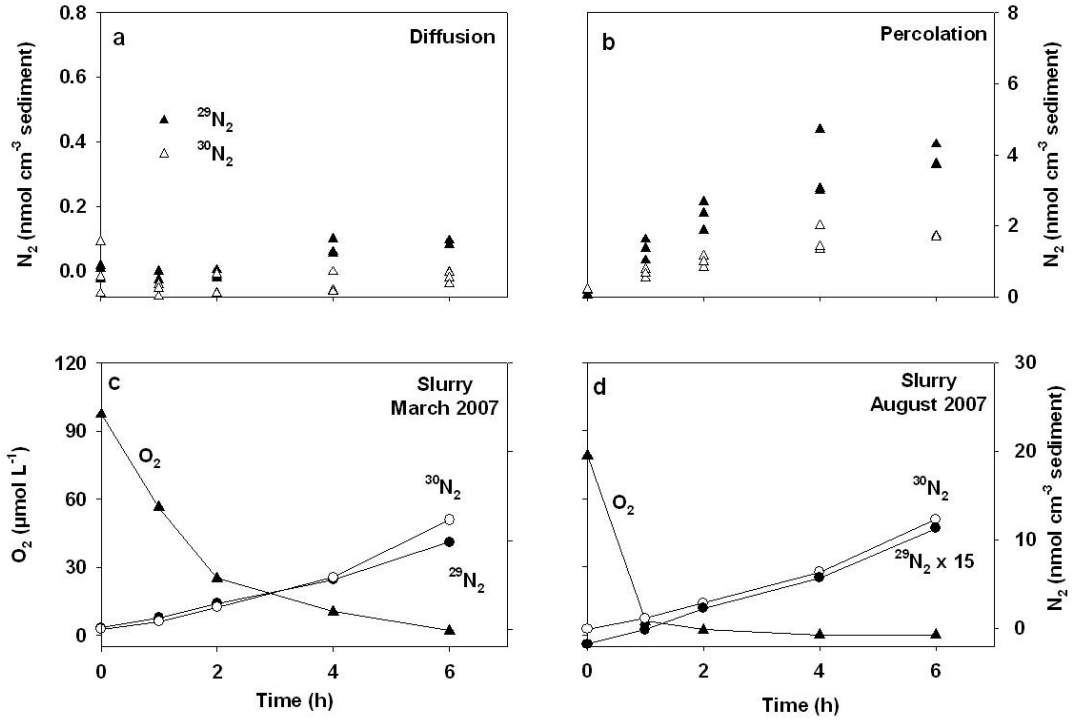

Figure 4: $^{29}N_2$ and $^{30}N_2$ concentration over time in intact core incubations simulating diffusive conditions (a) and advective conditions (b) in March 2007. Labeled N_2 and oxygen concentration over time in slurry incubations of the upper sediment (0-2cm) in March 2007 (c) and August 2007 (d). Note that $^{29}N_2$ in panel d was multiplied by 15 to fit the same scale.

Spatial and temporal variability of benthic N-loss—The temporal and spatial variability of N-loss rates measured either in slurries or percolated cores was minor. In March 2007, the N-loss rates in percolated cores were slightly higher at the upper flat in comparison to the middle flat (230 and 169 μmol N m^{-2} h^{-1}, respectively), while in August 2007 the N-loss rates were not significantly different between the same sampling sites (188 and 209 μmol N m^{-2} h^{-1}, respectively). In March and August 2007, N-loss rates obtained from slurry incubation were comparable to those obtained from percolated cores and showed similar deviations between the sampling sites (Table 2). In general, N-loss rates between the upper and middle flat in the 3 field campaigns were consistent (on

average ~ 200 μmol N m^{-2} h^{-1}) with the exception of the N-loss rate measured in the middle flat in October 2006, which was 5-fold increased. However, at the same time the N-loss rate at the upper flat was 238 μmol N m^{-2} h^{-1}, which was again similar to rates measured in March and August 2007 (Table 2).

Table 2. N-loss rates determined from intact core and slurry incubations at Janssand.

Sampling season	Sampling sites	N-loss rates (μmol m^{-2} h^{-1}) ± standard error		
		intact core incubation diffusion	intact core incubation percolation (down to 5 cm)	slurry incubation (integrated to 5 cm)
Oct 2006	upper flat	-----	238.4 ± 41.8	-----
	middle flat	9.5 ± 0.4	1056.2 ± 162.6	-----
Mar 2007	upper flat	4.7 ± 0.7	230.0 ± 24.0	303.4 ± 10.2
	middle flat	not detectable	168.9 ± 13.7	144.2 ± 11.8
Aug 2007	upper flat	18.9 ± 7.1	188.5 ± 43.7	179.3 ± 7.0
	middle flat	8.6 ± 1.3	209.2 ± 28.9	262.1 ± 24.5

Table 3. N-loss rates determined at sand flats along a transect in the East Frisian Wadden Sea.

Sampling season	Site No.	Site name	Latitude / Longitude	N-loss rates (μmol N m^{-2} h^{-1}) ± standard error
Oct 2006	1	Engelsmanplaat	53°26.2'N, 06°04.4'E	175.9 ± 57.4
	2	Simonszand	53°30.3'N, 06°25.3'E	185.1 ± 14.2
	3	Horsbornzand	53°29.17'N, 06°39.46'E	236.9 ± 8.4
	4	Kopersand	53°34'N, 07°01'E	288.6 ± 51.0
	5	Hohes Riff	53°41.5'N, 07°12.7'E	255.6 ± 101.1
	6	Janssand	53°44.11'N, 7°41.95'E	238.4 ± 41.8

In October 2006, N-loss rates were investigated at six stations along a transect through the East Frisian Wadden Sea. The rates were similar to those measured at

Janssand ranging from 176 to 289 μmol N m^{-2} h^{-1} (Table 3). The rates at the eastern stations (Sta. 3-6) were slightly increased compared to western stations (Sta. 1 and 2) (Fig. 1a). However, the variation along the 100 km transect was small. In summary, at the transect sites and during the three sampling campaigns at Janssand (Tables 2 and 3), N-loss rates in percolated cores varied by less than a factor of 2 (with the exception of the high rate at the middle flat in October 2006).

Modeled NO_x^- fluxes from overlying water into permeable sediments—Current velocities at 10-50 cm above the sediment were measured in July 2009 and April 2010. The velocities presented in Figure 5 were measured in April 2010 and averaged over 4 complete inundation periods (about 4 hours of a full tidal cycle). During the rising tide, an initial current velocity of 41.5 cm s^{-1} was measured, which decreased to a minimum of 7.6 cm s^{-1} at high tide. At falling water level, the current velocity increased to a maximum of 36 cm s^{-1} and, thereafter, decreased to 25 cm s^{-1} during the last hour of inundation. Current velocities during the individual inundation periods were consistent and comparable to current velocity measurements in July 2009. In general, current velocities in the Wadden Sea are governed by tidal forces and wind, and show little seasonal variation with the exception of storm events (Badewien et al. 2009; Bartholomä et al. 2009). Hence, the averaged values presented in Fig. 5 were used as U_0 to calculate the inward flow velocities into the sediment (U_{in}) from Eqs. 7-9.

In general, NO_x^- concentrations in the water column nearby Janssand exhibited a strong seasonal variability. NO_x^- concentrations ranging from below 1 to up to 110 μmol L^{-1} were measured by Grunwald et al. (2010) between January 2006 and December 2008. For the model, NO_x^- concentrations measured between October 2006 and October 2007 were applied. Concentrations were negatively correlated with temperature, but positively correlated with the loading of dissolved inorganic nitrogen estimated previously from riverine input (Van Beusekom and de Jonge 1998; Grunwald et al. 2010). In winter 2006 and early spring 2007, daily averaged NO_x^- concentrations in the water column increased to maximum values of 40 μmol L^{-1}. During early summer, the NO_x^- concentrations declined rapidly to values of around 1 μmol L^{-1}. NO_x^- concentration then gradually increased to 5-10 μmol L^{-1} in the late summer and autumn.

Measured NO_x^- concentrations (C_N) and modeled inward flow velocites (U_{in}) were used to calculate the NO_x^- flux (F_N) over a full inundation period according to Eq. 10. An example of modeled NO_x^- fluxes in March 2007 is shown in Figure 5. There, the mean NO_x^- concentration and temperature were 32 μmol L^{-1} and 7.3°C, respectively, and therefore, the simulated NO_x^- flux is responding to the current velocity only (*see* Eqs. 7-10). The estimated NO_x^- flux into the sediments was 700 μmol m^{-2} h^{-1} at low velocities and increased to 4.3×10^4 μmol m^{-2} h^{-1} at maximum velocities. The NO_x^- flux averaged over the full inundation period was $1.5 \times 10^4 \pm 3.0 \times 10^3$ μmol m^{-2} h^{-1} (Fig. 5).

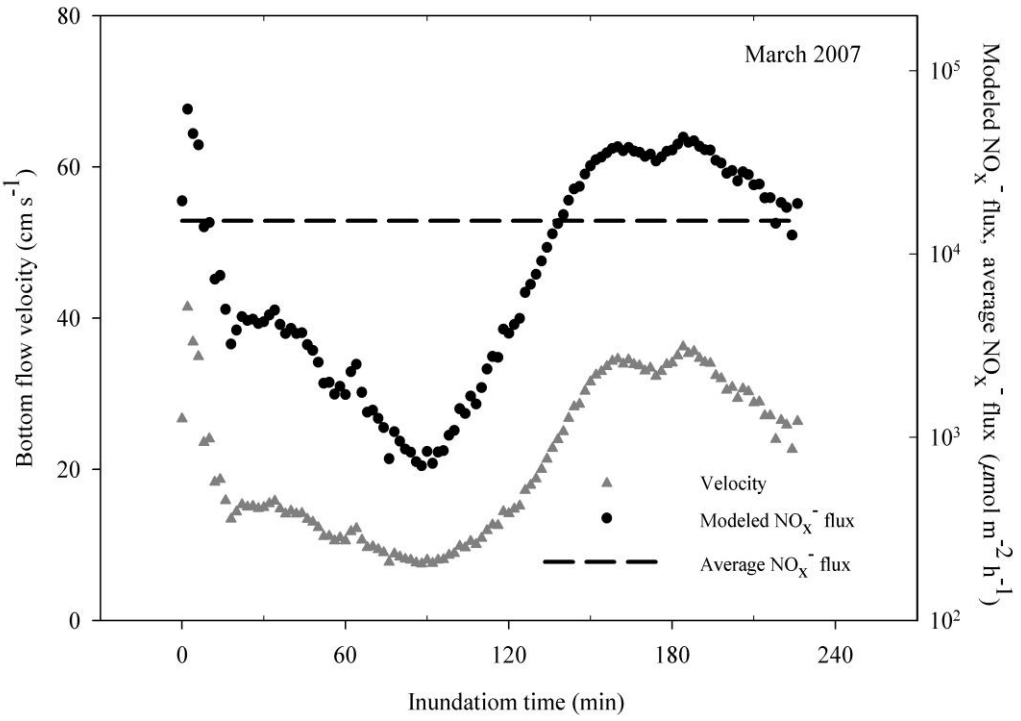

Figure 5: An example of modeled NO_x^- flux as a function of bottom flow velocity during inundation. The velocities in this plot (grey triangles) represent average values measured over 4 tidal cycles in April 2010. Modeled NO_x^- fluxes (black dots) were obtained from Eq. 10 using average NO_x^- concentrations (32.7 μmol L^{-1}) and temperatures (7.3°C) of the bottom water in March. The average NO_x^- flux (dashed line) was calculated from the modeled NO_x^- flux over one inundation period.

Over the seasonal cycle, modeled NO_x^- flux is a function of the available NO_x^- concentration in the overlying water (Fig. 6b). For example, increased NO_x^- concentration of 48.0 μmol L^{-1} in March 2007 with the temperature of 7.6°C caused the modeled NO_x^- flux to increase to 2.3×10^4 μmol m^{-2} h^{-1}. In contrast, although the temperature increased

by a factor of more than 2 in October 2006 and August 2007, decreased NO_x^- concentrations of ~ 0.7 μmol L^{-1} led to modeled NO_x^- fluxes decrease to ~ 700 μmol m^{-2} h^{-1}. Over the experimentally investigated seasons, modeled NO_x^- fluxes into permeable sediments were at least 2 times higher than the measured denitrification rates (Fig. 6, Table 2).

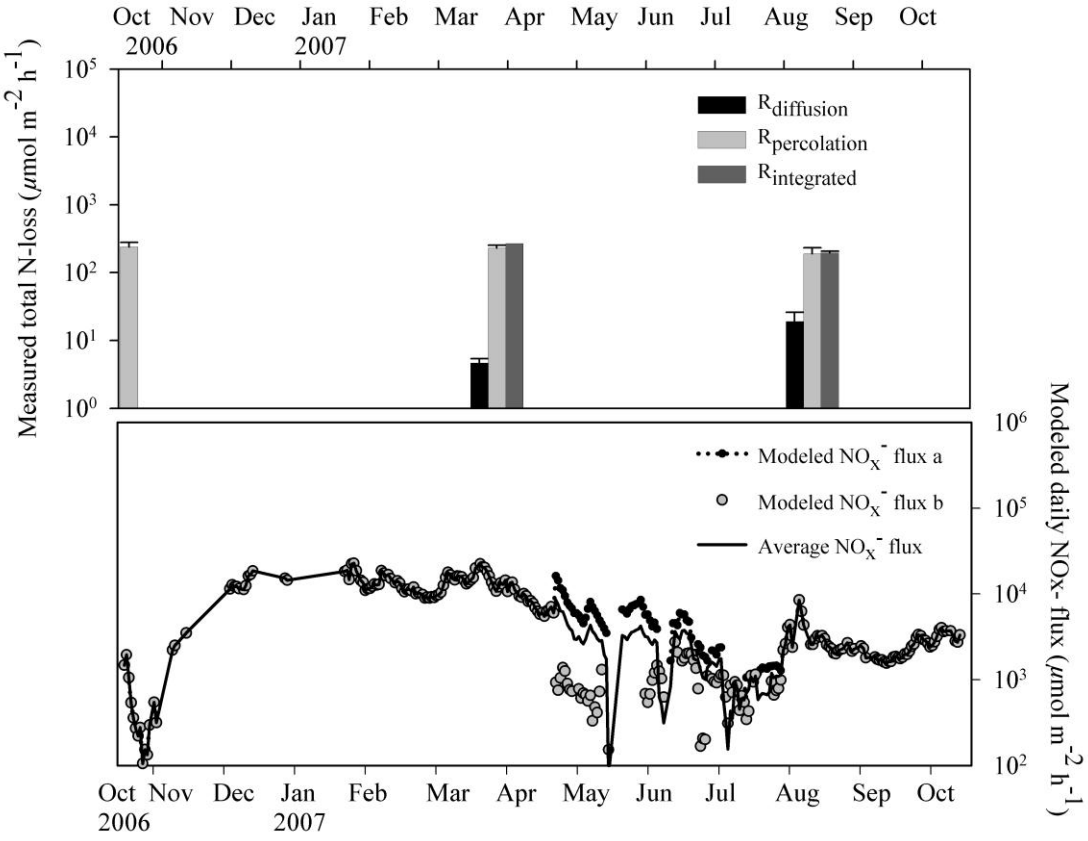

Figure 6. N-loss rates and NO_x^- fluxes determined from October 2006 to October 2007. (a) N-loss rates measured at the upper flat at Janssand using different incubation methods. (b) Modeled NO_x^- fluxes derived from ambient NO_x^- concentrations, which were measured at the time series station over the same time period. In place of missing data from April to July in 2007, the data from the same time period in 2006 (black dots) and in 2009 (gray dots) were shown in the figure. The average NO_x^- concentrations from April to July of both years were used to model the mean NO_x^- fluxes (black line) over the annual cycle. Note the different scales in panels a and b.

Discussion

N-loss from diffusive core incubations—In several previous studies, denitrification in permeable sediments was investigated by simulating diffusive transport conditions. Denitrification rates measured in these studies varied widely up to 133 μmol N m^{-2} h^{-1} (Table 4). In this study, N-loss rates obtained from intact cores under diffusive transport conditions (<19 μmol N m^{-2} h^{-1}, Table 2) were in the range of previously reported rates from the Wadden Sea permeable sediments (1-42 μmol N m^{-2} h^{-1}, Table 4). In contrast, N-loss rates obtained from intact cores under advective transport conditions (on average ~ 200 μmol N m^{-2} h^{-1}) were 1-2 orders of magnitude higher than those measured under diffusive flow conditions at the same sampling sites (Table 2). The increased N-loss under advective conditions was consistent with findings from permeable sediments in the South Atlantic Bight, where diffusive core incubations (Vance-Harris and Ingall 2005) and advective core incubations (Rao et al. 2007) from the same site deviated by 1-2 orders of magnitude. In this study, rates from percolated core incubations substantially exceed most denitrification rates reported from the northern coastal muddy sediments in Europe (Table 4) but agree well with the previous studies that observed enhanced N-loss rates due to advective transport in permeable sediments (Cook et al. 2006; Rao et al. 2007; Gihring et al. 2010).

N-loss from slurries and percolated core incubations—O_2 dynamics in permeable Wadden Sea sediments are largely influenced by advective porewater flow driven by waves and bottom water currents over uneven topography. Variable pressure gradients, caused by ripple migration, waves and variable currents, and the presence and absence of bottom water currents during times of inundation and exposure directly affect the porewater flow and thus the availability of oxygen and nitrate in the sediment. During inundation, advective porewater flow causes deep penetration of O_2 (~5 cm) (Werner et al. 2006; Billerbeck et al. 2006; Jansen et al., 2009), thus enlarging the oxic and suboxic biogeochemical zone and enhancing the remineralization rate of organic matter (de Beer et al. 2005; Franke et al. 2006). The oscillation between deep and shallow O_2 penetration depths during times of inundation and exposure may also favor the overlap of oxic and anoxic processes. Indeed, Gao et al. (2010) and Rao et al. (2007) reported substantial denitrification rates occurring in aerobic permeable surface sediments.

Furthermore, the advective porewater flow causes the deep penetration of NO_x^- into the sediment. Porewater profiles show that NO_x^- is still available at sediment depths of up to 6 cm (Fig. 3a). When the influx of NO_x^- ceases during exposure, consecutive porewater measurements show a rapid decrease of NO_x^- concentrations (Fig. 3b) indicating high NO_x^- consumption. NO_x^- consumption calculated from these porewater profiles was 6-fold higher (1.2 mmol N m^{-2} h^{-1}) compared to the average N-loss measured in slurry and percolated core incubations (0.2 mmol N m^{-2} h^{-1}). This suggests that the results from slurry and percolated core incubations may even underestimate the in situ N-loss under natural conditions.

The dynamic nature of porewater advection complicates the investigation of N-cycling in permeable sediments. Experiments used in this study, i.e. the incubation of slurries and percolated cores, aim to mimic a period of inundation when oxygenated and nitrate-containing bottom water is injected into the sediment, followed by a period of exposure during which porewater is stagnant and O_2 is consumed until anaerobic conditions prevail. Under the initial oxic condition, it can be expected that nitrification constantly adds $^{14}NO_x^-$ to the NO_x^- pool resulting in the decrease of $^{30}N_2$ relative to $^{29}N_2$ production over time. This would violate the steady state assumption behind the IPT method. However, during the first 4 hours of slurry and percolated core incubations no change of $^{30}N_2$ and $^{29}N_2$ production was observed (Fig. 4). In percolated core incubations this can be explained by the fact that the initial oxygen was rapidly consumed within the first 30 to 60 minutes of the incubation, i.e. between subsampling at 0 h and 1 h (*see* Gao et al. 2010, Fig.3). Hence, a change of the NO_x^- labeling percentage can be expected only in the first hour of the incubation. Thereafter, steady state conditions can be assumed. Likewise, steady state conditions are assumed in the slurry incubations in August 2007, when O_2 was consumed within the first 90 minutes (Fig. 4d). Finally, the oxygen consumption in the first hour of the incubation resulted in only minor changes of the labeling percentages. The decrease of $F'_{^{15}NO_3}$ (Eq. 6) relative to $F_{^{15}NO_3}$ (Eq. 5) was on average below 5% in the percolated core incubations and below 3% in the slurry incubations in August 2007.

In percolated core incubation, microbial cell densities remain unaffected, while cell densities in slurry incubations are diluted and, assuming constant cell specific respiration

rates, the change from oxic to anoxic condition may last longer. This was the case in March 2007, when oxic conditions in slurry incubations lasted for up to 6 hours (Fig. 4c). Nevertheless, N_2 production was constant within this period, because most of the initial oxygen (starting concentration ~300µmol L^{-1}) was consumed before the first subsampling, which resulted in a decrease of the initial labeling percentage ($F'_{^{15}NO_3}$ compared to $F_{^{15}NO_3}$) of 15% on average. Thereafter, the contribution of nitrification to the $^{14}NO_3^-$ pool was most likely insignificant. The potential error was estimated by calculating the amount of nitrified $^{14}NO_3^-$ from the O_2 consumed during the incubation (between 90 and 30 µmol L^{-1}) assuming an O_2/NO_3^- ratio of 138/16 (Jahnke et al. 1982). The maximum potential decrease in labeling percentage was 3.3% resulting in an increase of D_{tot} (Eq. 3) of less than 7%. In summary, we assume the NO_x^- pool to be in steady state in slurry and percolated core incubations - despite the initial dynamic oxygen regime.

NO_x^- availability under in situ conditions—Low N-loss rates measured under diffusive transport conditions are likely limited by NO_x^- availability. As diffusive transport conditions are not realistic in permeable surface sediments (Huettel et al. 1996, 1998, 2003), this limitation was overcome in core incubations where $^{15}NO_3^-$ enriched bottom water was percolated through the sediment. In percolated core incubations as well as in slurry incubations N-substrate was available throughout the incubation and therefore denitrification rates were not N-limited and may be considered as potential rates. However, we provide the following arguments suggesting that in situ denitrification rates are not N-limited in the first centimeters of permeable sediments.

At the same study site, repeated observations of deep O_2 penetration of several centimeters indicate significant advective transport of bottom water into the sediment (Werner et al. 2006; Billerbeck et al. 2006; Jansen et al., 2009). This advective transport stimulated oxygen consumption rates to increase 1-2 orders of magnitude (de Beer et al. 2005) – similar to the observed increase of denitrification in this study. In addition, NO_x^- is detected in porewaters down to depths of 6 cm and more (Fig. 3, *see* also Gao et al. 2010). The NO_x^- profiles were consistent with the modeled NO_x^- fluxes, which were sufficient during most of the year to support the measured N-loss rates. The modeled NO_x^- fluxes give conservative estimates since NO_x^- flux due to wave motion and bioirrigation and the NO_x^- contribution from nitrification was not considered.

Furthermore, in all rate measurements we observed the immediate start of a constant production of labeled N_2 (Fig. 4). Any adaptation to changing N-substrate availability, on either cell or community level, would have resulted in an initial lag phase of the N_2 production.

We also assume that the denitrifying community is well adapted to variable NO_x^- concentrations. First of all, the measured N-loss rates were similar in all slurry and percolated core incubations although the background nitrate concentrations differed by more than 80 μmol L^{-1}. Further evidence comes from experiments, in which Gao et al. (2010) used microsensors to measure NO_x^- consumption in a sediment core after percolation of bottom water. They observed a decrease of NO_x from 60 μmol L^{-1} down to submicromolar concentrations without significant change of rates suggesting that denitrification activity is not affected by low NO_x^- concentrations, such as those measured in the bottom water during summer. In summary, we suggest that N-loss rates from percolated core incubations provide reasonable estimates for in situ denitrification rates, while diffusive core incubations are inadequate because advective porewater transport is not considered.

Consistency of temporal and spatial N loss—N-loss rates obtained from advective core incubations were very similar at different sampling sites and throughout the different sampling periods (168 to 288 μmol m^{-2} h^{-1}, Table 2), although the background NO_x^- concentrations and the modeled NO_x^- influxes were highly variable. Modeled NO_x^- influxes varied from 1.9×10^3 to 2.2×10^4 μmol m^{-2} h^{-1} and significantly exceeded the demands for sustaining the measured denitrification rates. On average, modeled NO_x^- fluxes were 30 times higher compared to the measured rates. This suggests that N-loss rates in the upper 5 cm of the sediment were not limited by NO_x^- supply during most of the year.

The factors responsible for the consistent N-loss rates in the permeable sediments of the Wadden Sea remain speculative. The input or availability of organic carbon as a substrate for heterotrophic denitrification could potentially have limited the N-loss rates as has been shown in previous studies (Trimmer and Nicholls 2009). However, one would expect organic carbon concentration to be variable rather than uniform during the different sampling seasons. Alternatively, the consistent N-loss rate could depend on the

capacity of permeable sediment to host a microbial community. Compared to impermeable sediments with higher porosity and diffusive porewater transport, microorganisms in permeable sediments can colonize only the surface of the sand grains, since the pore space is exchanged with the pore water flow, which leads to fewer microorganisms per cm^{-3}.

Annual N loss from permeable Wadden Sea sediments—Based on the constant N-loss rates during the different sampling periods and at the various sampling sites (Table 2 and 4) we estimated the annual N-loss from permeable Wadden Sea sediments. The inundation periods of the studied intertidal sediments were 8-12 hours per day (i.e., 4-6 hours per cycle) with a mean of 10 hours per day (Table 5a). Since no substantial difference was observed between N-loss rates from percolated core and slurry incubations (Table 2), we used an average areal N-loss of 207 μmol N m^{-2} h^{-1} derived from percolated core incubations. Integrating these rates over the annual cycle, we assumed the areal N-loss to take place whenever the modeled NO_x^- fluxes were sufficient, i.e. higher than the measured rates. This was the case for 360 days of the year. For the remaining 5 days, modeled NO_x^- fluxes were lower than the experimentally derived N-loss and therefore rates during these days were conservatively set to zero. In summary, the annual N-loss per m^2 from the intertidal sand flats of the Wadden Sea is 745 ± 109 mmol N m^{-2} yr^{-1} (Table 5a), which is comparable to the mean annual N-loss rate of ~600 mmol N m^{-2} yr^{-1} estimated previously for the entire seafloor area of the Wadden Sea (Van Beusekom et al. 2008).

One third of the Wadden Sea area (~4700 km^2) is composed of sandy intertidal sediments (Common Wadden Sea Secretariat 2008). Based on our annual N-loss rate and the intertidal area, the annual N-removal from intertidal flats of the Wadden Sea is calculated to be 46 ± 7 × 10^6 kg N yr^{-1} (Table 5b). Furthermore, the subtidal flat areas (3700 km^2) and offshore areas (4900 km^2) are to a large extent covered by coarse permeable sediments (Common Wadden Sea Secretariat 2008), in which comparable advective porewater transport and oxygen penetration depths were observed (Janssen 2004). We conservatively estimated that 80 % of the subtidal Wadden Sea area is covered by permeable sediments. From the observed consistency of N-loss in the intertidal zones of Wadden Sea sediments, a similar N-loss of 207 μmol N m^{-2} h^{-1} was assumed for the

subtidal zones. Given that the subtidal zone is continuously inundated, the annual N-loss per m^2 in subtidal and offshore areas is estimated to be 1788 ± 263 mmol N m^{-2} yr^{-1} (Table 5b). Integrating over all intertidal and subtidal areas, the annual N-loss from permeable sediments of the entire Wadden Sea adds up to 218 ± 32 × 10^6 kg N yr^{-1} (Table 5b), which exceeds the previously reported estimate of ~112 × 10^6 kg N yr^{-1} (van Beusekom et al. 2008), and accounts for ~30% of the total annual N-input into the Wadden Sea (745 to 820 × 10^6 kg N yr^{-1}, van Beusekom et al. 2001). These results underline the importance of the sandy Wadden Sea seafloor as a major sink for riverine nitrogen loads that enter the German Bight.

Conclusions—Permeable sediments allow the advection of pore water, which accelerates the influx of NO_x^- from the bottom water. Modeled NO_x^- fluxes in this study suggest that even at times when NO_x^- concentrations in the bottom water are rather low the fluxes remain sufficiently high to support the experimentally measured rates of denitrification. Permeable sediments are wide spread in coastal areas and account for up to 70% of the shelf sediments (Johnson and Baldwin 1986). However, the mean annual N-loss from shelf sediments is currently estimated to be ~146 mmol N m^{-2} yr^{-1} (Galloway et al. 2004), which is only a fifth of the areal rates measured in this study. Therefore, the contribution of permeable sediments to the N-loss from shelf sediments should be re-evaluated, and the high potential of permeable sediments to regulate the flow of nitrogen at the land/sea boundary should be further investigated.

Table 4. Denitrification rates reported for coastal marine environments

Location	Sediment type	Method	Denitrification rate (μmol N m^{-2} h^{-1})	Reference
Texel, Wadden Sea	sand	acetylene block method	0.9 - 42	Kieskamp et al. 1991
Southern North Sea	fine sand	acetylene block method	5.8 - 8.9	Lohes et al. 1996
	fine sand	$^{15}N_2$ isotope paring method	8.9 - 11.9	Lohes et al. 1996; Devol 1991; Laursen and Seitzinger 2002
Svalbard	fine sand	N_2-flux	33.6	Devol et al. 1997
Mid-Atlantic Bight	sand	N_2-flux	68.8	Laursen and Seitzinger 2002
Washington state shelf	sand	N_2-flux	133.3	Devol1991
North Sea	sand and mud	NO_3^- consumption model	28.6	Billen 1978
Baltic Sea	sand and mud	Geochemical model	93.4	Shaffer and Ronner 1984
	sand and mud	$^{15}N_2$ isotope paring method	0.5 – 4.5; 13.4 – 28.7	Deutsch et al. 2010
Northern Baltic Proper Gulf of Finland	mud	$^{15}N_2$ isotope paring method	0 – 12.5 3 – 26.8	Tuominen et al. 1998
Aarhus Bay	silt	$^{15}N_2$ isotope paring method	12.2 - 20.8	Nielsen and Glud 1996

Table 5. Annual N-loss determined for the sandy seafloor of the Wadden Sea.

a) Intertidal sand flats.

	N-loss rate	Inundation time		N-loss rate integrated over inundation time and year	Annual N-loss rate
	(μmol N m^{-2} h^{-1})	hours per day	days per year	(mmol N m^{-2} per 3600 h)	(mmol N m^{-2} yr^{-1})
Experimental average	207.0 ± 30.4	10	360	745.2 ± 109.4	745.2 ± 109.4
Modeled NO_x^- flux	< 207.0 ± 30.4	10	5	-------	

b) Other areas where sands dominate the seafloor.

Geomorphological region of the Wadden Sea	Area	Percentage of sandy permeable sediments	Annual N loss rate	N loss estimate
	(km^2)	(%)	(mmol m^{-2} yr^{-1})	($\times 10^6$ kg N yr^{-1})
Intertidal flats	4700	93	745.2 ± 109.4	45.6 ± 6.7
Subtidal flats and gullies	3700	80 (almost all)	1788.5 ± 262.6	74.1 ± 10.9
Offshore area	4900	80 (almost all)	1788.5 ± 262.6	98.2 ± 14.4

References

Al-Raei, A. M., K. Bosselmann, M. Böttcher, B. Hespenheide, and F. Tauber. 2009. Seasonal dynamics of microbial sulfate reduction in temperate intertidal surface sediments: controls by temperature and organic matter. Ocean Dynam. **59:** 351-370.

Badewien, T. H., E. Zimmer, A. Bartholomä, and R. Reuter. 2009. Towards continuous long-term measurements of suspended particulate matter (SPM) in turbid coastal waters. Ocean Dynam. **59**: 227-238

Bartholomä, A., A. Kubicki, T. Badewien, and B. Flemming. 2009. Suspended sediment transport in the German Wadden Sea-seasonal variations and extreme events. Ocean Dynam. **59**: 213-225.

Billen, G. 1978. A budget of nitrogen recycling in North Sea sediments off the Belgian Coast. Estuar. Coast Mar. Sci. **7:** 127-146.

Billerbeck, M., U. Werner, L. Polerecky, E. Walpersdorf, D. de Beer, and M. Huettel. 2006. Surficial and deep pore water circulation governs spatial and temporal scales of nutrient recycling in intertidal sand flat sediments. Mar. Ecol. Prog. Ser. **326:** 61-76.

Braman, R. S., and S. A. Hendrix. 1989. Nanogram nitrite and nitrate determination in environmental and biological-Materials by vanadium(iii) reduction with chemi-luminescence detection. Anal. Chem. **61:** 2715-2718.

Cardenas, B. M., and L. J. Wilson. 2007. Dunes, turbulent eddies and interfacial exchange with permeable sediments. Water Resour. Res. **43:** 1-16.

Codispoti, L. A., J. A. Brandes, J. P. Christensen, A. H. Devol, S. W. A. Naqvi, H. W. Paerl, and T. Yoshinari. 2001. The oceanic fixed nitrogen and nitrous oxide budgets: Moving targets as we enter the anthropocene? Scientia Marina **65:** 85-105.

Codispoti, L. A. 2007. An oceanic fixed nitrogen sink exceeding 400 Tg Na-1 vs the concept of homeostasis in the fixed-nitrogen inventory. Biogeosciences **4:** 233-253.

Common Wadden Sea Secretariat. 2008. Nomination of the Dutch-German Wadden Sea as world heritage site -volume one. p. 10-28. Wilhelmshaven.

Cook, P. L. M., F. Wenzhofer, S. Rysgaard, O. S. Galaktionov, F. J. R. Meysman, B. D. Eyre, J. Cornwell, M. Huettel, and R. N. Glud. 2006. Quantification of denitrification in permeable sediments: Insights from a two-dimensional simulation analysis and experimental data. Limnol. Oceanogr.:Meth. **4:** 294-307.

De Beer, D., F. Wenzhofer, T. G. Ferdelman, S. E. Boehme, M. Huettel, J. E. E. Van Beusekom, M. E. Böttcher, N. Musat, and N. Dubilier. 2005. Transport and mineralization rates in North Sea sandy intertidal sediments, Sylt-Romo Basin, Wadden Sea. Limnol. Oceanogr. **50:** 113-127.

Deutsch, B., S. Froster, M. Wilhelm, J. W. Dippner, and M. Voss. 2010. Denitrification in sediments as a major nitrogen sink in the Baltic Sea: an extrapolation using sediment characteristics. Biogeosciences **7:** 3259-3271.

Devol, A. H. 1991. Direct measurement of nitrogen gas fluxes from continental-shelf sediments. Nature **349:** 319-321.

Devol, A. H., L. A. Codispoti, and J. P. Christensen. 1997. Summer and winter denitrification rates in western Arctic shelf sediments. Continental Shelf Res. **17:** 1029-1050.

Emery, K. O. 1968. Relict sands on continental shelves of the world. AAPG Bull. **52:** 445-464.

Eyre, B. D., and A. J. P. Ferguson. 2002. Comparison of carbon production and decomposition, benthic nutrient fluxes and denitrification in seagrass, phytoplankton, benthic microalgae- and macroalgae-dominated warm-temperate Australian lagoons. Mar. Ecol. Prog. Ser. **229:** 43-59.

Franke, U., L. Polerecky, E. Precht, and M. Huettel. 2006. Wave tank study of particulate organic matter degradation in permeable sediments. Limnol. Oceanogr. **51:** 1084-1096.

Galloway, J. N., F. J. Dentener, D. G. Capone, R. W. H. E. W. Boyer, S. P. Seitzinger, G. P. Asner, P. A. G. C. C. Cleveland, E.A. Holland, D.M. Karl, J. H. P. A. F. Michaels, A. R. Townsend, and C. J. Vöosmarty. 2004. Nitrogen cycles: past, present, and future. Biogeochemistry **70:** 153-226.

Gao, H., F. Schreiber, G. Collins, M. M. Jensen, J. E. Kostka, G. Lavik, D. de Beer, H. Y. Zhou, and M. M. M. Kuypers. 2010. Aerobic denitrification in permeable Wadden Sea sediments. ISME J. **4:** 417-426.

Gihring, T. M., A. Canion, A. Riggs, M. Huettel, and J. E. Kostka. 2010. Denitrification in shallow, sublittoral Gulf of Mexico permeable sediments. Limnol. Oceanogr. **55:** 43-54.

Gruber, N. 2004. The dynamics of the marine nitrogen cycle and its influence on atmospheric CO_2 variation, p. 97-148. *In* E. M. Follows and T. Oguz [eds.], The ocean carbon cycle and climate. Kluwer Academic.

Gruber, N. 2008. The marine nitrogen cycle: overview and challenges, p. 32-35. *In* D. G. Capone, D. Bronk, M. Mulholland and E. J. Carpenter [eds.], Nitrogen in the marine environment, 2nd ed. Academic Press/Elsevier.

Grunwald, M., O. Dellwig, G. Liebezeit, B. Schnetger, R. Reuter, and H. J. Brumsack. 2007. A novel time-series station in the Wadden Sea (NW Germany): First results on continuous nutrient and methane measurements. Mar. Chem. **107:** 411-421.

Grunwald, M., O. Dellwig, C. Kohlmeier, T. H. Badewien, M. Beck, S. Kotzur, N. Kowalski, G. Liebezeit, and H. J. Brumsack. 2010. Nutrient dynamics in a back barrier tidal basin of the Southern North Sea: Time-series, model simulations, and budget estimates, J. Sea Res. **64:** 199-212.

Guo, Z., and T. S. Zhao. 2002. Lattice Boltzmann model for incompressible flows through porous media. Phys. Rev. E **66:** 036304.

Hauck, R.D., S.W. Melsted, and P.E. Yankwich. 1958. Use of N-isotope distribution in nitrogen gas in the study of denitrification. Soil. Sci. 86: 287-291

Holtappels, M., G. Lavik, M. M. Jensen, and M. M. M. Kuypers. 2011. ^{15}N-Labeling Experiments to Dissect the Contributions of Heterotrophic Denitrification and Anammox to Nitrogen Removal in the OMZ Waters of the Ocean, p. 223-251 In Martin G. Klotz [ed.], Methods in Enzymology, Vol 486

Huettel, M., and G. Gust (1992) Impact of bioroughness on interfacial solute exchange in permeable sediments. *Mar. Ecol-Prog, Ser.* **89:** 253-267.

Huettel, M., W. Ziebis, and S. Forster. 1996. Flow-induced uptake of particulate matter in permeable sediments. Limnol. Oceanogr. **41:** 309-322.

Huettel, M., W. Ziebis, S. Forster, and G. W. Luther. 1998. Advective transport affecting metal and nutrient distributions and interfacial fluxes in permeable sediments. Geochim. Cosmochim. Ac. **62:** 613-631.

Huettel, M., and A. Rusch. 2000. Transport and degradation of phytoplankton in permeable sediment. Limnol. Oceanogr. **45:** 534-549.

Huettel, M., H. Røy, E. Precht, and S. Ehrenhauss. 2003. Hydrodynamical impact on biogeochemical processes in aquatic sediments. Hydrobiologia **494:** 231-236.

Jahnke R. A., S. R, Emerson, and J. W. Murray (1982). A model of oxygen reduction, denitrification, and organic matter mineralization in marine sediments. *Limnol. Oceanogr*. **27:** 610-623.

Janssen, F. 2004. Pore-water advection and organic matter mineralization in North Sea shelf sands. Dissertation University of Bremen. (http://nbn-resolving.de/urn:nbn:de: gbv:46-diss000101769)

Jansen, S., E. Walpersdorf, U. Werner, M. Billerbeck, M. Böttcher, and D. De Beer. 2009. Functioning of intertidal flats inferred from temporal and spatial dynamics of O_2, H_2S and pH in their surface sediment. Ocean Dynam. **59:** 317-332.

Johnson, H. D., and C. T. Baldwin. 1986. Shallow siliciclastic seas, p. 229-282 . *In* H. G. [ed.], Sedimentary environments and facies. 2nd ed. Blackwell Scientific Publications.

Jorgensen, B. B., and N. P. Revsbech. 1985. Diffusive boundary layers and the oxygen uptake of sediments and detritus. Limnol. Oceanogr. **30:** 111-122.

Kampmeyer, P. M. 1952. The Temperature dependence of viscosity for water and mercury. J. Appl. Phys. **23:** 99-102.

Kieskamp, W. M., L. Losh, E. Epping, and W. Helder. 1991. Seasonal variation in denitrification rates and nitrous oxide fluxes in intertidal sediments of the western Wadden Sea. Mar. Ecol. Prog. Ser. **72:** 145-151.

Laursen, A. E., and S. P. Seitzinger. 2002. The role of denitrification in nitrogen removal and carbon mineralization in Mid-Atlantic Bight sediments. Continental Shelf Res. **22:** 1397-1416.

Lohse, L., H. T. Kloosterhuis, W. van Raaphorst, and W. Helder. 1996. Denitrification rates as measured by the isotope pairing method and by the acetylene inhibition

technique in continental shelf sediments of the North Sea. Mar. Ecol. Prog. Ser. **132:** 169-179.

Nielsen, L. P. 1992. Denitrification in sediment determined from nitrogen isotope pairing. FEMS Microbiol. Ecol. **86:** 357-362.

Nielsen, L. P., and R. N. Glud. 1996. Denitrification in a coastal sediment measured in situ by isotope paring applied to a benthic flux chamber. Mar. Ecol. Prog. Ser. **137:** 181-186.

Perry, R. H., and D. Green. 1984. Physicl and chemical , p. 3-248–3-252. *In* Perry's Chemical Engineers' Handbook, 6th ed. E. McGraw-Hill.

Precht, E., and M. Huettel. 2003. Advective pore-water exchange driven by surface gravity waves and its ecological implications. Limnol. Oceanogr. 48: 16741684.

Precht, E., and M. Huettel. 2004. Rapid wave-driven advective pore water exchange in a permeable coastal sediment. J. Sea Res. **51:** 93-107.

Precht, E., U. Franke, L. Polerecky, and M. Huettel. 2004. Oxygen dynamics in permeable sediments with wave-driven pore water exchange. Limnol. Oceanogr. **49:** 693-705.

Rao, A. M. F., M. J. McCarthy, W. S. Gardner, and R. A. Jahnke. 2007. Respiration and denitrification in permeable continental shelf deposits on the South Atlantic Bight: Rates of carbon and nitrogen cycling from sediment column experiments. Continental Shelf Res. **27:** 1801-1819.

Rao, A. M. F., M. J. McCarthy, W. S. Gardner, and R. A. Jahnke. 2008. Respiration and denitrification in permeable continental shelf deposits on the South Atlantic Bight: N_2:Ar and isotope pairing measurements in sediment column experiments. Continental Shelf Res. **28:** 602-613.

Reimers, C. E., H. A. Stecher, G. L. Taghon, C. M. Fuller, M. Huettel, A. Rusch, N. Ryckelynck, and C. Wild. 2004. In situ measurements of advective solute transport in permeable shelf sands. Continental Shelf Res. 24: 183-201.

REUTER, R., T. H. BADEWIEN, A. BARTHOLOMA, A. BRAUN, A. LUBBEN, and J. RULLKOTTER. 2009. A hydrographic time series station in the Wadden Sea (southern North Sea). Ocean Dynam. **59:** 195-211.

Rusch, A., and M. Huettel. 2000. Advective particle transport into permeable sediments - evidence from experiments in an intertidal sandflat. Limnol. Oceanogr. **45:** 525-533.

Shaffer, G., and U. Rönner. 1984. Denitrification in the Baltic Proper deep-water. Deep-Sea Res. **31:** 197-220.

Thamdrup, B., and T. Dalsgaard. 2002. Production of N_2 through anaerobic ammonium oxidation coupled to nitrate reduction in Marine sediments. Appl. Environ. Microb. **68:** 1312-1318.

Thamdrup, B., and T. Dalsgaard. 2008. Nitrogen Cycling in Sediments, p. 527-568. *In* E. D. L. Kirchman [ed.], Microbial ecology of the oceans, 2nd ed. John Wiley & Sons.

Trimmer, M., and J. C. Nicholls. 2009. Production of nitrogen gas via anammox and denitrification in intact sediment cores along a continental shelf to slope transect in the North Atlantic. Limnol. Oceanogr. **54:** 577–589.

Tuominen, L., A. Heinanen, J. Kuparinen, and L. P. Nielsen. 1998. Spatial and temporal variability of denitrification in the sediments of the northern Baltic Proper. Mar. Ecol. Prog. Ser. **172:** 13-24.

van Beusekom, J. E. E., and V. N. de Jonge. 1998. Retention of phosphorus and nitrogen in the Ems estuary. Estuaries **21:** 527-539.

van Beusekom, J. E. E., H. Fock, F. de Jong, S. Diel-Christiansen, and B. Christiansen. 2001.Wadden Sea specific eutrophication criteria. Wadden Sea ecosystem No. 14. Common Wadden Sea Secretariat, Wilhelmshaven, Germany.

van Beusekom, J. E. E., S. Weigelt-Krenz, and P. Martens. 2008. Long-term variability of winter nitrate concentrations in the Northern Wadden Sea driven by freshwater discharge, decreasing riverine loads and denitrification. Helgol Mar. Res. **62:** 49-57

Vance-Harris, C., and E. Ingall. 2005. Denitrification pathways and rates in the sandy sediments of the Georgia continental shelf, USA. Geochem. T. **6:** 12-18.

Werner, U., M. Billerbeck, L. Polerecky, U. Franke, M. Huettel, J. E. E. van Beusekom, and D. de Beer. 2006. Spatial and temporal patterns of mineralization rates and

oxygen distribution in a permeable intertidal sand flat (Sylt, Germany). Limnol. Oceanogr. **51:** 2549-2563.

Ziebis, W., S. Forster, M. Huettel, and B. B. Jorgensen. 1996. Complex burrows of the mud shrimp Callianassa truncata and their geochemical impact in the sea bed. Nature **382:** 619-622.

Nitrification coupled to aerobic denitrification in the Wadden Sea intertidal permeable sediments

Hang Gao[1], Stefan Jansen[1,2], Moritz Holtappels[1], Marlene M Jensen [1,3], Gavin Collins [1,4], Frank Schreiber,[1,5] Sumei Liu[1,6], Joel Kostka[1,7], Dirk de Beer, [1] Gaute Lavik,[1] and Marcel MM Kuypers[1]

1 Biogeochemistry Department, Max Planck Institute for Marine Microbiology, Celsiusstr. 1, D-28359 Bremen, Germany

2 Current address: Deltares, Princetonlaan 6, 3584 CB, Utrecht, The Netherlands

3 Current address: Infrastructure and Environment, School of Engineering, University of Glasgow, Glasgow, Scotland, the United Kingdom

4 Current address: Institute of Biology and Nordic Center of Earth Evolution (NordCEE), University of Sothern Denmark, Campusvej 55, 5230 Odense M, Denmark

5 Current address: Dept. of Environmental Microbiology, Eawag - Swiss Federal Institute of Aquatic Science and Technology, Dübendorf, Switzerland

6 Current address: College of Chemistry and Chemical Engineering, Ocean University of China, Qingdao 266100, China

7 Current address: Department of Oceanography, Florida State University, Tallahassee, Florida, the United States

Acknowledgement

We thank Ingrid Dohrmann and Hani Tahsk for their field support, and Gabriele Klockgether and Daniela Franzke for their technical support in the lab. We are grateful to the Captains Ronald Monas, Ole Pfeiler for the ship time and excellent collaboration. We would especially thanks Phyllis Lam and Alexandra Rao for their constructive comments on this manuscript. Founding came from the Max Planck Society (Max Planck Gesellschaft, MPG), the German Research Foundation (Deutsche Forschung Gesellschaft, DFG), German Academic Exchange Center (Deutsche Akedemische Austausch Dienst, DAAD) and MPG (HG) and the Danish Research Council (MMJ).

Abstract

In permeable sediments, expansion of the oxic surface layer due to advection may favor nitrification and aerobic denitrification. However, little is known to date about the actual occurrence of and interactions between these N-cycling processes in permeable sediments. In this study, nitrification and its coupling to N-loss processes (including anammox and denitrification) in permeable Wadden Sea sediments were quantified using various ^{15}N-isotope-paring experiments. Experiments were conducted in March and August 2007, when NO_x^- (NO_3^- and NO_2^-) was enriched and depleted, respectively, in the overlying water column. The active occurrence of nitrification was verified by observed net $^{15}NO_x^-$ production. Interestingly, such produced NO_x^- appeared to be quickly consumed by other dissimilatory processes. Aerobic denitrification was the dominant N-loss process observed in these sediments. Although anammox did occur, it was at very low rates (<2 µmol N m^{-2} h^{-1}, <1 % of total N loss) and could explain only a small portion of the NO_x^- consumed. Nitrification coupled to aerobic denitrification was found to attribute to as much as 17 % of total N-loss especially in surficial permeable sediments which are most strongly influenced by advection. The rest of total N-loss (83 %) was attributed to NO_x^- from the overlying water due to advection. In fact, the coupling rate may be underestimated as O_2 limitation could have occurred due to the one-pulse percolation method used in incubations. The estimated potential gross nitrification rates indicate that nitrification is a significant *in situ* NO_x^- source in these sediments and might play a more important role in coupling with denitrification in the summer with depleted NO_x^- in overlying water compared to in the winter/spring with enriched NO_x^- in water column. The estimated potential gross nitrification is substantially greater than the measured conservative gross nitrification (the sum of net nitrification and the portion coupled to denitrification), implying that other NO_x^--consuming processes such as dissimilatory nitrate reduction to ammonium (DNRA) or assimilation are occurring. Hence, results from this study provide direct and quantitative evidence that nitrification plays a key role in linking N-sources and N-sinks in permeable Wadden Sea sediments.

Introduction

Denitrification, the reduction of NO_3^- or NO_2^- to N_2O or N_2, represent an important sink of fixed nitrogen (N) in coastal marine environments (Joye and Anderson 2008), where the anammox process ($NH_4^+ + NO_2^- \rightarrow N_2 + H_2O$) seems to be of less importance (Dalsgaards et al. 2005). In most marine sediments, denitrification is mainly limited by the availability of NO_x^- ($NO_2^- + NO_3^-$) (Canfield et al. 1993; Brandes and Devol 1995). The supply of NO_x^- is primarily derived from two sources: the overlying water column and nitrification in oxic surface sediments. The former source depends on the concentration of seawater NO_x^-, whereas the latter depends on the depth of oxygen penetration as an electron acceptor in the stepwise oxidation of ammonium to nitrite and nitrite to nitrate. These two steps in nitrification are performed by different groups of microorganisms (Lam and Kuypers 2010). Thus, nitrification, the main oxidative process in the N cycle, links mineralization of organic nitrogen to N loss via denitrification and anammox in the marine system (Jenkins and Kemp 1984; Rysgaard et al. 1993; Lam et al. 2007).

Under diffusive conditions, a thick layer of oxic surface sediments favors nitrification over ammonium loss across the sediment-water interface, and promotes denitrification coupled to nitrification rather than its reliance on NO_x^- from the overlying water (Nielsen et al. 1990; Jenkins and Kemp 1984; Seitzinger 1990). The significance of nitrification as an essential source of NO_x^- for denitrification in coastal fine-grained sediments under diffusive conditions, has been recognized for decades (Herbert 1999 and thereins; Ward 2008 and references thereins). However, although the majority (up to 68 %) of the continental shelves worldwide is covered by permeable, coarse-grained sediments (Emery 1969; Johnson and Baldwin, 1986), few studies have been done to investigate the role of nitrification in N cycling in permeable sediments, where advective transports, driven by tides and winds, predominate.

In contrast to diffusive transport in fine-grained sediments, the high permeability of sandy sediments promotes pore water flow and advective exchange of materials across the sediment-water interface (Huettel et al. 1998; 2003). Recent studies showed that O_2 penetrated down to ~5 cm in permeable sediments during inundation (Franke et al. 2006; Werner et al. 2006; Billerbeck et al. 2006; Jansen et al. 2009), leading to an enhanced thickness of the oxic sediment layer. Other studies have further shown an increase in N

loss via denitrification caused by advection, relative to those previous reported under diffusive conditions in permeable sediments (Cook et al. 2006; Rao et al. 2007; 2008; Gihring et al. 2010; Gao et al. *submitted*). Moreover, a tight coupling between nitrification and denitrification was reported in both the Gulf of Mexico and South Atlantic Bight sands (Rao et al. 2007; 2008; Gihring et al. 2010) based on isotope pairing in core incubations (Nielsen 1992). In the Wadden Sea, *in situ* monitoring efforts have shown clear tidal trend of water column NO_x^- enrichment appearing during low tide (Grunwald et al., 2010), suggesting that there might be a efflux of NO_x^- due to nitrification from sediments under advective pore water flows. In addition, an initial rapid net NO_x^- accumulation was observed in these permeable sediments under fully aerobic conditions, using simultaneous sensor measurements of O_2 and NO_x in intact cores during percolation experiments. The subsequent consumption of this accumulated NO_x^- indicated a tight coupling between nitrification and denitrification (Gao et al. 2010). Thus, there have been no direct quantitative assessments on nitrification and coupled nitrification-denitrification under simulated advective conditions with respect to O_2 in these permeable sediments.

In this study, we investigated nitrification and its importance as a NO_x^- source for N-loss processes in permeable Wadden Sea sediments, using ^{15}N-stable-isotope-paring experiments in slurry incubations. Furthermore, variation in activities of these microbial processes with depth was examined according to O_2 penetration. During expeditions in March and August 2007, our results examined: (1) The net NO_x^- produced by nitrification in sediments and the potential efflux of NO_x^- from the sediments, and (2) the role of coupled nitrification-denitrification in oxic surface layer of permeable Wadden Sea sediments, with anammox playing a negligible role.

Materials and methods

Study site description

Sampling and onboard incubations were carried out during two field expeditions in March and August 2007 on the Janssand intertidal sand flats in the German Wadden Sea (Fig. 1A). Janssand is located in the back-barrier area of Spiekeroog island, which belongs to the island chain separating the intertidal area from the open North Sea (Fig. 1B). The intertidal sand flat covers an area of 11 km^2 and is characterized by semi-

diurnal tides with tidal ranges of 1.5-2 m. During ebb tide, sediments of the sand flat are gradually exposed to air.

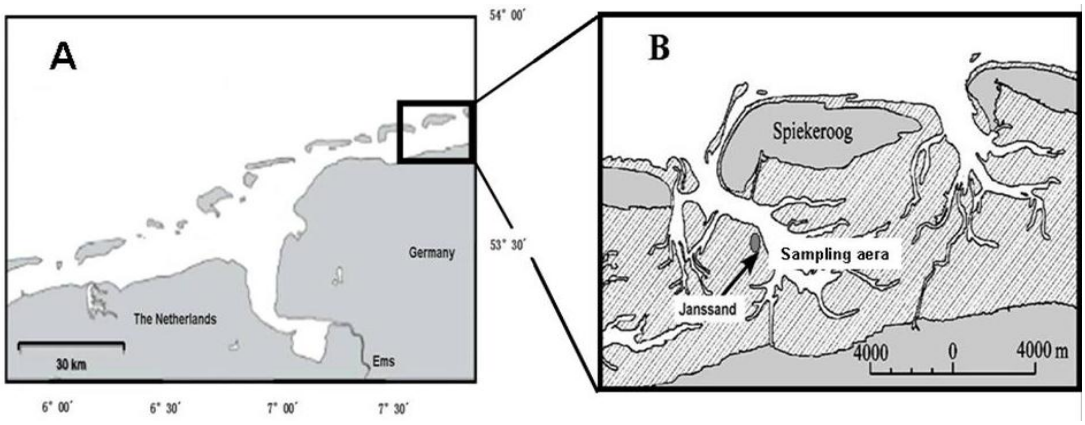

Fig. 1 A The location of Janssand sand flat in the Wadden Sea. B The investigated area at Janssand.

The sediments at Janssand are composed of well-sorted, fine quartz sands with a mean grain size of 176 µm and a permeability in the upper 15 cm of 7.2 x 10^{-12} m^2 (Billerbeck et al. 2006). The oxygen penetration depth ranges from 0.5-2 cm during exposure (low tide) to up to 5 cm during inundation (high tide) (de Beer et al. 2005; Billerbeck et al. 2006; Jansen et al. 2009).

Nitrate concentrations (NO_x^- = NO_3^- + NO_2^-) in the water column at Janssand are seasonally variable because of the seasonality of phytoplankton blooms. Water column NO_x^- ranges from <1 µM in summer to ~60 µM in winter. Correspondingly, the advective influx of NO_x^- into the permeable sediments, estimated by a porewater flux model (Gao et al. *submitted*), varied from 700 µmol m^{-2} h^{-1} in summer to 2.3×10^4 µmol m^{-2} h^{-1} in winter.

Recent studies have shown that the sediment biogeochemistry at Janssand, with respect to oxygen consumption, organic matter mineralization and N removal, is representative for Wadden Sea intertidal sand flats (de Beer et al. 2005; Røy et al. 2008; Gao et al. *in Rev.*). Hence, Janssand has been chosen for detailed studies of the role of nitrification in permeable sediment (Fig. 1B).

Sampling procedure

In situ pore water sampling was performed in sediments during exposure, using a Rhizon method modified from Seeberg-Elverfeldt et al. (2005). A metal plate with holes at 1-1.4 cm intervals down to 15 cm was pushed into sediments. Rhizon samplers were inserted into the undisturbed sediments and mounted through the holes on the metal plate with only the sampling ports protruding from the sediments. Pore water samples for dissolved inorganic nitrogen (DIN) were directly extracted from these ports with sterile hypodermic syringes.

Sediments for slurry incubations were sampled with push cores (inner diameter 9.5 cm). The upper 6 cm of each sediment core were sliced in 2-cm-thick interval. Parallel sections were pooled (142 cm^3 from each depth interval), homogenized and used for slurry incubations. Sea water used for incubations was collected during low tide and filtered through a 0.2 µm sterile filter. Subsamples were taken for dissolved inorganic nitrogen (DIN) measurements.

^{15}N labeling incubations

The sediment slurries were amended with ^{15}N labeled substrates and incubated in gas-tight bags (Thamdrup and Dalsgaard, 2002) to examine net nitrification, coupled nitrification to N-loss processes using 3 different treatments (Table 1). In treatment 1, samples were amended with NH_4^+ + $^{14}NO_X^-$ for the assessment of nitrification and its coupling to anammox and denitrification. In treatment 2, a nitrification inhibitor (allylthiourea, ATU) was further added with $^{15}NH_4^+$+ $^{14}NO_3^-$ to exclude the contribution from nitrification. Finally, total N-loss via anammox, denitrification and coupled nitrification-denitrification combined was examined in treatment 3 ($^{15}NO_3^-$). In all three treatments, nitrate/nitrite and ammonium were respectively amended to a final concentration of 200µmol L^{-1}, while allylthiourea (ATU) was added to a final concentration of 86 µmol L^{-1} to inhibit ammonium oxidation (Jensen et al. 2007). Complete details of the incubation procedures are described in Gao et al. (2010). In brief, all the slurry incubations were performed in the dark at *in situ* temperature with 200 mL amended air-saturated seawater to simulate the initial oxic conditions driven by advection. Samples for nutrient measurements were taken before and after substrate addition to determine the final ^{15}N-enrichment. Slurries were well mixed after the

amendment of ^{15}N-labeled substrates and incubated for 30 mins to ensure in *in situ* temperature conditions during incubations. Subsamples were taken from the well-mixed slurries after that 30-min inicubation with the sampling time marked as 0, 1, 2, 4, 6, 8, 16 and 24 hours, and preserved in 6 ml Exetainer ^{TM} vials (Labco, U.K.) pre-filled with 100 μl of saturated $HgCl_2$.

Table 1: Slurry incubation treatments and investigated N cycling processes.

Treatment	Added N-substrates and inhibitors	Investigated process	Equation
1	$^{15}NH_4^+ + {}^{14}NO_3^-$ (in March) $^{15}NH_4^+ + {}^{14}NO_2^-$ (in August)	net nitrification + anammox + nitrification-denitrification	Eq. 2 Eq. 4 Eq. 12
2	$^{15}NH_4^+ + {}^{14}NO_3^-$ + ATU	anammox	Eq. 4
3	$^{15}NO_3^-$	anammox + denitrification + nitrification-denitrification	Eq. 4 Eq. 9 Eq. 14

^{15}N-N_2 measurements

A 1 mL helium (He) headspace was introduced to each sample vial. The isotope ratio of dinitrogen gas ($^{28}N_2$, $^{29}N_2$ and $^{30}N_2$) in the headspace was determined by gas chromatography-isotope ratio mass spectrometry (GC-IRMS; VG Optima) by direct injection of the sample headspace. Concentrations of $^{30}N_2$ and $^{29}N_2$ were determined from the excess relative to air. Incubations without a significant linear trend in concentration with time ($p > 0.05$) were discarded.

DIN measurements

All DIN samples from seawater, porewater and subsamples from incubations were kept frozen at -20 °C immediately after sampling and until further analysis. Dissolved ammonium (NH_4^+) concentrations were determined using a flow injection analyzer (Hall

and Aller, 1992). Nitrate + nitrite (NO_x^-) was determined by chemiluminescence after reduction to NO with acidic vanadium (II) chloride (Braman and Hendrix, 1989).

Oxygen determinations

In situ dissolved oxygen concentrations was measured at high-resolution depth intervals with autonomous profiling microsensors as described in Glud et al. (1999) and Wenzhöfer et al. (2000). The Clark-type oxygen microelectrodes had a tip diameter of 2 µm and a response time of less than 5 s (t90). In March 2006, the profiler was placed on the flat during low tide with the microsensors initially positioned 1 to 2 cm above the sediment surface. Profiles were measured over at least one tidal cycle to a sediment depth of 6 cm at intervals of 1 mm. Repeated profiles were measured every 20 to 60 min.

Using oxygen microsensors, O_2 concentration was measured in every slurry subsample shortly after subsampling from the bags and before introducing the headspace. The sample vials were uncapped, a calibrated O_2 microsensor was inserted into the bottom of each vial for ~10 seconds until the sensor signal stabilized. Sample vials were recapped immediately to avoid significant gas exchange (Jensen et al, 2007; Gao et al. 2010). Oxygen consumption rates at all depth intervals were calculated in the first 2 or 4 time points of incubations when O_2 were measurable and linearly consumed. The mean rate for each depth interval was obtained by averaging over all measured rates in those three paralleled slurry incubations.

Rate determinations

Net NO_X production

In treatment 1 (added $^{15}NH_4^+$ and $^{14}NO_3^-$), the net production of NO_x^- via nitrification was determined from the accumulation of $^{15}NO_x^-$ in the Exetainers. After ^{15}N-N_2 production had been measured in these Exetainers, all N_2 gas was removed by purging with He. Subsequently, NO_x^- in the subsamples was converted into N_2 gas by reduction with spongy cadmium and then sulfamic acid according to Fuessel et al. (*submitted*). The isotope composition of thus generated ^{15}N-N_2 was analyzed as described above (in section of ***^{15}N-N_2 measurements***). The production of $^{15}NO_x^-$ was then calculated according to the converted $^{29}N_2$ and $^{30}N_2$ production:

$$^{15}NO_X = {}^{29}N_2 + 2 \cdot {}^{30}N_2 \qquad (1)$$

The production of $^{15}NO_x^-$ ($p^{15}NO_X$) in March was calculated from the increase of $^{15}NO_X$ concentration over the first 2 hours (0-2 cm depth) and 4 hours (2-4 cm and 4-6 cm depth). In August, $^{15}NO_X$ was already decreasing after the first 30 mins (see results below). Therefore, in summer, the actual incubating time zero (T0') is when ^{15}N-labelled substrates were immediately added, 30 mins ahead of the marked T0 sampling time-0h. $p^{15}NO_X$ was calculated from the increase of $^{15}NO_X$ concentration between the actual incubating time zero (T0') and the first marked T0 subsampling (i.e. 30 min). Considering the labeling percentage, the net nitrification rate (N^{net}) is calculated by:

$$N^{net} = pNO_X = p^{15}NO_X / F_{^{15}NH_4} \quad (2)$$

where $F_{^{15}NH_4}$ is the ^{15}N-mole fraction of ammonium calculated from the added $^{15}NH_4^+$ and the measured $^{14}NH_4^+$ in the initial seawater and porewater samples:

$$F_{^{15}NH_4} = {}^{15}NH_4^+ / \left({}^{14}NH_4^+ + {}^{15}NH_4^+\right) \quad (3)$$

Anammox

In treatment 2 (added $^{15}NH_4^+$, $^{14}NO_3^-$ and ATU), the N_2 production via anammox (A) was calculated over the first 4 hours (linear production phrase) under aerobic conditions according to:

$$A = p^{29}N_2 / F_{^{15}NH_4} \quad (4)$$

where $F_{^{15}NH_4}$ is calculated in the same way according to equation (3).

Denitrification

In treatment 3 (added $^{15}NO_3^-$), the $^{29}N_2$ production via denitrification was derived by correcting the production of $^{29}N_2$ ($p^{29}N_2$) with the $^{29}N_2$ production via anammox subtracted:

$$p^{29}N_{2(Den)} = p^{29}N_2 - A \cdot F_{^{15}NO_3} \quad (5)$$

Here it has been assumed that anammox rates in treatment 2 and 3 are similar. $F_{^{15}NO_3}$ is the ^{15}N-mole fraction of nitrate calculated from the added $^{15}NO_3^-$ and the measured $^{14}NO_3^-$ in the initial seawater and porewater samples:

$$F_{^{15}NO_3} = {}^{15}NO_3^- / \left({}^{15}NO_3^- + {}^{14}NO_3^-\right) \quad (6)$$

The denitrification rates of $^{15}NO_X$ (D_{15}) and $^{14}NO_X$ (D_{14}) are calculated over the first 4 hours under aerobic conditions from the corrected $^{29}N_2$ production and the $^{30}N_2$ production according to Nielsen (1992):

$$D_{15} = p^{29}N_{2(Den)} + 2 \cdot p^{30}N_2 \quad (7)$$

$$D_{14} = \left(p^{29}N_{2(Den)} / \left(2 \cdot p^{30}N_2\right)\right) \cdot \left(p^{29}N_{2(Den)} + 2 \cdot p^{30}N_2\right) \quad (8)$$

Accordingly, the total denitrification rate (D_{tot}) is calculated as

$$D_{tot} = D_{14} + D_{15} \quad (9)$$

Coupled nitrification-denitrification

In treatment 1 (added $^{15}NH_4^+$ and $^{14}NO_3^-$), the production of $^{29}N_2$ ($p^{29}N_2$) over the first 4 hours under aerobic conditions has to be corrected for the $^{29}N_2$ production via anammox to derive the $^{29}N_2$ production via denitrification:

$$p^{29}N_{2(Den)} = p^{29}N_2 - A \cdot F_{^{15}NH_4} \quad (10)$$

with the assumption that anammox rates in treatment 1 and 2 are similar.

Since all $^{15}NO_X$ that is denitrified derived from the nitrification of $^{15}NH_4^+$ under aerobic conditions (in the first 4 hours), D_{15} represents the coupled nitrification-denitrification of $^{15}NO_X$:

$$D_{15} = p^{29}N_{2(Den)} + 2 \cdot p^{30}N_2 \quad (11)$$

To calculate the total coupled nitrification-denitrification rate ($D^{nit}_{(treat\_1)}$), the labeling percentage of $^{15}NH_4^+$ has to be considered:

$$D^{nit}_{(treat\_1)} = D_{15} / F_{^{15}NH_4} \quad (12)$$

In treatment 3, the $^{14}NO_X$ originates either from the added seawater or from nitrification. To distinguish between the two sources that fuel the denitrification of $^{14}NO_X$ (D_{14}), the denitrification of $^{14}NO_X$ from the added seawater is calculated according to Nielsen (1992):

$$D^w_{14} = D_{15} \cdot F_{^{15}NO_3} / (1 - F_{^{15}NO_3}) \quad (13)$$

Whereas, the denitrification of $^{14}NO_X$ coupled to nitrification is calculated from:

$$D^{nit}_{(treat\_3)} = D_{14} - D^w_{14} \quad (14)$$

In this treatment nitrification did not produce any $^{15}NO_X$. Therefore, $D^{nit}_{(treat\_3)}$ is essentially the rate of coupled nitrification-denitrification.

Conservative gross nitrification

Conservative gross nitrification under aerobic conditions in treatment 1 and 3 was calculated by adding N^{net} to $D^{nit}_{(treat\_1)}$ and $D^{nit}_{(treat\_3)}$, respectively.

$$N_{(treat\_1)} = N^{net} + D^{nit}_{(treat\_1)} \quad (15)$$

$$N_{(treat\_3)} = N^{net} + D^{nit}_{(treat\_3)} \quad (16)$$

Areal rates

To calculate areal rates, the volumetric rates were vertically integrated from 0 to 5 cm. This depth interval was chosen, because during inundation a O_2 penetration depth of ~5 cm was measured at the same study site (Billerbeck et al. 2006; Jansen et al. 2009), indicating that at least the upper 5 cm of the sediment were affected by advective porewater transport.

Results

In situ DIN and O_2 concentrations

O_2 penetration depth varied from 2 to 4 cm over the tidal cycle (Fig. 2A). During ebb tide (1h before exposure), O_2 was measurable down to 4 cm, whereas the O_2 penetration depth decreased to 2 cm at low tide (4hrs after exposure) when advective pore water flow ceased (Fig. 2A).

At 2.5 hour after exposure, NO_x^- (i.e. NO_3^- + NO_2^-) and NH_4^+ were detected throughout the entire sampling depth (0-10 cm). NO_x^- concentrations increased from 5 μM at 1 cm depth to a maximum of 10 μM at 3 cm depth (Fig. 2A). At 4 cm, the concentration decreased down to 4 μM and stayed constant towards deeper depths. A local minimum of NH_4^+ concentration (7 μM) was correlated with the maximum of NO_x^- concentration at 3.5 cm depth. Above and below this depth, NH_4^+ concentrations were around 16 μM, and from there decreased towards deeper depths and towards the sediment surface.

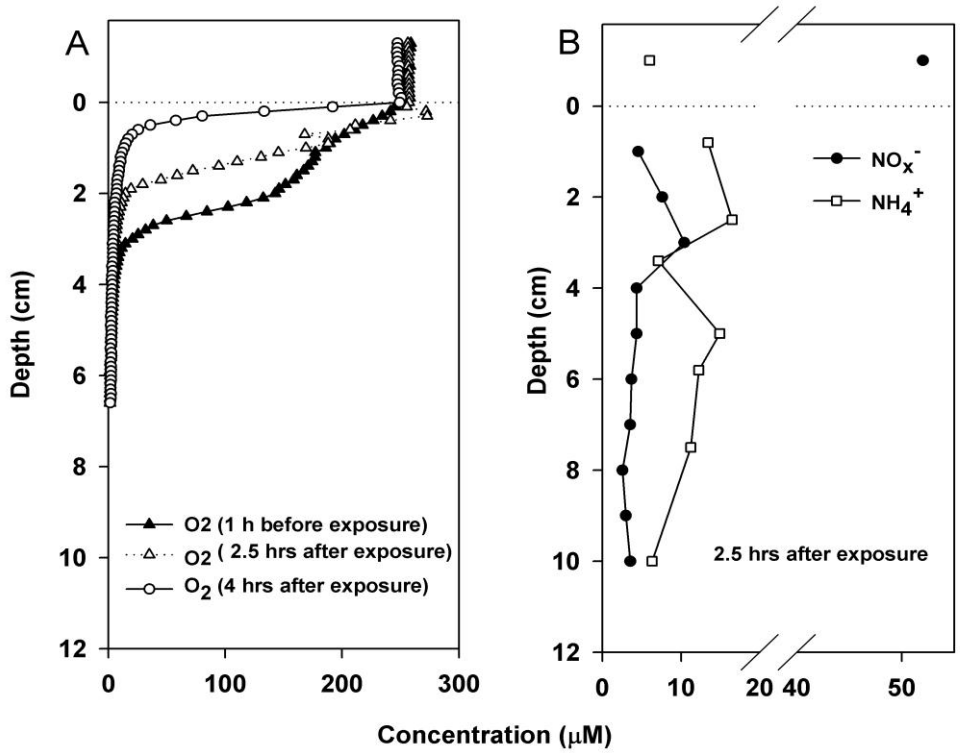

Fig. 2 *In situ* O_2, NO_x^- and NH_4^+ concentrations in the pore water of permeable sediments at Janssand flat in March 2007. (A) O_2 dynamics over exposure. Data were obtained from ebb tide (1 hour before exposure) to low tide (4 hours after exposure). Black triangles, white triangles and white dots are O_2 concentrations respectively at 1 hour before exposure, 2.5 hours and 4 hours after exposure. (B) NO_x^- and NH_4^+ concentrations at 2.5 hours after exposure. Black dots and white squares are respectively NO_x^- and NH_4^+ concentrations.

Oxygen consumption rates in the sediments

The average oxygen consumption rate showed similar variation with depth in March and August 2007 (Fig. 3). Rates were comparable at 0-2 and 4-6cm depth intervals in March (~35 mmol $m^{-3}_{\ sediments}\ h^{-1}$) and in August (~120 mmol $m^{-3}_{\ sediments}\ h^{-1}$). Lower rates were determined at 2-4 cm depth interval, 25 mmol $m^{-3}_{\ sediments}\ h^{-1}$ in March and 90 mmol $m^{-3}_{\ sediments}\ h^{-1}$ in August. Oxygen consumption rates showed seasonal variation. Rates in August (100-120 mmol $m^{-3}_{\ sediments}\ h^{-1}$) exceeded those in March (20-35 mmol $m^{-3}_{\ sediments}\ h^{-1}$) by factors of 3-5 (Fig 3 and Table 3). The areal O_2 consumption rate integrated to 5 cm was 3 times higher in August (5-6 mmol $m^{-2}_{\ sediments}\ h^{-1}$) than that in winter (1-2 mmol $m^{-2}_{\ sediments}\ h^{-1}$).

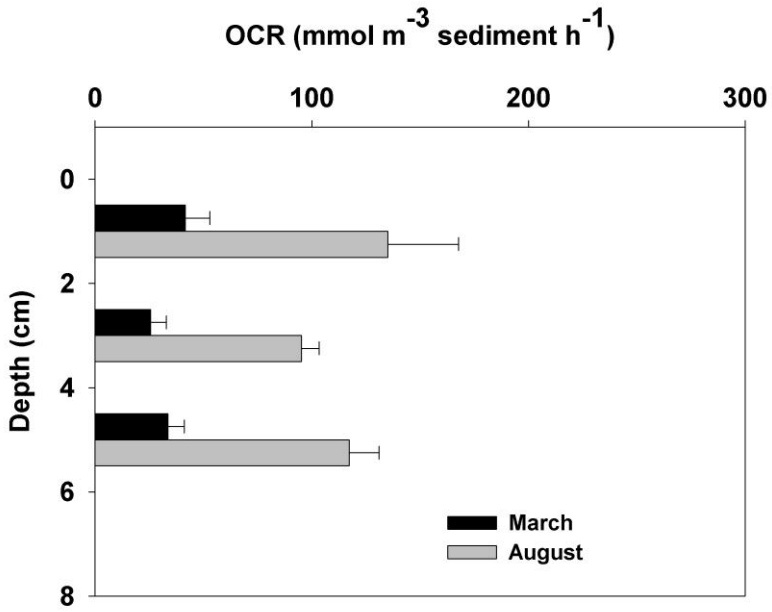

Fig. 3 Oxygen consumption rates (OCRs) in average in permeable sediments in 2007. Black and grey bars respectively present the OCRs data March and August.

Net NO_x^- production

In treatment 1 (added $^{15}NH_4^+$, $^{14}NO_x^-$), net production of $^{15}NO_x^-$ was determined under aerobic conditions thus verifying nitrification activity (Fig. 4). In March, $^{15}NO_x^-$ produced via nitrification accumulation was observed in the first 2-4 hours of the incubation, while O_2 decreased down to 15-50 µM (Fig. 4 A, B and C). The maximum of produced $^{15}NO_x^-$ was 592 µmol m^{-3}sediment in the upper layer (0-2 cm) and increased to the highest concentration of 2200 µmol m^{-3}sediment in the deep layer (4-6 cm). Net NO_x^- nitrification rates (N^{net}, see equation 2) were comparable (190 and 180 µmol N m^{-3}_{sediment} h^{-1}) at the depth intervals of 0-2 and 2-4 cm and the rate in the deep layer (4-6 cm) was 2-fold higher (350 µmol N m^{-3}_{sediment} h^{-1}). The vertically integrated rate to 5 cm was 11µmol N m^{-2} h^{-1} (Table 2).

In August, the $^{15}NO_x^-$ pool was assumed to have peaked between the actual starting time point of incubation and the time point of the first subsampling (i.e. 30 mins), because $^{15}NO_x^-$ produced via nitrification start to decrease from this time onwards in spite of O_2 concentrations at 70-130 µM (Fig. 4 D, E and F). The maxima of $^{15}NO_x^-$ concentrations at time point of the first subsampling were one-tenth to one-third of those in March. Similar to the March sampling, however, lower max NO_x^- concentrations (47

µmol m^{-3} $_{sediment}$) were observed in the upper layer and the highest concentrations (615 µmol m^{-3} $_{sediment}$) was measured in the deep layer. Correspondingly, net nitrification (N^{net}, see equation 2) increased from 30 to1200 µmol N m^{-3} $_{sediment}$ h^{-1} towards the deeper depth. The vertical integrated net nitrification rate (0-5 cm) was 28 µmol N m^{-2} h^{-1}, and exceeded the rate measured in March by a factor of ~3 (Table 2). The reduction in net $^{15}NO_x^-$ accumulation with time observed in both seasons, clearly indicated the occurrence of NO_x^- consuming processes in the same samples.

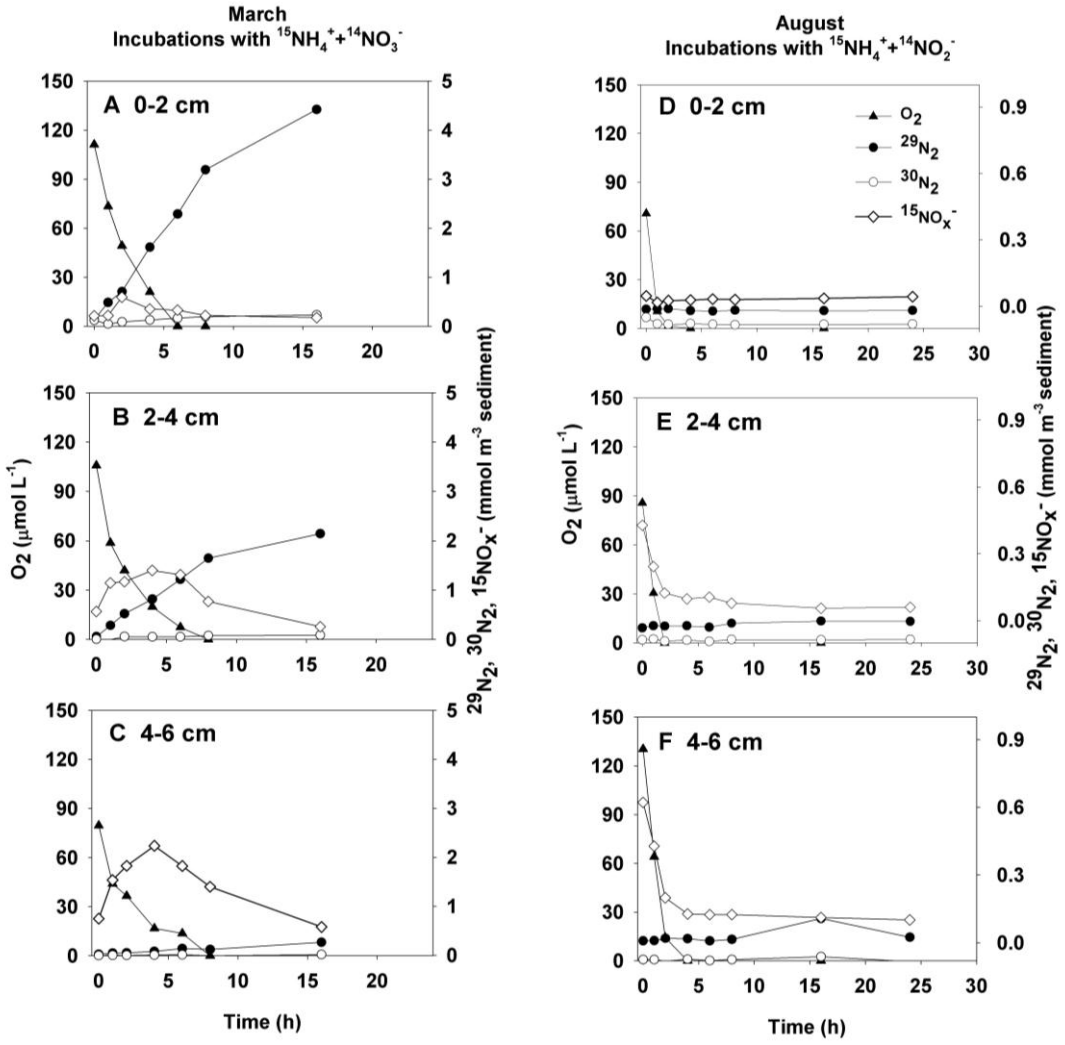

Fig. 4 O_2 concentrations (black triangles), $^{29}N_2$ (black dots) and $^{30}N_2$ productions (white dots) as well as net $^{15}NO_x^-$ productions (white diamonds) in incubations adding $^{15}NH_4^+$ and $^{14}NO_3^-$ ($^4NO_2^-$). Panels A, B and C presented the incubations in March at the depth intervals of 0-2, 2-4 and 4-6 cm, respectively. While panels D, E and F presented the incubations in August at the depth intervals of 0-2, 2-4 and 4-6 cm, respectively. Due to the first sampling after 30 mins of the incubation, the incubated time zero (0h) is not the real zero point for these reactions.

Anammox

The $^{29}N_2$ production in treatment 2 (added $^{15}NH_4^+$, $^{14}NO_3^-$ and ATU) is due to mere anammox since the aerobic oxidation of $^{15}NH_4^+$ is inhibited by ATU. In general, production rates were low or even below the detection limit (Fig. 5). When detected, $^{29}N_2$ concentrations increased linearly over time. Anammox rates calculated from equation 4 were below 51 µmol N m^{-3} $_{sediment}$ h^{-1} in March as well as in August (Table 2). After the complete consumption of O_2 at 2-4 hour in March and 1 hour in summer, no significant increase in $^{29}N_2$ production due to anammox was observed. Anammox rates were less than 1% of total denitrification rates (see below) at all the depth intervals (Table 2).

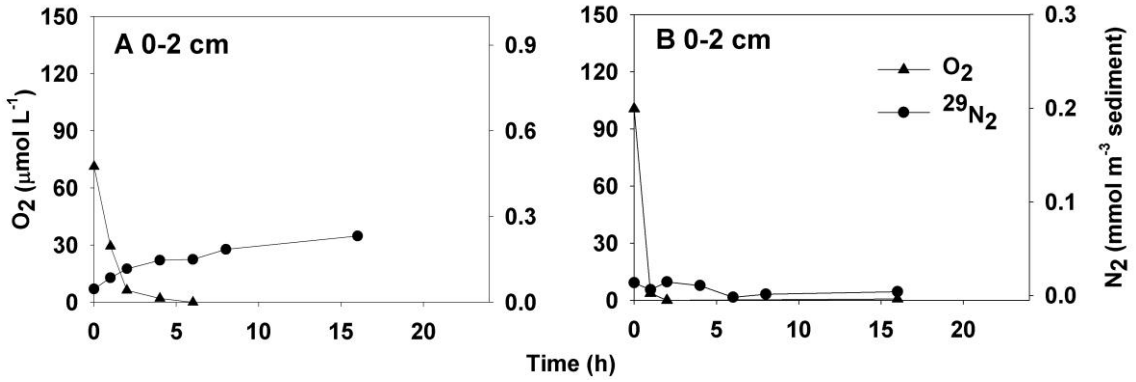

Fig. 5 O_2 concentration (black triangles) and $^{29}N_2$ production (black dots) in slurry incubations with treatment 1 ($^{15}NH_4^+$,$^{14}NO_3^-$ and ATU). Panels A and B presented the data at depth interval of 0-2 cm in March and August 2007.

Denitrification

In treatment 3 (added $^{15}NO_3^-$), the concentrations of $^{29}N_2$ and $^{30}N_2$ increased from the very beginning of the incubation experiments, even though O_2 was initially present in high concentrations (Fig. 6). In March, the production of $^{29}N_2$ and $^{30}N_2$ was constant in the first 4 hours of the incubation. Thereafter the production increased between hour 4 and 8, and decreased again between hours 8 and 16. In August, O_2 was consumed within the first 2-4 hours. The productions of $^{29}N_2$ and $^{30}N_2$ were generally constant in the first 8 hours of the incubation. Thereafter the production gradually decreased between hours 8 and 24. For further calculations (equations 5-9), the production of $^{29}N_2$ and $^{30}N_2$ over the first 4 hours under oxic conditions was used.

Total denitrification (D_{tot}) varied between 2200 and 7100 µmol N m^{-3} $_{sediment}$ h^{-1} (Table 2). In March as well as in August, maximum denitrification was measured in the 2-4 cm depth interval (7100 and 5200 µmol N m^{-3} $_{sediment}$ h^{-1}, respectively), whereas the lowest rates were found at 4-6 cm depth (2200 and 2600 µmol N m^{-3} $_{sediment}$ h^{-1}, respectively). Integrated rates were higher in March (270 µmol N m^{-2} h^{-1}) compared to those measured in August (190 µmol N m^{-2} h^{-1}).

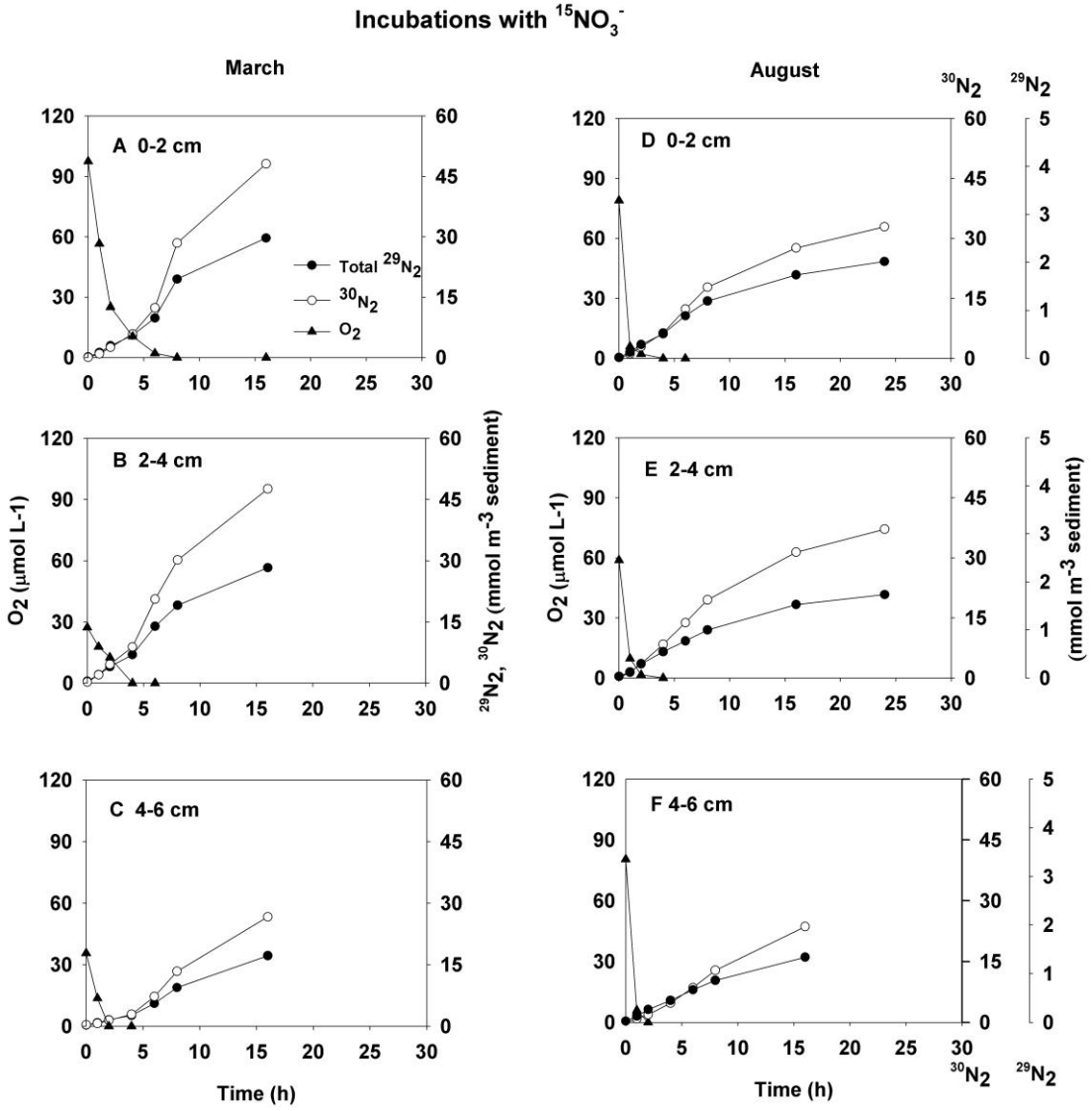

Fig. 6 O_2 concentrations (black triangles), $^{29}N_2$ (black dots) and $^{30}N_2$ productions (white dots) versus time in slurry incubations with $^{15}NO_3^-$ (treatment 2). Panel A, B and C present incubations at the depth intervals of 0-2, 2-4 and 4-6 cm, respectively, in March 2007. Panels D, E and F present incubations at the depth intervals of 0-2, 2-4 and 4-6 cm, respectively, in August 2007. Panel A, B and C were presented by Gao et al. (2010)

Coupled nitrification-denitrification

In treatment 1 (added $^{15}NH_4^+$, $^{14}NO_x^-$), the production of $^{29}N_2$ and $^{30}N_2$ was constant over the first 6-8 hours in March, whereas no production of labeled N_2 was detected in August (Fig. 4). In March, denitrified $^{15}NO_x^-$ was found predominantly in the $^{29}N_2$ fraction, whereas the contribution of $^{30}N_2$ to D_{15} (equation 11) was less than 20%. Rates of coupled nitrification-denitrification ($D^{nit}_{(treat\_1)}$, see equation 12) varied from 330 µmol N m^{-3} $_{sediment}$ h^{-1} in the upper layer to 14 µmol N m^{-3} $_{sediment}$ h^{-1} in the deep layer (Table 2).

In treatment 3 (added $^{15}NO_3^-$), the calculated rates of coupled nitrification-denitrification ($D^{nit}_{(treat\_3)}$, see equation 14) varied between 350 and 860 µmol N m^{-3} $_{sediment}$ h^{-1} in March and between 90 and 140 µmol N m^{-3} $_{sediment}$ h^{-1} in August (Table 2). $D^{nit}_{(treat\_3)}$ decreased from highest rates in the upper layer (0-2 cm) to lowest rates in the deep layer (4-6 cm). Vertically integrated to 5 cm, $D^{nit}_{(treat\_3)}$ was 34 µmol N m^{-2} h^{-1}, which is 3 times higher than the coupled nitrification-denitrification rates measured in treatment 1 ($D^{nit}_{(treat\_1)}$). The contribution of coupled nitrification-denitrification to the total denitrification (C_1) was greater in March (10-17%) than in August (2-5%) (Table 2).

Conservative gross nitrification

In March 2007, the conservative gross nitrification rates, combining net NO_3^- production and coupled nitrification-denitrification, $N_{(treat\_1)}$ and $N_{(treat\_3)}$ (equations 15-16) decreased from the upper layer (0-2 cm) (1050 and 520 µmol m^{-3} $_{sediment}$ h^{-1}, respectively) towards the deep layer (4-6 cm) (700 and 360 µmol m^{-3} $_{sediment}$ h^{-1}, respectively) (Fig. 7 and Table 2). $N_{(treat\_3)}$ was twice as high as $N_{(treat\_1)}$ at all the depth intervals.

In contrast with the observations in March, $N_{(treat\_3)}$ increased towards the deep layer in August (Table 2). The lowest rates (180 µmol m^{-3} $_{sediment}$ h^{-1}) were measured in the upper layer, whereas the highest rates (1260 µmol m^{-3} $_{sediment}$ h^{-1}) were found in the

deep layer. The integrated rate of $N_{(treat\_3)}$ in March (45 µmol m^{-3} $_{sediments}$ h^{-1}) was slightly higher than that in August (34µmol m^{-3} $_{sediments}$ h^{-1}) (Table 2).

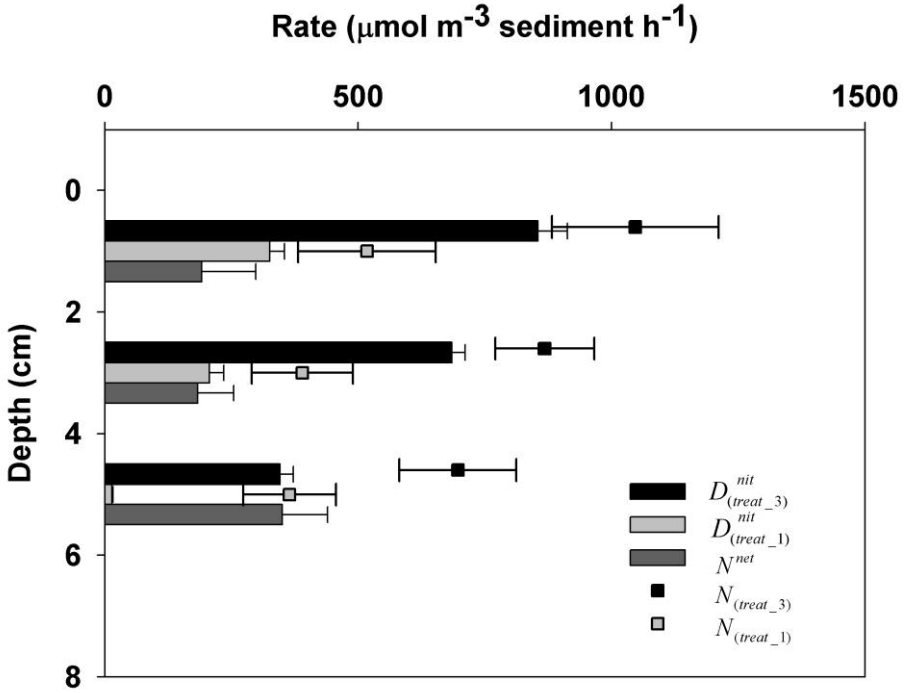

Figure 7 Total nitrification rates $N_{(treat\_3)}$ (black squares with error bars) in incubations with $^{15}NO_3^-$ and $N_{(treat\_1)}$ (grey squares with error bars) in incubations with $^{15}NH_4^+ + ^{14}NO_3^-/14NO_2^-$ in permeable sediments in March 2007. Black, light and dark grey bars respectively represent coupled nitrification-denitrification $D^{nit}_{(treat\_3)}$, $D^{nit}_{(treat\_1)}$ and net nitrification (N^{net}).

Discussion

O_2 dynamics in permeable Wadden Sea sediments are largely influenced by advective pore water flows driven by tides and winds. During inundation, advective pore water flow leads to maximum O_2 penetration down to ~ 5 cm (Franke et al. 2006; Werner et al. 2006; Billerbeck et al. 2006; Jansen et al., 2009), thus extending the oxic biogeochemical zone and enhancing the remineralization of organic matter (de Beer et al. 2005; Werner et al. 2006). The oscillation between deep and shallow O_2 penetration depths during times of inundation and exposure (Fig 2) may also favor the overlap of oxidative and reductive processes such as nitrification and aerobic denitrification. Indeed, Substantial denitrification rates was found to occur in aerobic surface sediments of the Wadden Sea, while NO_x^- was rapid but transient accumulated and was almost consumed under saturated O_2 conditions (Gao et al. 2010). Therefore, it indicated that NO_x^-, produced *in situ* via nitrification might be involved in the N dissimilatory processes—denitrification and anammox.

Net NO_x^- production—direct proof of nitrification

In this study, the net NO_x^- production observed provide direct evidence of *in situ* nitrification as examined under in situ conditions and simulated oxic conditions in incubations (Fig.2 and 4). Accumulation of net NO_x^- was found within the O_2 penetration depth in the pore water during exposure (Fig. 2). NO_x^- accumulation could be attributed to ongoing nitrification during exposure or it originates from nitrification during the last pulse of advection, just before exposure. Net NO_x^- production was also determined under oxic conditions in slurry incubations wirh (Fig. 4). In treatment 1 ($^{15}NH_4^+ + ^{14}NO_3^-$), NO_x^- accumulated under aerobic conditions over the first 2-4 hours in March, and as fast as within 30 minutes of incubation in August (Fig. 4). Considering that the upper 4-5 cm of the sediment is oxygenated during inundation, it is reasonable to calculate the net NO_x^- production as net nitrification rates in the first hours when oxygen was still available. In summary, the porewater profiles and the net NO_x^- productions parallel support the active occurrence of nitrification in these sediments at the study site and that nitrification is an important *in situ* source of NO_x^-. Nevertheless, both in March and August, the decreases in net $^{15}NO_x^-$ accumulation with time were observed in the treatment 1 ($^{15}NH_4^+ + ^{14}NO_3^-$)l,

implying NO_x^- loss by concurrent dissimilatory processes, such as anammox or denitrification.

N-loss processes—anammox and denitrification

Anammox or denitrification was individually investigated in slurry incubations with treatment 2 ($^{15}NH_4^+$+$^{14}NO_3^-$+ATU) and 3 ($^{15}NO_3^-$) (Fig. 5 and 6) The dynamic nature of porewater advection complicates the investigation of N-cycling in permeable sediments. The experimental design used in this study aims to mimic a period of inundation when oxygenated bottom water is injected into the sediment, followed by a period of exposure and stagnant porewater during which O_2 is consumed until anaerobic conditions prevail.

The incubated sediment slurries were amended with 200µM of N-substrate and, therefore, processes were not N-limited. Because N limitation under *in situ* conditions cannot be fully excluded, the rates measured in the sediment slurries may have to be considered as potential rates. However, NO_x^- and NH_4^+ concentrations in the porewater profiles (Fig. 2) suggest that *in situ* nitrification, denitrification and anammox were not N-limited. This is supported by the immediate start of the production of labeled N_2 right from the time point of first subsampling (0h) (Fig. 5+6), since any adaptation to the increased N-substrate availability, on either cell or community level, would have resulted in an initial lag phase of the N_2 production.

The results of $^{29}N_2$ productions in treatment 2 (Fig.5) showed the contribution of potential anammox to the total N-loss was less than 1% (Table 2), in March as well in August. These rates were determined in the presence of oxygen concentrations (>20µM) that usually inhibit anammox (Jensen et al. 2007). Alternatively, the production of $^{29}N_2$ under oxic conditions in treatment 2 can be attributed to coupled nitrification-denitrification with crenarchaea as nitrifiers, since crenarchaea tolerate higher concentration of allylthiourea than bacteria (Martens-Habbena et al. 2010) and may not have been fully inhibited. Hence, in our incubations, anammox could have been overestimated. In summary, although recent studies have reported the importance of anammox in marine sediments as another N loss pathway (Thamdrup and Dalsgaard et al. 2002; Engsroem et al. 2005; Kuypers et al. 2006), N-loss due to anammox is negligible in these shallow permeable sediments of the Wadden Sea.

In treatment 3, the total $^{15}N\text{-}N_2$ ($^{29}N_2+^{30}N_2$) showed that substantial denitrification occurred under aerobic conditions in the surficial sediments (Fig. 6). One recent results showed that areal rates integrated to 5 cm (190-270 µmol m^{-2} $_{sediments}$ h^{-1}) from slurry incubations in March and August were comparable to rates determined from intact core incubations at the same study site (Gao et al. *submitted*). The measured denitrification rates are, however, 10-20 fold higher than rates determined from muddy sediments in Aarhus Bay (Nielsen and Glud 1996), Gulf of Finland and Northern Baltic Proper (Tuominen et al. 1998) and Baltic Sea (Deutsch et al., 2010), in which the diffusive transport of N-substrates probably limited denitrification. Gao et al. (*in Rev.*) calculated that the mere influx of NOx from the bottom waters driven by advection is sufficient to these high rates during most of the year.

Coupled nitrification to denitrification

The calculation of coupled nitrification-denitrification rates from treatment 3 ($D^{nit}_{(treat\_3)}$) is based on the fact that the ^{15}N-mole fraction ($F_{NO_3^-}$) of the initial NO_3^- pool differs from that calculated from the $^{29}N_2$ and $^{30}N_2$ production (assuming binomial distribution of $^{28}N_2$, $^{29}N_2$ and $^{30}N_2$). The underlying assumption is that both the first step of denitrification (i.e. NO_3^- reduction to NO_2^-) and the first step of nitrification (i.e. NH_4^+ oxidation to NO_2^-) fuel an extracellular NO_2^- pool that is the source for all consecutive steps of denitrification. If nitrification in treatment 2 is absent, the ^{15}N % of the NO_3^- pool remains the same in the NO_2^- pool and, thus, agrees with the label percentage calculated from $^{29}N_2$ and $^{30}N_2$ production. Any nitrification would dilute the ^{15}N % in the NO_2^- pool resulting in ratios of $^{30}N_2$ to $^{29}N_2$ production that are below those expected from the initial $F_{NO_3^-}$.

If denitrifiers are present that perform all denitrifying steps without releasing the intermediate NO_2^- to the ambient pool, two different pools (NO_3^- and NO_2^-) with different ^{15}N % have to be considered when calculating denitrification from the production of $^{29}N_2$ and $^{30}N_2$. This leads to a set of equations with too many unknowns to fully determine the respective rates. Nevertheless, assuming denitrification via the extracellular nitrite pool only, results in rather conservative rate estimates, because any additional denitrification from the heavily labeled nitrate pool would have to be

compensated by increased denitrification rates from the less labeled nitrite pool in order to produce the observed production of $^{29}N_2$ and $^{30}N_2$.

Apart from the calculated coupled nitrification-denitrification rates $D^{nit}_{(treat\_3)}$, due to the negligible contribution of anammox in the N-loss, the observed $^{29}N_2$ as well as $^{30}N_2$ productions in the treatment 1 ($^{15}NH_4^+$+$^{14}NO_3^-$) is the direct proof of couple nitrification to denitrification presented by $D^{nit}_{(treat\_1)}$. Coupled nitrification-denitrification rates ($D^{nit}_{(treat\_1)}$) were only 30% of those measured in treatment 3 ($D^{nit}_{(treat\_3)}$) in March (Table 2), and were most likely underestimates the true rates, because the labeling percentage in equation 12 was calculated based on the initial $^{14}NH_4^+$ concentrations, not accounting for the $^{14}NH_4^+$ released from organic matter mineralization during the experiment. In August $D^{nit}_{(treat\_1)}$ was not detected at all. In March $^{14}NO_3^-$ was added, whereas $^{14}NO_2^-$ was added in August. Assuming that the extracellular NO_2^- pool is the source for all consecutive steps of denitrification, the $^{15}NO_2^-$ produced from $^{15}NH_4^+$ via nitrification was most probably too much diluted by the addition of 200µM $^{14}NO_2^-$ and thus could not be detected as $^{29}N_2$ and $^{30}N_2$.

Although absolute values of $D^{nit}_{(treat\_1)}$ and $D^{nit}_{(treat\_3)}$ were different, they showed similar trends of decreasing sediment depth (Fig. 4 and Table 2), indicating that nitrification-denitrification was tightly coupled in the upper 4 cm of sediments that are periodically oxygenated. In addition, the seasonal variation of $D^{nit}_{(treat\_3)}$ suggests that coupled nitrification-denitrification relies on O_2 availability and is favored by the expanded oxic surface layer driven by advection in these permeable sediments. Seasonal variations of coupling rates are negatively correlated with the O_2 consumption rates (Fig. 7 and Table 2). If oxygen is consumed more rapidly, as observed in the August experiments, oxygen is available for a shorter time period and nitrification becomes oxygen limited. Since all incubations were performed with a one-pulse addition of aerated bottom water instead of a continuous flushing, which can be assumed under *in situ* conditions, $D^{nit}_{(treat\_3)}$ in August was probably underestimated.

The seasonal variation of coupling rates and NO_x^- in water column was suggested to be positively correlated. Bottom water NO_x^- (~60 µM) and the modeled pore water NO_x^- influx (2.3×10^4 µmol m^{-2} h^{-1}) in March were one order of magnitude higher than

those in August (Gao et al. *in Rev.*), higher coupling rates — $D^{nit}_{(treat\_3)}$ (680-850 μmol m^{-3} sediment h^{-1}) and $D^{nit}_{(treat\_1)}$ (210-320 μmol m^{-3} sediment h^{-1}) were found in March as well (Table 2). It suggested that denitrification is more tightly coupled to nitrification rather than overlying water NO_x^-, in the expanded oxic surface layer driven by advection in these permeable sediments. Coupled nitrification-denitrification could probably be stimulated by the influx of oxic water into the sediment. $D^{nit}_{(treat\_3)}$ in August was underestimated due to the O_2 limitation in the slurry incubations. Therefore, the combined data in this study seem to coupled nitrification-denitrification is a significant NOx source for N-loss processes in permeable sediments, especially in summer.

Implications of nitrification

Direct observation on NO_x^- accumulation in presence of O_2 in the pore water profile combined with rate determinations on the conservative gross nitrification ($N_{(treat\_1)}$ and $N_{(treat\_3)}$) confirmed that substantial nitrification occurred in the surficial permeable sediments during the whole semi-diurnal tidal cycle (Fig.2 +7). The rates, $N_{(treat\_1)}$ and $N_{(treat\_3)}$, integrated to 5 cm (22-45 μmol m^{-2} sediments h^{-1}) (Table 2) are in the range of previous reported nitrification rates in sediments (10 μmol -18 mmol m^{-2} sediments h^{-1}) (Henriksen and Kemp 1988; Gilbert et al. 2003; Mortimer et al. 2004; Ward 2008).

Since nitrification is also an important sink for oxygen in marine environments by consuming O_2 to oxidize NH_4^+ to NO_x^-, the gross nitrification rate could be estimated from the aerobic respiration according to the classic Redfield stoichiometry (Redfield et al. 1963):

$(CH_2O)x(NH_3)y(H_3PO_4) + (x+2y)O_2 \rightarrow xCO_2 + yHNO_3 + (x+y)H_2O$

When x=106 and y=16, in this formulation, oxygen consumption should be inversely related to NO_3^- production with a slope of 138/16 = 8.6. In fully oxygenated sediments (i.e., carbon loading is not sufficient to exhaust the available oxygen), such relationships are often found (Grundmanis and Murray 1982; Jahnke et al. 1982). The permeable sediments of the Wadden Sea are fully aerated with deep O_2 penetration depth down to 5 cm (Billerbeck et al. 2006; Jansen et al. 2009) under the advection conditions during inundation or down to 2-4 cm even during exposure (Fig. 2). Moreover, the ratio of

POC:PON in seawater is 7:1(Billerbeck et al. 2006), which is consistent with the Redfield ratio of C:N (106:16). Therefore, it is reasonable to present their potential gross nitrification by the stoichiometry between the NO_3^- production and oxygen consumption. Although the estimated gross nitrification rates ($G_{nit}/G_{nit'}$) are 4-7 times higher than the conservative gross nitrification ($N_{(treat\_1)}/N_{(treat\_3)}$) (Table 2 +3), the range of rates (0.15-0.7 mmol m^{-2} $_{sediments}$ h^{-1}) are comparable with previously reported nitrification rates in sediments (10 μmol -18 mmol m^{-2} $_{sediments}$ h^{-1}) (Henriksen and Kemp 1988; Gilbert et al., 2003; Mortimer et al., 2004; Ward 2008). G_{nit} showed the seasonal variation and the integrated rate was >3 times higher in August (0.6-0.7 mmol m^{-2} $_{sediments}$ h^{-1}) than in March (0.15-0.2 mmol m^{-2} $_{sediments}$ h^{-1}). It suggests that nitrification is an important NO_x^- source to support for denitrification in NO_x^--depleted season when there is only low NO_x^- influx from bottom sea water, although no direct proof on coupling rates of $D^{nit}_{(treat\_1)}$ was obtained in August. It was due to the dilution of immediate nitrification implied by net NO_x^- production within 30 mins of incubation before the first subsampling. Regardless, the substantial potential gross nitrification based on OCRs strongly suggested that nitrification plays an important role as being a significant NO_x^- source in the Wadden Sea sediment system, especially in the summer when ambient NO_x^- availability is low.

The differences between the potential gross nitrification and the conservative gross nitrification ($G_{nit}/G_{nit'}$ and $N_{(treat\_1)}/N_{(treat\_3)}$) were in a wide range from 0.1 mmol m^{-2} $_{sediments}$ h^{-1} in March to 0.5 mmol m^{-2} $_{sediments}$ h^{-1} in August (Table 2 and Table 3). This difference suggested that other process such as dissimilatory nitrate reduction to ammonium (DNRA) or assimilation might occur in these sediments.

Altogether, our results showed that nitrification is an important NOx source in permeable Wadden Sea sediments, especially for N-loss through aerobic denitrification. Tightly coupled nitrification-denitrification observed in surficial sediments (in the upper 2 or 4 cm) suggests that the coupling is stimulated by O_2 availabilty and favored by the expanded oxic layer under advection. Net NO_x^- productions via nitrification determined in these sediments might further imply these sediments as a potential source for the efflux of NO_x^- into water column driven by the advective pore water flow. Our results supported the hypotheses that the sufficient NO_x^- availability for intensive denitrification

in permeable Wadden Sea sediments is ascribed to nitrification as well as bottom water NO_x^- influx, and the former might play a more important role in N loss especially in the summer when the ambient seawater NO_x^- availability is low. Therefore, our results showed that nitrification in these permeable sediments when directly coupled to denitrification plays a significant role in the marine N-removal by providing a start circuit from reduced N to N-loss.

Table 2 Rates of anammox, denitrification, coupled nitrification-denitrification, and nitrification measured in treatment 1, 2, and 3.

Expedition	Depth	A	$D^{nit}_{(treat\_3)}$	$D^{nit}_{(treat\_1)}$	N^{net}	$N_{(treat\_3)}$	$N_{(treat\_1)}$	D_{tot}	C_1	C_2
	cm	μmol N m^{-3} $_{sediment}$ h^{-1}								%
Mar 2007	0-2	51 ± 8	855 ± 58	323 ± 29	192 ± 106	1047± 164	518 ± 135	5190 ± 121	16.5	81.7
	2-4	25 ± 5	685 ± 26	212 ± 29	183 ± 71	868 ± 97	390 ± 100	7082 ± 270	9.7	78.9
	4-6	3 ± 1	346 ± 26	15 ± 2	350 ± 90	696 ± 100	364 ± 92	2234 ± 206	15.5	49.7
	Areal rates (0-5)	2 ± 0.1*	34.2 ± 1.9*	10.8± 1.2*	11.0 ± 4.4*	45.3 ± 6.2*	21.8 ± 3.5*	267.8 ± 9.9*	12.8	75.5
Aug 2007	0-2	No sig.	143 ± 10	----	34	177 ± 10	----	3201 ± 302	4.5	80.7
	2-4	9 ± 4	110 ± 4	----	799	909 ± 4	----	5184 ± 205	2.1	12.1
	4-6	17 ± 5	92 ± 6	----	1172	1264 ± 6	----	2634 ± 190	3.5	7.3
	Areal rates (0-5)	0.3 ± 0.1*	6.0 ± 0.3*	----	28.4*	34.4± 0.3*	----	194.0± 12.0	3.1	17.4

* in the unit of μmol m^{-2} h^{-1}

---- No significant

C_1 –the contribution of the coupled nitrification-denitrification to the total denitrification (D_{tot}) ($D^{nit}_{(treat\_3)} / D_{tot}$)

C_2 - the coupling efficiency of nitrification-denitrification ($D^{nit}_{(treat\_3)} / N_{(treat\_3)}$)

Table 3 The potential gross nitrificaiton rates based on the aerobic organic matter mineralization in incubations in March and August 2007

Expedition	Depth	OCR	OCR'	G_{nit}	$G_{nit'}$
	cm	mmol m^{-3} sediment h^{-1}		mmol m^{-3} sediment h^{-1}	
March 2007	0-2	30.8 ± 4.7	36.8 ± 10.4	3.6 ± 0.5	4.3 ± 1.2
	2-4	35.0 ± 9.7	11.6 ± 0.9	4.0 ± 1.1	1.3 ± 0.1
	4-6	25.2 ± 6.8	31.4 ± 4.3	2.9 ± 0.8	3.6 ± 0.5
	Integrated 0-5cm	1.57 ± 0.36*	1.28 ± 0.27*	0.18 ± 0.04 *	0.15 ± 0.03 *
August 2007	0-2	106.3	128.6	12.3	14.9
	2-4	97.1	86.6	11.2	10.0
	4-6	116.8	131.2	13.5	15.2
	Integrated 0-5cm	5.24*	5.62*	0.60 *	0.65 *

* in µmol m^{-2} h^{-1}

OCR and OCR' represented the oxygen consumption rates in incubations with $^{15}NH_4^+/^{14}NO_3^-$ and $^{15}NO_3^-$, respectively.

G_{nit} and $G_{nit'}$ represented the estimated gross nitrification from OCRs in incubations with $^{15}NH_4^+/^{14}NO_3^-$ and $^{15}NO_3^-$, respectively.

References

Billerbeck, M., U. Werner, K. Bosselmann, E. Walpersdorf, and M. Huettel. 2006. Nutrient release from an exposed intertidal sand flat. Mar. Ecol-Prog. Ser. **316:** 35-51

Brandes, J. A., and A. H. Devol. 1995. Simultaneous NO_3 and O_2 respiration in coastal sediments: Evidence for Discrete Diagenesis. J. Mar. Res. **53:**771-797

Braman, R. S., and S. A. Hendrix. 1989. Nanogram Nitrite and Nitrate Determination in Environmental and Biological-Materials by Vanadium(Iii) Reduction with Chemi-Luminescence Detection. Anal. Chem. **61:** 2715-2718

Capone, D. G., D. Bronk, M. Mulholland, and E. J. Carpenter. 2008. Nitrogen in the Marine Environment. 2nd edition. San Diego: Academic Press/ Elsevier.

Canfield, D. E., B. B. Jørgensen, H. Fossing, R. N. Glud, J. K. Gundersen, B. Thamdrup, J. W. Hansen, L. P. Nielsen, and P. O. J.Hall. 1993. Pathways of organic carbon oxidation in three continental margin sediments. Mar Geol **113:**27–40

Cook, P. L. M., F. Wenzhofer, S. Rysgaard, O. S. Galaktionov, F. J. R. Meysman, B. D. Eyre et al. 2006. Quantification of denitrification in permeable sediments: Insights from a two-dimensional simulation analysis and experimental data. Limnol. Oceanogr-Meth. **4:** 294-307

Dalsgaard, T., B. Thamdrup, and D. E. Canfield. 2005. Anaerobic ammonium oxidation (anammox) in the marine environment. Res Microbiol **156:** 457–464.

de Beer, D., F. Wenzhofer, T. G. Ferdelman, S. E. Boehme, M. Huettel, J. E. E. van Beusekom et al. 2005. Transport and mineralization rates in North Sea sandy intertidal sediments, Sylt-Rømø Basin, Wadden Sea. Limnolo. Oceanogr. **50:** 113-127

Deutsch, B., S. Froster, M. Wilhelm, J. W. Dippner, and M.Voss. 2010. Denitrification in sediments as a major nitrogen sink in the Baltic Sea: an extrapolation using sediment characteristics. Biogeosci. **7:** 3259-3271

Emery, K. O. 1968. Relict sands on continental shelves of the world. Am. Assoc. Petrol.Geo. Bull. **52:** 445-464

Engström, P., T. Dalsgaard, S. Hulth, and R. C. Aller. 2005. Anaerobic ammonium oxidation by nitrite (anammox):Implications for N2 production in coastal marine sediments.Geochim. Cosmochim. Acta. **69:** 2057–2065

Franke, U., L. Polerecky, E. Precht, and M. Huettel. 2006. Wave tank study of particulate organic matter degradation in permeable sediments. Limnol. Oceanogr. **51:** 1084-1096

Galloway, J. N., F. J. Dentener, D. G. Capone, R. W. H. E. W. Boyer, S. P. Seitzinger, G. P. Asner, P. A. G. C. C. Cleveland, E. A., Karl D. M. Holland, J. H. P. A. F. Michaels, A. R. Townsend, and C. J. Vöosmarty. 2004. Nitrogen cycles: past, present, and future. Biogeochem. **70:** 153-226

Gao, H., F. Schreiber, G. Collins, M. M. Jensen, J. E. Kostka, G. Lavik, D. de Beer, H. Y. Zhou, and M. M. M. Kuypers. 2010. Aerobic denitrification in permeable Wadden Sea sediments. ISME Journal. **4:** 417-426

Gao, H., M. Matyka, B. Liu, A. Khalili, J. E. Kostka, G. Collins, S. Jansen, M. Holtappels, M. M. Jensen, et al. Limnol. Oceanogr. *(In Rev)*

Gihring, T. M. A., Canion, A. Riggs, M. Huettel and J. E. Kostka. 2010. Denitrification in shallow, sublittoral Gulf of Mexico permeable sediments. Limnol. Oceanogr. **55:** 43-54

Gilbert, F., R.C. Aller and S. Hulth. 2003. The influence of macrofaunal burrow spacing and diffusive scaling on sedimentary nitrification and denitrification: an experimental simulation and model approach. J Mar. Res. **61:** 101-125

Glud, R. N., J. K. Gundersen and O. Holby. 1999. Benthic in situ respiration in the upwelling area off central Chile. Mar. Ecol. Prog. Ser. **186:**9–18

Grundmanis, V., and J. W. Murray. 1982. Aerobic respiration in pelagic marine sediments. Geochim. Cosmochim. Acta. **46:** 1101-1120

Grunwald, M., O. Dellwig, C. Kohlmeiter, T. H. Badewien, M. Beck, S. Kotzur N., Kowalski, G. Liebezeit, and H. J. Brumsack. 2010. Nutrient dynamics in a back barrier tidal basin of the Southern North Sea: Time-series, model simulations, and budget estimates, J. Sea Res. **64:** 199-212

Hall, P. J., and R. C. Aller 1992. Rapid, small-volume, flow injection analysis for ΣCO_2, and NH_4^+ in marine and freshwaters. Limnol. Oceanogr. **37:** 1113-1119

Henriksen, K., and W. M. Kemp. 1988. Nitrification in estuarine and coastal marine sediments: Methods, patterns and regulating factors. In H. Blackburn and J. Sorensen [eds.], Nitrogen cycling in coastal marine environments. Wiley. **pp.** 207-250

Howarth, R. W., R. Marino, J. Lane and J. Cole. 1988. Nitrogen fixation in freshwater, estuarine and marine ecosystems. 1. Rates and importance. Limnol. Oceanogr. **33:** 660–687

Hulth, S., R. C. Aller, D. E. Canfield, T. Dalsgaard, P. Engstrom, F. Gilbert et al. 2005. Nitrogen removal in marine environments: recent findings and future research challenges. Mar. Chem. **94:** 125-145

Huettel, M., W. Ziebis, S. Forster, and G. W. Luther. 1998. Advective transport affecting metal and nutrient distributions and interfacial fluxes in permeable sediments. Geochim. Cosmochim. Ac. **62:** 613-631

Huettel, M., H. Roy, E. Precht, and S. Ehrenhauss. 2003. Hydrodynamical impact on biogeochemical processes in aquatic sediments. Hydrobiologia. **494:** 231-236

Jahnke, R. A., S. R. Emerson, and J. W. Murray. 1982. A model of oxygen reduction, denitrification, and organic matter mineralization in marine sediments. Limnol. Oceanogr. **27:** 610-623

Jansen, S., E. Walpersdorf, U. Werner, M. Billerbeck, M. Böttcher, and D. de Beer. 2009. Functioning of intertidal flats inferred from temporal and spatial dynamics of O_2, H_2S and pH in their surface sediment. Ocean Dynam. **59:** 317-332

Jenkins, M. C., and W. M. Kemp. 1984.The coupling of nitrification and denitrification in two estuarinesediments. Limnol. Oceanogr. **29:** 609-19

Jensen, M. M., B. Thamdrup, and T. Dalsgaard. 2007. Effects of specific inhibitors on anammox and denitrification in marine sediments. Appl. Environ. Microbiol. **73:** 3151-8

Johnson, H. D., and C. T. Baldwin. 1986. Shallow siliciclastic seas. In Reading, HG (Ed.)

Sedimentary environments and facies (2nd ed.). Blackwell Scientific Publications, Oxford, **pp** 229-282

Joye, S. B., and I. C. Anderson. 2008. Nitrogen cycling in Estuarine and Nearshore Sediments. In: Capone, D., Bronk, D., Carpenter, E. and Mulhollond, M. (Eds), Nitrogen in the Marine Environment, Springer Verlag, Chapter 19, **pp** 868-915.

Keepers, M. M. M., G. Lavik, and B. Thamdrup. 2006. Anaerobic ammonium oxidation in the marine environment, In Past and Present Marine Water Column Anoxia (ed. L. N. Neretin), Springer. **pp.** 311-336

Lam, P., M. M. Jensen, G. Lavik, D. F. McGinnis, B. Müller, C. J. Schubert, R. Amann, B. Thamdrup, and M. M. M. Kuypers. 2007. Linking crenarchaeal and bacterial nitrification to anammox in the Black Sea. PNAS. 104: 7104-7109

Lam, P., and M. M M. Kuypers. 2011. Microbial Nitrogen Cycling Processes in Oxygen Minimum Zones. Annu. Rev. Mar. Sci. **3**: 317-345

Martens-Habbena, W., H. Urakawa, S. Tiquia, A. Devol, A. Ingalls, and D. Stahl. 2010. 13th ISME-Meeting, Seattle, WA, USA, August 22 – 27

Mortimer, R. J. G., S. J. Harris, M. D. Krom, T. Freitag, J. Prosser, and J. Barnes, et al. 2004. Anoxic nitrification in marine sediments. Mar. Eco. Prog. Ser. **276:** 37-51

Nielsen, L. P., P. B. Christensen, N. P. Revsbech, and J. Smensen. 1990. Denitrification and photosynthesis in stream sediment studied with microsensor and whole-core techniques. Limnol. Oceanogr. **35**: 1135-l 144

Nielson, L P. 1992. Denitrification in sediments determined from nitrogen isotope pairing. FEMS Microbiol. Ecol. **86**:357-362

Nielsen, L. P., and R. N. Glud. 1996. Denitrification in a coastal sediment measured in situ by isotope paring applied to a benthic flux chamber. Mar. Ecol. Prog. Ser. **137:** 181-186

Rao, A. M. F., M. J. McCarthy, W. S. Gardner, and R. A. Jahnke. 2007. Respiration and denitrification in permeable continental shelf deposits on the South Atlantic Bight: Rates of carbon and nitrogen cycling from sediment column experiments. Cont. Shelf Res. **27:** 1801-1819

Rao, A. M. F., M. J. Mccarthy, W. S. Gardner, and R. A.Jahnke. 2008. Respiration and denitrification in permeable continental shelf deposits on the South Atlantic Bight: N2:Ar and isotope pairing measurements in sediment column experiments. Cont. Shelf Res. **28:** 602-613

Redfield, A. C., B. H. Ketchum, and F. A. Richards. 1963. The influence of organisms on the composition of sea-water. In M.N. Hill (ed.) The Sea. Vol.2, pp.554. John Wiley & Sons, New York. **pp.**26-77

Revsbech, N. P. 1989. An oxygen microsensor with a guard cathode. Limnol. Oceanogr. **34:** 474-478

Rysgaard, S., N. Risgaard-Petersen, L. P. Nielsen, and N. P.Revsbech. 1993. Nitrification and Denitrification in Lake and Estuarine Sediments Measured by the 15N Dilution Technique and Isotope Pairing. Appl. Environ. Microbiol. **59:** 2093-2098

Røy, H., J. S. Lee, S. Jansen, D. de Beer. 2008. Tide-driven deep pore-water flow in intertidal sand flats. Limnol. Oceanogr. **53:** 1521-1530

Seeberg-Elverfeldt, J., M. Schlüter, T. Feseker, and M. Kölling. 2005. Rhizon sampling of porewaters near the sediment-water interface of aquatic systems. Limnol. Oceanogr-Meth. **3:** 361-371

Seitzinger, S. P. 1990. Denitrification in aquatic sediments. In: N.P. Revsbech and J. Sorensen, (editors), Denitrification in soil and sediment. Plenum Press. **pp.** 301-322

Thamdrup, B., and T. Dalsgaard. 2002. Production of N_2 through Anaerobic Ammonium Oxidation Coupled to Nitrate Reduction in Marine Sediments. Appl. Environ. Microbiol. **68:** 1312-1318

Tuominen, L., A. Heinanen, J. Kuparinen, and L. P. Nielsen. 1998. Spatial and temporal variability of denitrification in the sediments of the northern Baltic Proper. Mar. Ecol. Prog. Ser. **172:** 13-24

Ward, B. B. 2008. Nitrification. In: Nitrogen in the Marine Environment. Eds. D. G. Capone, D. A. Bronk, M. R. Mulholland, and E. J. Carpenter. Elsevier, Amsterdam. **pp.** 199 – 262

Wenzhöfer, F., O. Holby, R. N. Glud, H. K. Nielsen. 2000. In situ microsensor studies of a shallow hydrothermal vent at Milos, Greece. Mar. Chem. **69:**43–54

Werner, U., M. Billerbeck, L. Polerecky, U. Franke, and M. Huettel. 2006. Spatial and temporal patterns of mineralization rates and oxygen distribution in a permeable intertidal sand flat (Sylt, Germany). Limnol. Oceanogr. **51:** 2549-2563

Conclusions and outlook

This thesis focuses on the importance and regulation of nitrogen (N) loss in the Wadden Sea permeable sediments under advective conditions and the general importance of permeable sediments for the removal of N in marine environments. As the oxygen penetration and solute transports into permeable sediments are both enhanced by advection, the study mainly addresses the following questions: 1) How does oxygen influence the activity of N-loss processes in the oxic layers of the sediment impacted by pore water advection? 2) Are there spatial and seasonal variations in nitrogen loss from these permeable sediments and what is the annual N-loss rate? 3) How do other N-cycling processes such as nitrification interact with N-loss processes, and what are the implications on total N-loss?

To answer the first question, multiple experimental approaches under simulated *in situ* conditions were applied to investigate N-loss by denitrification in relation to O_2 dynamics. Substantial denitrification rates of 0.19-0.32 mmol N m^{-2} h^{-1} were found even in the presence of nearly 90 µM O_2 using the modified intact core incubation with one-pulse percolation and well–mixed slurry incubations. Furthermore, co-respiration of NO_x^- and O_2 was demonstrated by simultaneous measurements using a NO_x biosensor and O_2 microsensor, respectively. The existence of anoxic microniches was excluded by the vigorously-mixed sediment slurry incubation in a flow-through stirred retention reactor, providing further evidence for aerobic denitrification independent from coupled nitrification. The consistent results from various approaches showed that O_2 may not act as the primary or exclusive control of N_2 production in permeable sediments, especially in the upper 4 cm where O_2 and NO_x^- co-occurred. The ecological significance of the co-respiration of NO_x^- and O_2 in permeable sediments of the Wadden Sea was proposed as a selective environmental adaptation of denitrifiers to recurrent tidally induced redox oscillations.

To understand the role of permeable sediments in the oceanic N-budget, N-loss rates were determined in permeable sediments of the Wadden Sea on spatial and seasonal scales using a combination of stable N isotopes and model simulation approaches. Three different incubation methods that employed the isotope pairing technique (IPT) were used: Intact core incubations simulating either (i) diffusive or (ii) advective transport conditions

and (iii) slurry incubations. Advective transport of pore water in the sediment increased total N loss rates by factors of 1-2 orders of magnitude compared to diffusion. These permeable sediments are generally characterized by substantial N-loss rates (on average 0.2 mmol N $m^{-2}_{sediment}$ h^{-1}) over spatial and temporal scales. It was hypothesized to be due to sufficient NO_x^- availability driven by advection. A 2-D empirical model was developed to estimate the NO_x^- availability by simulating the influx of NO_x^- driven by advection using annual *in situ* monitoring data as input parameters, which included temperature, bottom current velocity and ambient NO_x^- concentrations in the overlying seawater. The simulated result of the model showed that sufficient NO_x^- influx in the sediments exceeded the amount required to support measured N loss rates during most of the year. Annual N-loss for the Wadden Sea permeable sediments was estimated to be 0.22 Tg N y^{-1} based on the annual average N-loss rate of 750 mmol N m^{-2} y^{-1} at intertidal flats as determined from experimental and model simulation results and the consequent extrapolated rate of 1788 mmol N m^{-2} y^{-1} at subtidal flats, gullies and offshore areas. The sandy seafloor is therefore considered as a major sink for riverine N loads into the Wadden Sea and permeable sediments have great potential to regulate the flow of nitrogen at the land-sea boundary.

The enhanced thickness of oxic zone in permeable sediments due to advection might favor nitrification. The importance of nitrification in the Wadden Sea permeable sediments, nitrification and its coupling to N-loss processes, mainly aerobic denitrification, were quantified using various ^{15}N-isotope-paring experiments. Net NO_x^- production via nitrification was examined under aerobic conditions in these sediments. Results showed that the NO_x^- accumulation in sediments is attributed to nitrification, and the subsequence consumption of accumulated NO_x^- suggested that nitrification could be the NO_x^- source for other dissimilatory processes (i.e. anammox and denitrification) or the potential efflux of NO_x^- from the sediments. As Anammox occur at very low rates (<2 µmol N m-2 h-1, <1 % of total N loss), aerobic denitrification was the dominant N-loss process observed in these sediments. Nitrification coupled to denitrification was found to contribute to as much as 17% of total N-loss especially in surface sediments and the rest of total N-loss was fueled by NO_x^- from the overlying water. Both nitrification and the influx of NO_x^- from the overlying water were strongly influenced by advection. Here, coupled nitrification-denitrification might be underestimated, especially in the summer, due to the

O_2 limitation during incubations instead of *in situ* continuous aerated advective porewater flushing. In summary, by being tightly coupled to aerobic denitrification, nitrification plays a significant role linking N-source and N-sink in these permeable Wadden Sea sediments, especially in overlying water NO_x^- depleted season.

This thesis shows that permeable sandy sediments, accounting for 58-70% of the continental shelves, play a key role in global marine N-loss, and that they act as efficient filters for the increasing N-inputs from terrestrial/freshwater systems that would otherwise reach the Ocean. Aerobic denitrification has been found in these sediments as the predominant N-loss process. However, the microbial mechanism remains unclear. Co-metabolism of both NO_x^- and O_2 in single cells or co-inhabiting of distinct denitrifying and oxygen respiring populations in this redox zone should be investigated in future studies using molecular biological techniques. The substantial denitrification rates in these permeable sediments are neither restrained by O_2 or by NO_x^- availability. Another important factor in the regulation of denitrification activity is organic matter. Hence, the seasonal availability of organic matter should be further investigated to verify if it is sufficient to support the high denitrification rates over a year. The difference between potential and conservative gross nitrification rates suggested there may be the interactions with DNRA, which would channel some of NO_x^- produced by nitrification back to NH_4^+ and thus preventing direct N-loss, or benthic primary production, which will produce O_2 as well, though also providing more organic matter, etc. Therefore, to understand the whole N-cycling, those questions should be focused on in the future.

Acknowledgements

First of all I would like to specially thank Marcel Kuypers for accepting me as PhD student to work in the Nutrient Group at our institute with such a nice atmosphere of easy collaboration. I have to say, though my name appears on the cover of this dissertation, a great many people have contributed to its production. I would like to thank all those people who have made this dissertation possible, and because of whom my experience has been one that I will cherish forever.

My deepest gratitude is to my supervisor, Marcel Kuypers, for his inspiring advice and comments, enthusiastic and encouraging discussions, and for reviewing the thesis. He opened the door for me to the field of N-cycling and shed the light for me through the darkness. Do learn from him how to dig the importance out of the numerous irrelevances. His support helped me overcome the crisis and finish this dissertation.

I would like to thank Joel Kostka, Gaute Lavik as co-supervisors who greatly supported me in numerous ways. I'm specially thankful to Joel Kostka for teamwork and fun time during various expeditions, his supervision on carefully reading and commenting on countless revisions of the manuscripts. I'm deeply grateful to Gaute Lavik for sharing the experience of technical details of my work, supporting for the isotope measurements and introducing me to the mysteries of isotope paring stoichiometry.

In particular, I would like to thank Kai-Uwe Hinrichs and Gerhard Bohrmann for their help and supports to proceed to my defense, and Kai-Uwe Hinrichs is specially thanked for reviewing the thesis.

Many thanks go to my dear Watt-partners, Gavin Collins, Marlene Jensen, Sumei Liu for the teamwork in expeditions, for their friendships, collaborations and great time during and after the work. I also would like to thank Dirk de Beer, Stefan Jansen, Hans Roy, Frank Schreiber, Lubos Polerecky and Christy Wu from microsensor group for the collaborations of sharing their experience, technical supports and joyful time in the "Watt" field expeditions, as well as Bo Liu, Maciej Matyka and Arzhang Khalili from

mathematics modeling group for their collaborations and sharing the knowledge on model build-up.

I would specially thank Phyllis Lam for her selfless help and support on constructive comments on my thesis, and daily chocolate offer to fuel my brain for the thesis preparation. Moritz Holtappels is thanked so much for a lot of help, especially helpful discussion and constructive comments on manuscripts.

For their help and technical assistance in the field trip and laboratory I want to thank all technicians in Biogeochemistry department, especially Ingrid Dohrmann, Gabi Klockgether, Daniela Franzke. I would further like to thank the captains Ronald Monas and Ole Pfeiler for the ship time and excellent collaborations. I also would like to thank Melanie Beck, Thomas Badewien from ICBM of University Oldenburg and Maik Grunwald from Helmholtz-Zentrum Geesthacht for their collaboration and sharing the knowledge on the Wadden Sea.

All dear colleagues in the Nutrient Group and the BioGeo Group are thanked for their warmth and open minds which make me feel like home. I want to thank all my dear friends, especially Olivera Svitlica, Clelia Dona, Alexandra Rao, Casey and Anna-Maria Hubert, Aude Picard, Sarah Sokoll, Annina Huber, Hannah Marchant, and all friends from BFBC, for their help and supports in these years, bringing the sunshine into my life and accompanying with me through the difficulty. Here, Alexandra Rao, Casey and Anna-Maria Hubert, Hannah Marchant are specially thanked for commenting on my thesis or improving my English. I also would like to thank my former Chinese supervisor, Huai-yang Zhou, for his long term supports from China. I am also grateful to my families for their love, encouragement and solid supports.

Finally I would like to acknowledgement the DAAD, MPG and DFG for providing the funding of the work.